FREE AND FORCED TROPICAL VARIABILITY: ROLE OF THE WIND-EVAPORATION-SEA SURFACE TEMPERATURE (WES) FEEDBACK

A Dissertation

by

SALIL MAHAJAN

Submitted to the Office of Graduate Studies of
Texas A&M University
in partial fulfillment of the requirements for the degree of

DOCTOR OF PHILOSOPHY

December 2008

Major Subject: Atmospheric Sciences

FREE AND FORCED TROPICAL VARIABILITY: ROLE OF THE WIND-EVAPORATION-SEA SURFACE TEMPERATURE (WES) FEEDBACK

A Dissertation

by

SALIL MAHAJAN

Submitted to the Office of Graduate Studies of
Texas A&M University
in partial fulfillment of the requirements for the degree of

DOCTOR OF PHILOSOPHY

Approved by:

Chair of Committee,	R. Saravanan
Committee Members,	Kenneth P. Bowman
	Ping Chang
	Gerald R. North
Head of Department,	Kenneth P. Bowman

December 2008

Major Subject: Atmospheric Sciences

ABSTRACT

Free and Forced Tropical Variability: Role of the Wind-Evaporation-Sea Surface Temperature (WES) Feedback. (December 2008)

Salil Mahajan, B. Arch, Indian Institute of Technology, Kharagpur;

M.S., Texas A&M University

Chair of Advisory Committee: Dr. R. Saravanan

The Wind-Evaporation-Sea Surface Temperature (WES) feedback is believed to play an important role in the tropics, where climate variability is governed by atmosphere-ocean coupled interactions. This dissertation reports on studies to distinctly isolate the WES feedback mechanism over tropical oceans using a modified version of an NCAR-Community Climate Model (CCM3) thermodynamically coupled to a slab ocean model, where the WES feedback is deliberately suppressed in the bulk aerodynamic formulation for surface heat fluxes. A comparison of coupled integrations using the modified WES-off CCM3 to those carried out using the standard CCM3 conclusively identifies the role of the WES feedback in enhancing the inter-annual variability over deep tropical oceans and the westward propagation of the equatorial annual cycle. An important role for near surface humidity in tropical climate variability in enhancing inter-annual variability and in sustaining the equatorial annual cycle is also suggested. Statistical analyses over the tropical Atlantic reveal that the free coupled meridional mode of the Atlantic Ocean is amplified in the presence of the WES feedback. Similar analyses of coupled model integrations, when forced with an artificial El Niño Southern Oscillation (ENSO)-like SST cycle in tropical Pacific, reveal that only in the presence of the WES feedback is the meridional mode the preferred mode of response of the Atlantic to ENSO forcings. It is also found that WES feedback reinforces the tendency of the ITCZ to stay north of the equator

over the Atlantic during El-Nino events. Comparative studies between Last Glacial Maximum (LGM) equivalent imposed northern hemispheric sea-ice experiments with the WES-off model and the standard model indicate a dominant role for the WES feedback in the southward shift of the ITCZ as indicated by paleo-climate records. However, it is found not to be the sole thermodynamic mechanism responsible for the propagation of high latitude cold SST anomalies to the tropics, suggesting significant roles for other mechanisms in the tropical response to high latitude changes.

To my family, for their unshakeable love and support

ACKNOWLEDGMENTS

I would not have delved into the unfathomable depths of the pursuit of a doctorate without the strong encouragement of Prof. Gerald R. North, for which I am forever indebted to him. I would like to extend my gratitude to Prof. R. Saravanan, who took me under his guidance as my advisor, and has also been a mentor all these years. I have learned both science and scientific conduct from him. Prof. Ping Chang has been supporting and reviewing this work from its start, and I am very grateful for his advice. I would like to acknowledge the guidance and support of Prof. Kenneth P. Bowman, who has had a constant presence across my graduate education. I would like to thank Dr. Link Ji and Dr. Hank Seidel, from whom I have relentlessly sought help throughout.

It is beyond my writing abilities to express in words, the gratitude I feel towards my family and friends for their unconditional support. The least I can say is - 'Thank you'.

TABLE OF CONTENTS

CHAPTER Page

LIST OF FIGURES

FIGURE Page

FIGURE Page

FIGURE Page

FIGURE Page

FIGURE Page

FIGURE Page

FIGURE Page

CHAPTER I

INTRODUCTION

Atmosphere-ocean coupling generates predictable modes of variability in the climate system. The decay time-scale of intrinsic atmospheric perturbations ranges from days to months, whereas coupled variability could last for multiple years as is vividly seen in the El Niño Southern Oscillation (ENSO) phenomenon, which is a product of the dynamic interactions between the atmosphere and the ocean. Lesser attention has been paid to the thermodynamic coupling between the two components of the climate system. Traditionally, the atmosphere had been considered to be a stochastic noise generator that forces the ocean (Hasselmann, 1976; Frankignoul and Hasselmann, 1977). Recent work reveals that thermodynamic coupling and feedbacks between the atmosphere and the ocean increase the thermal variance of both the atmosphere and the oceans at low frequencies (Barsugli and Battisti, 1998; Saravanan, 1998) and have been hypothesized to cause decadal oscillations (Chang et al., 1997). Although the thermodynamic coupling between the atmosphere and the oceans is weak, and may not give rise to self-sustained oscillations, non-normal growth caused by the non-local effects of coupling could provide potential predictability (Chang et al., 2004).

Over the tropical oceans, the thermodynamic wind-evaporation-SST (WES) feedback has been proposed to be one such mechanism causing decadal cross-equatorial dipole-like oscillations over the tropical Atlantic (Chang et al., 1997; Xie, 1999). An analogous meridional mode is also found in the Pacific (Yukimoto et al., 2000; Chiang and Vimont, 2004). In addition to its possible role in decadal oscillations, the WES feedback is also proposed to play significant roles in the seasonal and inter-annual vari-

---

The journal model is *Journal of Climate*.

ability of the coupled system over the deep tropics - amplifying the cross-equatorial variability (Carton et al., 1996; Saravanan and Chang, 2004), causing the latitudinal asymmetry of tropical climate (Xie, 1996) and playing a central role in the equatorial annual cycle and the westward propagation of equatorial anomalies in the Pacific and the Atlantic basins (Xie, 1994; Liu, 1996). A recent study has also proposed the WES feedback as a mechanism for the propagation of high latitude cooling, associated with abrupt climate change, to the tropics and the subsequent southward transition of the ITCZ (Chiang and Bitz, 2005). Even though the WES feedback received its current nomenclature in a later study (Xie, 1996), it was in fact, initially introduced as a mechanism to explain the asymmetry of the ITCZ by Xie and Philander (1994).

The cross equatorial WES feedback works as follows. An anomalous development of a northward cross equatorial SST gradient (CESG) causes the development of anomalous cross-equatorial southward pressure gradient due to hydrostatic adjustment (Lindzen and Nigam, 1987). This generates anomalous northward cross equatorial winds which turn to their left south of the equator and right to the north of the equator due to Coriolis force. The anomalous south-westerly (south-easterly) winds diminish (enhance) the north-easterly (south-easterly) background trade winds over the northern (southern) side of the equator, decreasing (increasing) the latent heat flux release from the oceans to the atmosphere, leading to a local warming (cooling) of the region amplifying the initial anomaly. A stepwise illustration of the feedback as discussed above is shown in a schematic in Figure 1. The positive feedback exists in regions where the mean background zonal trade winds are easterlies. In regions where the zonal mean winds are westerlies, the WES feedback manifests itself as a negative feedback. Modeling studies reveal that an equatorially asymmetric steady state solution is reached by the balancing effect of the non-linearities in the system, such as the SST threshold for deep convection in the atmosphere and the minimum

wind speed requirement for the calculation of surface latent and sensible heat fluxes (Xie, 1996). At decadal time-scales, an oscillatory solution has been proposed, in which the WES feedback is counteracted by advection caused by meridional oceanic currents (Chang et al., 1997) and by the poleward advection due to Ekman pumping (Xie, 1999).

While the WES feedback has been proposed to be a leading cause of inter-hemispheric interactions (Carton et al., 1996; Chang et al., 1997) in simple modeling studies, statistical analysis of tropical oceans reveals little negative correlation between the two hemispheres across the equator (for e.g. Czaja et al., 2002; Nobre and Shukla, 1996). It is possible that the atmospheric internal noise forces the SST in each hemisphere independently, lowering correlation between inter-hemispheric anomalies (Chang et al., 2001). Okajima et al. (2003) propose that WES feedback is weakened if the axis of symmetry in the deep tropical oceans is shifted from the equator, as is the case in the eastern Pacific and the Atlantic. In the presence of a symmetric climate with the axis of symmetry and the climatological ITCZ at the equator in an AGCM, strong correlation between inter-hemispheric anomalies is observed. However, in an asymmetric climate where the ITCZ stays north of the equator, the correlation across the ITCZ vanishes due to the stronger Coriolis force off the equator preventing an cross-ITCZ meridional flow. This result finds support in observations where a stronger inter-hemispheric coherence is observed in spring over the Atlantic, when the ITCZ is close to the equator. However, the reasoning is somewhat circular because the ITCZ is proposed to be asymmetric because of the WES feedback.

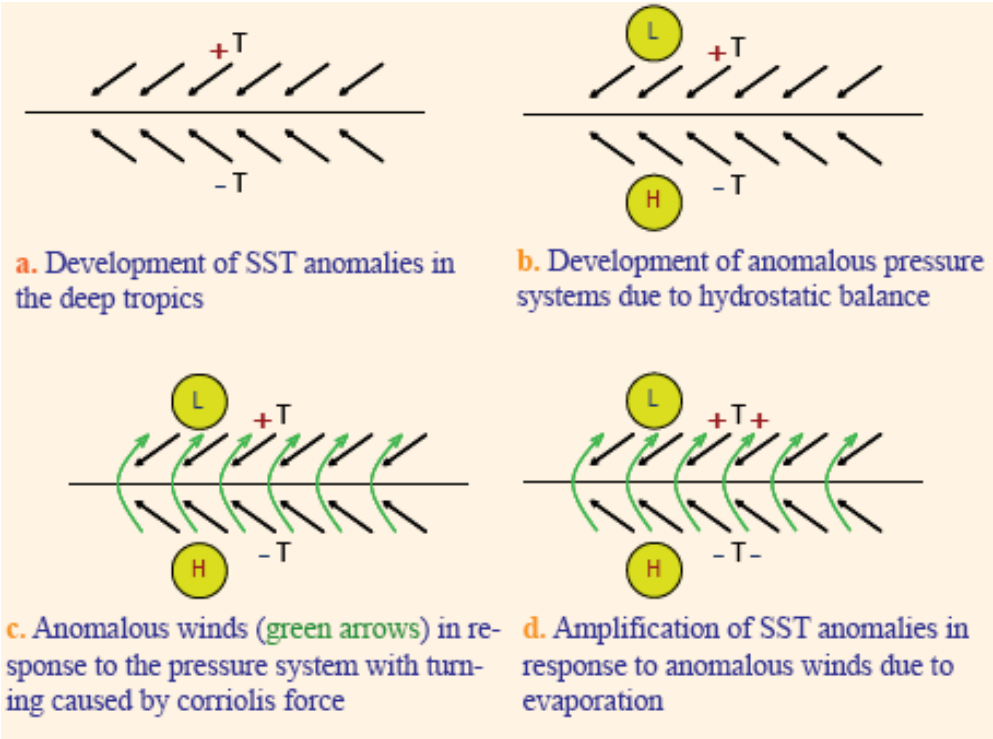

Fig. 1. An illustration of the WES feedback. The horizontal line represents the equator, and the black arrows indicate trade winds.

A. Proposed Roles of the WES Feedback in Tropical Climate Variability

In the following sections, the specific proposed roles of the WES feedback in tropical climate variability are listed starting with its role in maintaining the ITCZ asymmetry, followed by its role in the westwards propagation of the equatorial annual cycle. Its roles in the free and forced meridional variability of the tropical Atlantic are also described. Finally, the proposed role of the WES feedback in the propagation of high latitude cooling to the tropics is illustrated.

1. ITCZ Asymmetry

The reasons for the northern hemispheric preference of the ITCZ over the eastern Pacific and the Atlantic have been studied for some time, and the trio of land, air and sea have been found to play significant roles in the asymmetry of the ITCZ (Xie, 2005). The existence of the ITCZ at the equator over the eastern Pacific and the Atlantic is ruled out because of the presence of colder SSTs over the equator due to ocean upwelling (Xie and Philander, 1994) caused by zonal winds over the equator. In fact, even over the western Pacific warm pool, where there is a broad equatorial SST maximum, the ITCZ exists off the equator - the physics of which is not well understood (Xie, 2005). Xie and Philander (1994) found that in the presence of air-sea interactions a symmetric ITCZ about the equator over the oceans is unstable, and the ITCZ relapses to one of the hemispheres. The choice of the northern hemispheric location for the ITCZ in the present climate is attributed to the north-western tilt of the eastern Pacific coastlines, the north African continental bulge, the stratus cloud-SST feedback (Philander et al., 1996) and the subsidence of dry air by the Andes over the south-eastern tropical Pacific (Takahashi and Battisti, 2007) that create the initial asymmetry in the eastern coastal SSTs. The SST asymmetry in

combination with the associated wind pattern with anomalous south westerlies in the north and south-easterlies in the south forms the WES mode. Xie (1996) showed using a simple coupled atmosphere-ocean model that the WES mode over the eastern oceans propagates westward in the presence of air-sea interaction as westward propagating Rossby waves that arise as a response to any asymmetric atmospheric and oceanic anomalies (Gill, 1980), generating basin-wide asymmetry.

2. Equatorial Annual Cycle over Tropical Oceans

Another westward propagation mechanism involving the WES feedback exists in the equatorial Pacific and Atlantic oceans, though on the seasonal time-scale, and is responsible for the westward propagation of air-sea anomalies over the equatorial oceans resulting in the westward propagating annual cycle. Horel (1982) found an annual cycle of SST in the equatorial eastern Pacific whose phase propagates westwards, even in the presence of a semi-annual solar cycle at the equator. This annual cycle is a result of intensification of southerlies in the fall and their reduction in the spring at the equator as they converge onto the northern ITCZ (Xie, 1994; Wang, 1994). During boreal fall, southerlies over the equatorial Pacific intensify leading to stronger evaporation at the surface and upwelling over the eastern equatorial Pacific, resulting in reduced SSTs. The SSTs respond to the changed winds in the eastern Pacific with a timescale of a few weeks because of the shallower thermocline in the eastern Pacific as compared to the rest of the basin. Similarly, in the spring when the trade winds diminish, SSTs rise in the eastern equatorial Pacific.

The westward propagation of this annual cycle originating in the eastern Pacific can be explained by a zonal manifestation of the WES feedback as follows (Xie, 1994): In the boreal spring, when the southerlies diminish, and the SSTs rise in the eastern pacific, an anomalous low pressure develops in the region. This leads

to development of anomalous westerlies in the western neighborhood of the eastern pacific. These westerlies weaken the background easterly trade winds and thus reduce the evaporation in the region, consequently leading to higher SSTs, extending the low-pressure region from the eastern pacific westwards. This WES feedback leads to westward propagation of warm SST anomalies. Cold anomalies also propagate westward similarly starting in boreal fall. Using a simple linear coupled model, Liu (1996) shows that the equator-ward propagation of the off-equatorial annual cycle, which also involves the coupled WES feedback in addition to wind forced vertical mixing, is also a plausible mechanism for the equatorial annual cycle. A similar annual cycle is also observed over the equatorial Atlantic (Mitchell and Wallace, 1992; Philander and Chao, 1991) with the west African monsoon also influencing the southerly winds over the eastern equatorial Atlantic (Okumura and Xie, 2004).

3. Free Meridional Mode of Tropical Atlantic

The meridional mode of variability in the tropical Atlantic, also known as the inter-hemispheric mode or the dipole mode, is about as strong as the Atlantic Niño mode (e.g. Ruiz-Barradas et al., 2000), distinguishing the Atlantic from the neighboring tropical Pacific, where the zonal El Niño Southern Oscillation (ENSO) mode dominates. While random cross-equatorial dipole sea surface temperature (SST) patterns have been known to occur over the tropical Atlantic (Enfield and Mayer, 1997; Enfield et al., 1999), they do not characterize the meridional mode. Statistical analysis studies (Houghton and Tourre, 1992; Rajagopalan et al., 1998; Enfield et al., 1999; Mehta, 1998; Enfield et al., 1999) reveal that the meridional mode does not manifest itself as a simple cross-equatorial anti-symmetry of SSTs at inter-annual time-scales, as was previously suggested (e.g. Moura and Shukla, 1981), but exists as cross equatorial SST gradients (CESG) that result in dipole like anomalies of atmospheric variables

(e.g. Enfield et al., 1999).

The physical mechanisms of the meridional mode and its associated time-scales, however, have remained elusive. Observational studies clearly indicate decadal variability of both northern and southern tropical Atlantic SSTs independently. A decadal variability of the CESG, suggesting a meridional cross-equatorial relation, is also noted (e.g. Carton et al., 1996; Rajagopalan et al., 1998). A modeling study by Seager et al. (2001) using ocean models forced by observed winds show that the observed variability in the tropical Atlantic SSTs on decadal time-scales can be explained primarily by the influence of winds on SST via surface fluxes with the ocean circulation merely acting to damp the effects of winds. Carton et al. (1996) in an ocean modeling study also find that inter-annual and inter-decadal tropical Atlantic SST variability can be well explained by the influence of climatological winds. However, studies using simple and complex coupled models raise the possibility of the existence of an oscillatory dipole-like meridional mode of the tropical Atlantic SST on the inter-annual and decadal time-scales caused by the coupled dynamics of atmosphere-ocean system (Chang et al., 1997; Curtis and Hastenrath, 1995; Kushnir et al., 2002; Saravanan and Chang, 2000; Giannini et al., 2000; Xie, 1999; Huang and Shukla, 1997). An important mechanism contributing to the meridional mode that emerges among various studies is the positive Wind-Evaporation-SST (WES) feedback, the mechanics of which are the focus of this study.

The positive WES feedback is balanced by other oceanic processes such as the meridional transport of SST anomalies by advection due to cross-equatorial currents (Chang et al., 1997), and poleward SST advection by Ekman flow (Xie, 1999), leading to decadal oscillations. Chang et al. (2001) show that the balancing effect of damping by just the climatological ocean circulation is enough to cause decadal oscillations. Low frequency variability of the tropical Atlantic has also been shown to be caused by

the selective amplification of random forcing, either intrinsic to the tropical Atlantic or from external sources such as ENSO or NAO by the WES feedback (Kushnir et al., 2002).

4. Atlantic Ocean's Response to ENSO

Regression of ENSO indices on SST over the Atlantic reveal a CESG pattern similar to the meridional mode (Enfield and Mayer, 1997; Ruiz-Barradas et al., 2000; Saravanan and Chang, 2000) indicating that it is the preferred mode of response of the Atlantic to ENSO events, with about 30% of the variability of the Atlantic meridional mode explained by ENSO. The understanding of the precise mechanisms of the response of ENSO on the Atlantic through atmospheric tele-connections and the associated potential predictability are subjects of on-going research. Several observational studies have found significant warming (cooling) in the north Tropical Atlantic in response to El Niño (La-Niña) (Curtis and Hastenrath, 1995; Enfield and Mayer, 1997; Klein et al., 1999). Much of the warming during El Niño events has been attributed to a reduction in latent heat fluxes over the north sub-tropical and tropical Atlantic, due to the reduction in trade winds in a number of studies (Curtis and Hastenrath, 1995; Enfield and Mayer, 1997; Klein et al., 1999; Saravanan and Chang, 2000).

Several mechanisms causing the change in trade wind strength over the Atlantic in response to ENSO have been proposed in the literature. By one mechanism, which involves the Pacific North American (PNA) tele-connection (e.g Wallace and Gutzler, 1981; Nobre and Shukla, 1996), El Niño events cause lower sea level pressures (SLP) over the northern sub-tropical and mid-latitude Atlantic ocean. which induce anomalous south-westerlies in the region, acting to reduce the mean wind speed as they oppose the background north-easterly trades. The warming in the north sub-tropical ocean causes anomalous south-easterly winds south of the warming, possibly

due to reduction in the SLP in the region of warming, warming up the tropical Atlantic and influencing the south-equatorial Atlantic as well (Enfield and Mayer, 1997; Chiang et al., 2002). Giannini et al. (2000) argued that the high pressure anomaly developed during an El Niño in the tropical Atlantic acts together with the low pressure anomaly in the sub-tropical Atlantic for developing the south-westerly anomalies. Another proposed mechanism involves the modification of the Walker and Hadley circulations during ENSO events (Klein et al., 1999), where the subsidence in the equatorial Atlantic associated with the anomalous Walker circulation in response to El Niño reduces the meridional Hadley circulation, and associated trade winds, over the tropical Atlantic. The change in convection in the tropical Atlantic due to changes in the Walker and Hadley circulation also effects the shortwave fluxes. Alexander and Scott (2002) also find significant contributions of sensible heat flux, also affected by winds, and shortwave heat flux in the response of northern tropical Atlantic to ENSO. Tropical tropospheric warming during ENSO warm events also causes a warming of the SSTs over the tropical Atlantic (Chiang and Sobel, 2002), where warming of the eastern Pacific troposphere during El Niño spreads throughout the tropics (e.g. Charney, 1963; Schneider, 1977; Held and Hou, 1980; Sobel and Bretherton, 2000). These mechanisms are illustrated in a schematic in Figure 2. An increase of specific humidity, which effects the latent heat flux, over the northern tropical Atlantic during El Niño, also works to increase the SST in the region (Saravanan and Chang, 2000). There are also dynamic feedbacks excited by ENSO which complicate the remote ENSO influence in the tropical Atlantic, as shown by Chang et al. (2006).

Modeling studies show that the response of the Atlantic atmosphere to external forcings is weak in the absence of air-sea coupling which allows for feedbacks, and the atmosphere anomalies persist longer in the presence of these feedbacks (e.g Lau and Nath, 2001). Over the north tropical and equatorial Atlantic, it has been proposed

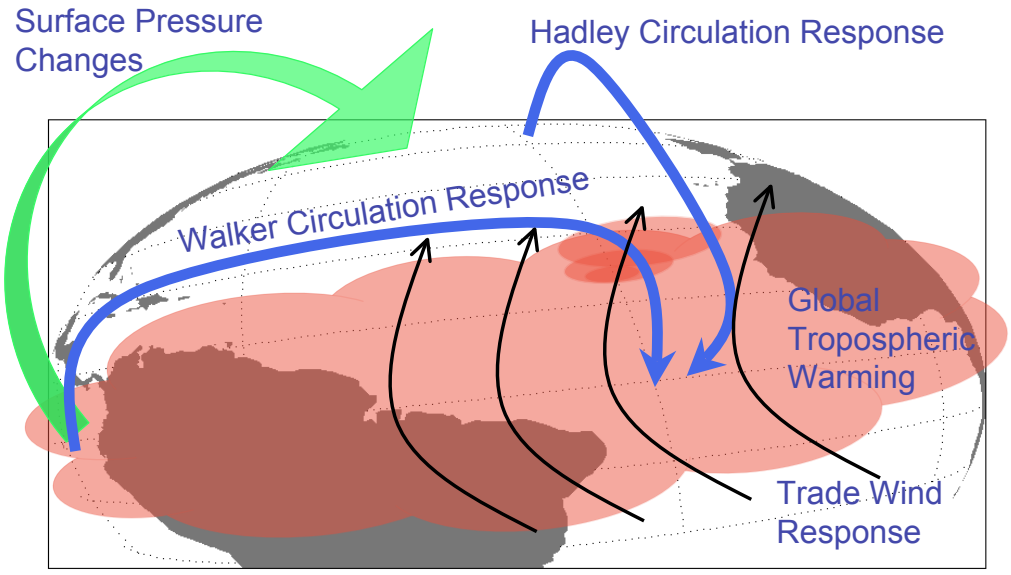

Fig. 2. A schematic of the influence of warm ENSO events on the tropical Atlantic.

that small SST anomalies grow to reach observed amplitudes through amplification by the thermodynamic Wind-Evaporation-Sea Surface Temperature (WES) feedback (Enfield and Mayer, 1997; Xie and Carton, 2004). However, only a weak response associated with the WES feedback is observed over the equatorial south tropical Atlantic (Enfield and Mayer, 1997). The mid-latitude north Atlantic's response to ENSO is also believed to be affected by positive feedbacks between the ocean and the atmosphere (Lau and Nath, 1996). Here, the role of the WES feedback in generating a tropical Atlantic response to ENSO is investigated.

5. Response of the Tropical Oceans to High Latitude Cooling

The tropics have been known to actively influence the extra-tropics by transporting heat to solar radiation-starved higher latitudes by oceanic advection and atmospheric heat transport mechanisms. Recent interest has grown over the possibility of higher latitude climate change forcings impacting the tropics. Studies have particularly focused on the impact of high latitude cooling on the tropics, as that associated with the Last Glacial Maximum (LGM) and Heinrich events, when the Atlantic Meridional Overturning Circulation (AMOC) is believed to be weaker than the current state (for e.g. Manabe and Broccoli, 1985; Broccoli, 2000; Chiang et al., 2003; Chiang and Bitz, 2005; Cheng et al., 2007; Dahl et al., 2005; Dong and Sutton, 2002; Vellinga and Wood, 2002; Zhang and Delworth, 2005).

A weaker AMOC does imply a weaker poleward ocean heat transport by advection, but it alone cannot explain the accompanying cooling that is observed in the entire northern hemisphere (Seager et al., 2002). The atmosphere, which is a more potent transporter of heat, has been proposed to be the stronger tele-connection medium for global impacts of AMOC slowdown (Dong and Sutton, 2002; Seager et al., 2002). However, since sea-ice formation is sensitive to ocean heat transport (Thorndike,

1992), a weaker AMOC is responsible for the initiation of sea-ice formation in the North Atlantic and an increased ice cover due to ice-associated feedbacks, causing further cooling (Maykut and Untersteiner, 1971) over the North Atlantic. In addition to AMOC changes, small changes in surface wind-stress over the sea-ice edge, have been shown to cause rapid changes in sea-ice coverage (Gildor and Tziperman, 2003; Kaspi et al., 2004). As had long been proposed (Dansgaard et al., 1989; Alley et al., 1993; Broecker, 2000; Denton et al., 2005), these changes in sea-ice have then been shown in Global Climate Models (GCMs) (Li et al., 2005) to influence dominantly the climate of entire high and mid-latitudes via atmospheric heat transports, consistent with the paleo-climate records of Greenland, particularly explaining the warming episodes known as the Dansgaard-Oeschger events (Dansgaard et al., 1993) during the last glacial period (50-10 kyr BP).

Also, paleo-climate observational studies correlating tropical proxy records (e.g. Peterson et al., 2000; Kennett and Ingram, 1995) with Greenland ice-core records (Stuiver and Grootes, 2000) have indicated that during cold events in the northern high latitudes, the ITCZ moved southwards and exhibited more symmetry about the equator (Lynch-Stieglitz, 2004). GCM studies that simulate the climate response to AMOC slowdown simulated by large freshwater input into the sub polar North Atlantic (Broccoli, 2000; Vellinga and Wood, 2002; Dahl et al., 2005; Stouffer et al., 2006; Timmermann et al., 2005; Cheng et al., 2007), or to imposed northern hemisphere LGM land and sea-ice conditions (Chiang et al., 2003; Chiang and Bitz, 2005) also note a robust cooling of the entire northern hemisphere, in addition to a southward migration of the ITCZ and the associated development of a cross-equatorial SST gradient (CESG). The altered Hadley circulation associated with the shift in ITCZ dries the northern hemisphere in the simulations, hence causing cooling due the reduction of the greenhouse water vapor (Chiang and Bitz, 2005). The southern extratropics

exhibit a tangible warming in response to AMOC shutdown in most studies (e.g. Vellinga and Wood, 2002; Dahl et al., 2005; Zhang and Delworth, 2005). This hemispherically asymmetric response of GCMs, when forced with LGM conditions, has been known for a while (Manabe and Broccoli, 1985), but the search for responsible mechanisms has gained interest only recently.

Atmospheric GCMs (AGCMs) coupled to both static ocean models (Chiang et al., 2003; Chiang and Bitz, 2005) or dynamic ocean models (Vellinga and Wood, 2002; Zhang and Delworth, 2005; Cheng et al., 2007; Stouffer et al., 2006) exhibit tropical responses similar to each other when forced with changes in high latitudes, suggesting possible oceanic as well as atmospheric tele-connection mechanisms. Oceanic Kelvin and Rossby waves originating in the Atlantic generated from the AMOC slowdown have been proposed to propagate to the Atlantic (e.g. Kawase, 1987; Yang, 1999) and into the tropical Pacific via the Indian ocean affecting the equatorial pacific thermocline depth and the El Niño Southern Oscillation (ENSO) phenomenon (e.g. Huang et al., 2000; Cessi et al., 2004; Timmermann et al., 2005). There is more oceanic teleconnection than just the oceanic wave mechanisms. Chang et al. (2008) is an example who find that the interaction between the thermohaline circulation and the wind-driven tropical circulations cause changes in the African Monsoon. Chiang et al. (2003); Chiang and Bitz (2005) find that just the thermodynamic coupled interaction between the atmosphere and the upper ocean can act as a mechanism for the communication between the high latitudes and the tropics within a short period of five years as compared to the decadal length time-scales associated with oceanic tele-connection. Northward atmospheric heat transport by the altered Hadley circulation transporting heat from the southern tropics to the northern hemisphere and transient and stationary eddies over the mid-latitudes - caused by the increased temperature gradient between the poles and the tropics, in AMOC slowdown or imposed

ice simulations have also been suggested (Cheng et al., 2007; Broccoli et al., 2006).

Over the Atlantic, experiments of Chiang et al. (2003) with an atmospheric GCM thermodynamically coupled to a slab ocean model (SOM) lead them to suggest that the north high latitude forcing would cause a meridional mode response over the tropical Atlantic. Their argument being that the meridional mode in the current climate is the preferred mode of response to external forcings like NAO and ENSO (Kushnir et al., 2002; Seager et al., 2000; Xie and Tanimoto, 1998; Czaja et al., 2002), both of which first initiate changes in the north Atlantic similar in effect to changes associated with high latitude cooling. Chiang et al. (2003) also find that thermodynamic interactions are largely responsible for the meridional mode response of the tropical response, with a GCM forced with prescribed LGM SSTs not being able to generate the response. Chiang and Bitz (2005) further propose that once the high latitude cooling signal reaches the northern tropics, further southward propagation over global oceans is carried out by the WES feedback, which is also the leading proposed mechanism of the meridional mode over the Atlantic (Chang et al., 1997; Servain et al., 1999). Mechanisms associated with the ITCZ, like deep convection-SST positive feedback, changes in humidity, high cloud cover, along with the WES feedback are further proposed to be responsible for the southward propagation of the ITCZ, and the development of a cross-equatorial SST gradient (CESG) with cooling in the northern side and warming in the southern side (Chiang and Bitz, 2005).

In the response of the tropics to cooling at higher latitudes, the WES feedback as proposed by Xie and Philander (1994) works as follows in the deep tropics: An initial southward CESG would result in the development of a northward pressure gradient due to hydrostatic adjustment (Lindzen and Nigam, 1987) generating southward wind anomalies. The induced wind anomalies would however, turn westwards (eastwards) in the northern (southern) side of the equator due to the Coriolis force, exhibiting

a C-shaped profile, adding to the background north-easterly (south-easterly) winds to increase (decrease) the wind speed locally. The increased (decreased) winds on the northern (southern) side increase (decrease) the latent heat flux release from the oceans to the atmosphere, cooling (warming) the SSTs and further amplifying the initial CESG forming a positive feedback. The ITCZ follows the warming SSTs in the southern side migrating southwards. A new steady state is reached by the balancing effect of the convective cloud - SST negative feedback with cooler SSTs in the northern side, warmer SSTs on the southern side and a more symmetric ITCZ (Chiang and Bitz, 2005) as mentioned earlier. A manifestation of the WES feedback as proposed by Chiang and Bitz (2005), active in the trade wind region when cooling occurs in the high and mid-latitudes works as follows. When the mid-latitude cold SST 'front' reaches the trade wind region, it induces a northward pressure gradient that generates easterlies in the trade wind region south of the 'front', which add on to the background easterly winds, increasing latent heat release from the oceans and cooling the mixed layer immediately south of the front, hence propagating the front southwards into the deep tropical northern oceans.

Unlike the Atlantic, the response over the tropical Pacific is not robust across various GCMs in response to a slowdown of the AMOC. As noted by Xie et al. (2008), in some fully coupled models, the eastern tropical Pacific demonstrates an equatorially asymmetric pattern (Vellinga and Wood, 2002; Zhang and Delworth, 2005), while in others a zonally asymmetric response both in the El Niño mode (Dong and Sutton, 2002) and the La-Niña mode (Wu et al., 2007) is observed . In the AGCM coupled to the SOM model of Chiang and Bitz (2005), the strongest ITCZ southward displacement in response to imposed high latitude ice is seen in the tropical eastern and central Pacific. However, in an AGCM-SOM experiment of Zhang and Delworth (2005), where northern Atlantic cooling is emulated by ocean heat flux adjustments

in the northern high latitudes, the response in the tropical Pacific is much weaker.

In addition to the thermodynamic WES mechanism, mentioned above, propagating cold anomalies from the high latitude Pacific to the tropical Pacific (Chiang and Bitz, 2005) and shifting the ITCZ southwards, other atmospheric and oceanic tele-connection mechanisms have been suggested. Timmermann et al. (2007) find that increased northeasterly trade winds across the central American isthmus, caused by WES mechanism over the deep tropical Atlantic in response to a weakened AMOC, causes cold SST anomalies in the north eastern tropical Pacific, which could again be amplified by the deep tropical WES feedback mechanism, and Ekman pumping generating an anomalous CESG over the eastern tropical Pacific and causing the ITCZ to move southwards. Since the tropical Pacific annual cycle is closely tied with the northward location of the ITCZ over the eastern tropical Pacific (Xie, 1994), a southward displacement of the ITCZ due to northern high latitude cooling causes a change in the mean state/annual cycle of the tropical Pacific, which is proposed to intensify ENSO by non-linear frequency entrainment (Timmermann et al., 2007). On the other hand, ocean wave dynamics and baroclinic adjustment cause a weakening of ENSO due to the decrease in the thermocline depth of the equatorial eastern Pacific on decadal time-scales (Timmermann et al., 2005). Xie et al. (2008) note that in simulations where the ITCZ shifts southwards, the intensification of ENSO caused by a reduced annual cycle over the eastern equatorial Pacific is strong enough to overcome the weakening caused by the oceanic tele-connection as is seen in the response of several AGCMs to a weakened AMOC (Timmermann et al., 2007).

While other boundary conditions like ice-topography, greenhouse gases and orbital forcings are important for the zonal response of high and mid-latitudes to cooling in GCMs' high latitudes (Seager et al., 2002; Cheng et al., 2007), Chiang et al. (2003) found that the effect of high latitude ice albedo is dominant over other boundary

conditions and external forcings associated with the LGM in generating the tropical responses to high latitude cooling. In addition, Chiang and Bitz (2005) found that adding LGM land-ice and sea-ice anomalies separately over the high latitudes in two different runs of the GCM produced similar responses at the tropics, suggesting a climate response independent of the longitudinal placement of the forcing and similar mechanisms in action under the two forcing scenarios. In this study, only the impacts of additional sea-ice on the tropics are focused upon, with the expectation that the effect of additional land-ice would be similar.

B. Approach

Since its formal introduction by Xie and Philander (1994), the WES feedback has been hypothesized to contribute significantly to tropical climate variability in many studies as discussed above. In these observational and modeling studies, the existence of the WES feedback is suggested by correlated and co-varying patterns of SSTs, surface heat fluxes and winds (e.g. Carton et al., 1996; Chang et al., 1997; Saravanan and Chang, 2000). Hierarchical modeling studies (e.g. Lau and Nath, 1996, 2001; Saravanan and Chang, 2000; Chang et al., 1997), where an atmospheric GCM is first forced using SSTs as boundary conditions and then compared to a coupled atmosphere-ocean model also suggest the existence of feedbacks in the atmosphere-ocean system manifested as the increased variance of the coupled model. Another approach is to force an ocean model with climatological wind stress forcing and monthly forcings separately, to identify a role of thermodynamic interactions over SST (Carton et al., 1996). However, these studies do not directly implicate the WES feedback but rather only the cumulative effect of all atmosphere-ocean feedbacks, which include reduced thermal damping (Barsugli and Battisti, 1998), thermodynamic mixed layer feedback (Sara-

vanan and Chang, 1999), the stratus cloud-SST negative feedback (Philander et al., 1996) and the ITCZ convective clouds and SST feedback (Tanimoto and Xie, 2002). While most studies invoking the WES feedback to explain a physical mechanism are supported by strong theoretical arguments, few explicitly demonstrate the presence of the WES feedback. The goal of this investigation is to identify and quantify the role of the WES feedback in tropical climate variability in a full physics atmospheric GCM coupled to a slab ocean model. The role of the WES feedback is isolated by performing simulations where the WES feedback is literally switched off, and comparing the results with those of a control run.

Here the role of the WES feedback in the low frequency variability of the Atlantic is studied using an atmospheric Global Climate Model (GCM) - NCAR Community Climate Model (CCM3) coupled to a Slab Ocean Model (SOM). In addition to the standard control runs of CCM3-SOM model, simulations, termed as WES-off, are carried out with the WES feedback turned off by modifying the bulk aerodynamic formulations of surface sensible and latent heat fluxes over the oceans. The SOM is a static ocean model interacting with the atmospheric model only thermodynamically, allowing us to focus on thermodynamic processes like the WES feedback. The lack of ocean dynamics in the SOM prevents the balancing of the WES feedback by oceanic circulation. Instead, steady state solutions are reached by a balance between the WES feedback and the non-linearities of the atmospheric model like the minimum wind speed requirement for the calculation of surface sensible and latent heat fluxes and the convective cloud SST feedback (Xie, 1996). An oscillatory mechanism of the tropical Atlantic, which depends on transport of SST anomalies by ocean circulation as found in modeling studies of Chang et al. (2001), Huang and Shukla (1997) and Xie (1999), is not expected to exist in such a model set-up. An analysis of CCM3-SOM, however, still allows for the study of variability associated with the WES feedback. The role

of the WES feedback in free tropical variability and in tropical Atlantic forced by the remote influence of ENSO is investigated here. The NAO is also believed to influence the tropical Atlantic, however recent studies find little impact of the NAO on the tropical Atlantic (e.g. Ruiz-Barradas et al., 2000; Rajagopalan et al., 1998). Hence, here we consider the NAO to be a part of intrinsic free tropical Atlantic atmospheric variability in CCM3, and not as an external forcing. CCM3-SOM imposed with anomalous sea-ice is further applied to clearly identify the role of the WES feedback in the propagation of cold anomalies from the higher latitudes to the tropics.

The rest of the dissertation is structured as follows. A brief description of CCM3-SOM, along with a description of the procedure carried out to switch off the WES feedback in WES-off simulations, follows in chapter II. Chapter III demonstrates the role of the WES feedback as evident from comparative analysis of WES-off runs and control runs in free tropical variability including the westwards propagating oceanic equatorial annual cycle and the Atlantic meridional mode. Further, the role of the WES feedback in forced tropical variability as that associated with the response of tropical Atlantic to ENSO, and the response of tropical oceans to high latitude sea-ice forcing are detailed in chapter IV. The results of the study are finally summarized in chapter V.

CHAPTER II

MODEL SET-UP

Our basic model is the NCAR-Community Climate Model (CCM3), an atmospheric general circulation model (Kiehl et al., 1998) coupled to a static Slab Ocean Model (SOM) with spatially varying but temporally constant ocean mixed layer thickness. The mixed layer thickness is based on observations and is shown in Figure 3. The model integrations are conducted at a triangular spectral resolution of T42, equivalent to a horizontal resolution of about 2.81° x 2.81°. We use the older CCM3 as compared to the complex and newer Community Atmospheric Model (CAM3) as the former has a better throughput than latter, and also because the improvements in CAM3 as compared to CCM3 are not important for this mechanistic study.

Varying sea-ice in climate models increases the sensitivity of the model, and require longer spin-up times. Also, small perturbations of sea-ice in higher latitudes, as seen in the current climate, have little impact on the atmosphere of the tropical regions, the region of focus of this study. Hence, for further computational efficiency, CCM3 used in this study is modified such that the sea-ice in the model is non-interactive, and is prescribed for all experiments. The SOM interacts with the atmospheric model only thermodynamically. The changes in the ocean mixed layer temperature, which is the same as the SST, is caused only by changes in the surface heat fluxes, with the thermal inertia of the ocean being proportional to the ocean depth. The lack of ocean dynamics, although not realistic, clearly isolates thermodynamic air-sea interactions. The lack of heat transport by the ocean circulation is corrected by artificially adding heat fluxes, namely Q-fluxes, to the mixed layer at model ocean grid points (Kiehl et al., 1996) so that the model follows the monthly mean SST climatology as follows:

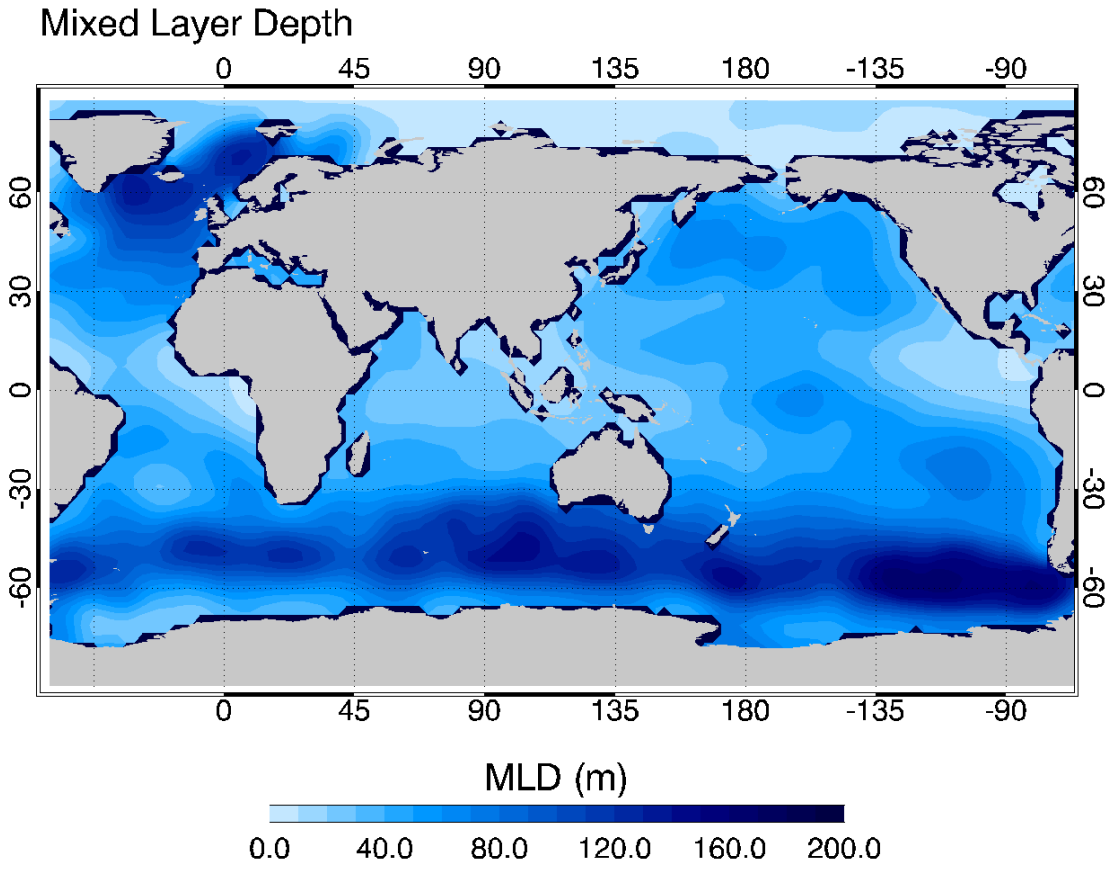

Fig. 3. Spatial distribution of the ocean mixed layer depth used in the Slab Ocean Model.

$$\rho_w C_w h_w \frac{\partial T}{\partial t} = F + Q \tag{2.1}$$

where, ρ_w is the density of sea water, C_w is the specific heat capacity of sea water, h_w is the mixed layer depth, T is the SST at the grid point, F is the net ocean surface heat flux and Q is the corrective heat flux. In the CCM3-SOM setting, the monthly climatology of F is derived from a stand-alone CCM3 run forced with fixed monthly SST climatological boundary conditions. The monthly mean Q-flux is then computed as (Kiehl et al., 1996):

$$Q^n = \rho_w C_w h_w \frac{T^{n+1} - T^{n-1}}{d^{n+1} - d^{n-1}} - F^n \tag{2.2}$$

where, T^n is the climatological monthly mean SST for month n, d^n is the number of days in month n, F^n is the monthly mean climatology of net surface flux into the ocean for month n computed from the stand-alone CCM3 simulation. The derived Q^n from the equation above is thus the climatological monthly mean corrective heat flux used by CCM3-SOM.

The latent and sensible heat fluxes over the ocean surface in CCM3 are computed via bulk aerodynamic formulations, which incorporate the stability of the atmosphere and turbulent scales in exchange coefficients (Kiehl et al., 1998). The bulk formulations can be simplified for our purposes here as:

$$Q_{lh} = - \; u^* \; \Delta q \; C_e \; \rho \; L_{vap} \tag{2.3}$$

$$Q_{sh} = - \; u^* \; \Delta T \; C_d \; \rho \; C_p \tag{2.4}$$

where, Q_{lh} and Q_{sh} are the latent and sensible heat fluxes defined to be positive for an upwards transfer from the ocean to the atmosphere, u^* is a product of the wind

speed at the lowest atmospheric level and a neutral momentum exchange coefficient, Δq is the difference $(q - q_s)$ in the specific humidity (q) of the lowest atmospheric surface and the surface saturation specific humidity (q_s) and C_e is a neutral tracer exchange coefficient, ΔT is the difference $(T_a - T_s)$ in the potential temperature of the lowest atmospheric surface (T_a) and the ocean surface temperature (T_s), C_d is a neutral heat exchange coefficient, ρ is the density of air at the lowest atmospheric surface, C_p is the specific heat capacity of moist air and L_{vap} is the latent heat of vaporization of water. Positive values of Q_{lh} and Q_{sh} imply upwards flux.

The surface latent and sensible heat fluxes are related to the winds through these parameterizations. In addition to control runs using the standard CCM3-SOM model, we carry out WES-off runs where we suppress the effect of winds on surface fluxes by prescribing u^* for the computation of surface heat fluxes in CCM3. CCM3 is modified to read in prescribed values of u^* and use them to compute the surface fluxes instead of the model generated u^*. This suppression of the effect of fluctuations in the winds on surface fluxes eliminates the feedbacks between winds and surface fluxes, namely the WES feedback. In such a set-up, while anomalies in SSTs would still be influencing the winds, the model wind anomalies would have no direct impact on the latent and sensible heat fluxes and hence the SSTs, thus breaking the WES feedback loop. The prescribed monthly-averaged u^* climatology is computed from the control CCM3-SOM integration and is used to force the modified CCM3. The use of the control run u^* climatology in the modified CCM3 simulation ensures similar climate mean states in the control run and the WES-off run, to first order. However, non-linearities in equations 2.3 and 2.4 involving anomalies of u^*, Δq, and ΔT can potentially induce deviations in the WES-off mean climate state. To ensure similar climate mean states for the control runs and the perturbed runs, heat flux adjustments, referred to as Q-flux as described in the next section, are applied.

Hereafter, the control run is referred to CCM3-SOM integration and the modified run is named as the WES-off-SOM integration. The analyses of these runs presented in the following section, which compare mean state of the two integrations, and subsequent chapters are based on 70 years of integration of both versions of the model after discarding the first five years of run as spin-up time. All of the model integrations carried out for this study are listed with their names and a brief description in Table I.

A. Model Mean-State

A Q-flux adjustment following Kiehl et al. (1996) was performed to ensure that surface heat flux between the control run and the perturbed WES-off-SOM run would be the same. This also causes the resulting SST field in the two integrations to be close to each other over the tropics. Q-fluxes for the CCM3-SOM integration are computed from observational SST using the method (Kiehl et al., 1996) described in the previous section. The simulated annual mean SST and ocean surface latent heat fluxes in CCM3-SOM are shown in Figure 4. Surface winds and convective precipitation as simulated by CCM3-SOM are also shown in Figure 5. The simulation is found to be fairly realistic and consistent with other CCM3 studies (Hurrell et al., 1998; Saravanan, 1998).

Q-fluxes for the WES-off-SOM run are computed as follows. First, the modified CCM3 is integrated in a stand-alone mode with the prescribed CCM3-SOM generated SST climatology, computed from 30 years of the control run. The modified stand-alone CCM3 is also prescribed with control run CCM3-SOM generated u^* climatology in the boundary layer heat flux formulations. The climatology of the net surface fluxes is then computed from this stand-alone CCM3 integration. Q-fluxes for the perturbed

Table I. List of model integrations

Model Run	**Description**
CCM3-SOM	Control integration of CCM3 coupled to a Slab Ocean Model (SOM)
WES-off-SOM	Integration of the modified CCM3 coupled to the SOM with the WES feedback switched off
WES-off-NoANN	WES-off integration with prescribed annual mean u^* instead of u^* climatology
CCM3-SOM-ENSO	CCM3-SOM integration with prescribed SST in the tropical Pacific representing an ideal constant amplitude 4 year ENSO cycle
WES-off-ENSO	WES-off integration with prescribed SST in the tropical Pacific representing an ideal constant amplitude 4 year ENSO cycle
CCM3-SICE	CCM3-SOM integration with prescribed LGM sea-ice conditions in the northern high latitudes. 4 ensemble member runs were carried out.
WES-off-SICE	WES-off integration with prescribed LGM sea-ice conditions in the northern high latitudes. 4 ensemble member runs were carried out.

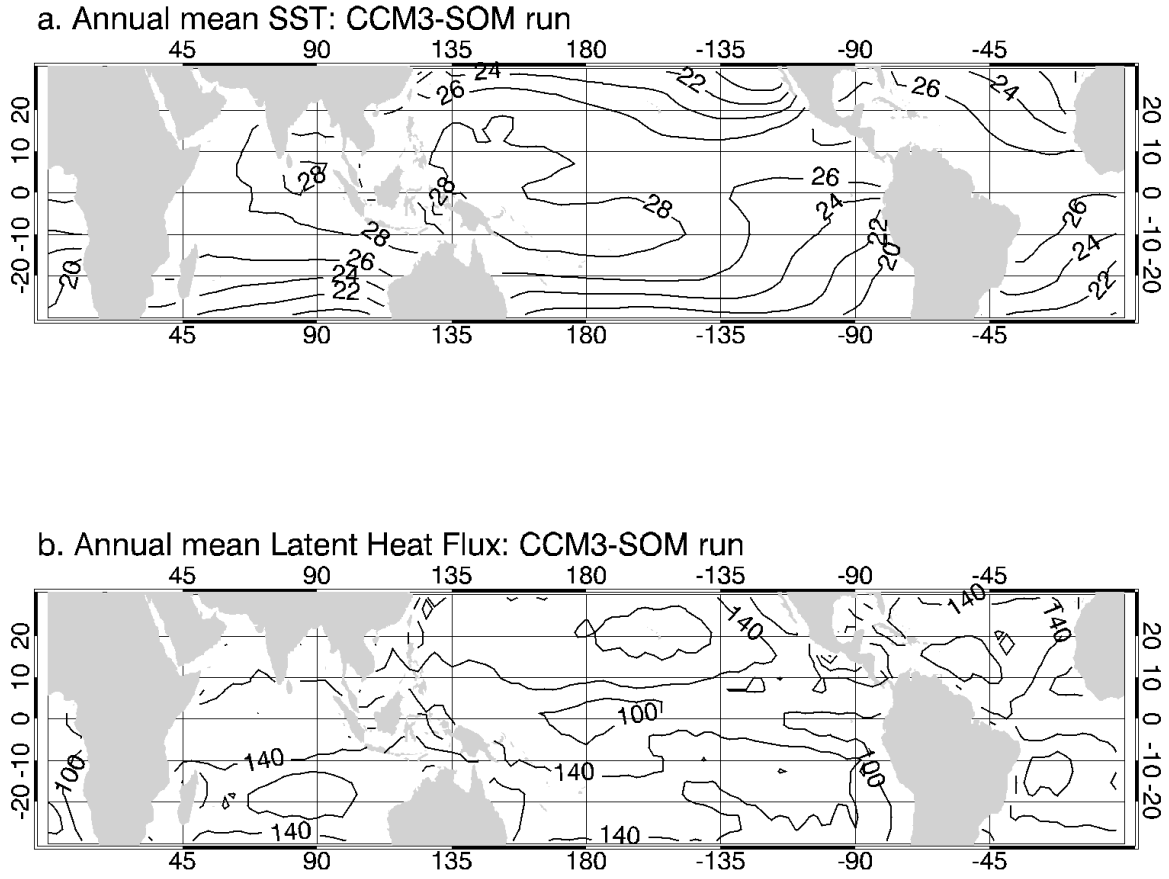

Fig. 4. Annual mean (a) SST (contour interval: 2 K) and (b) latent heat flux (contour interval: 40 W/m^2) as simulated in CCM3-SOM.

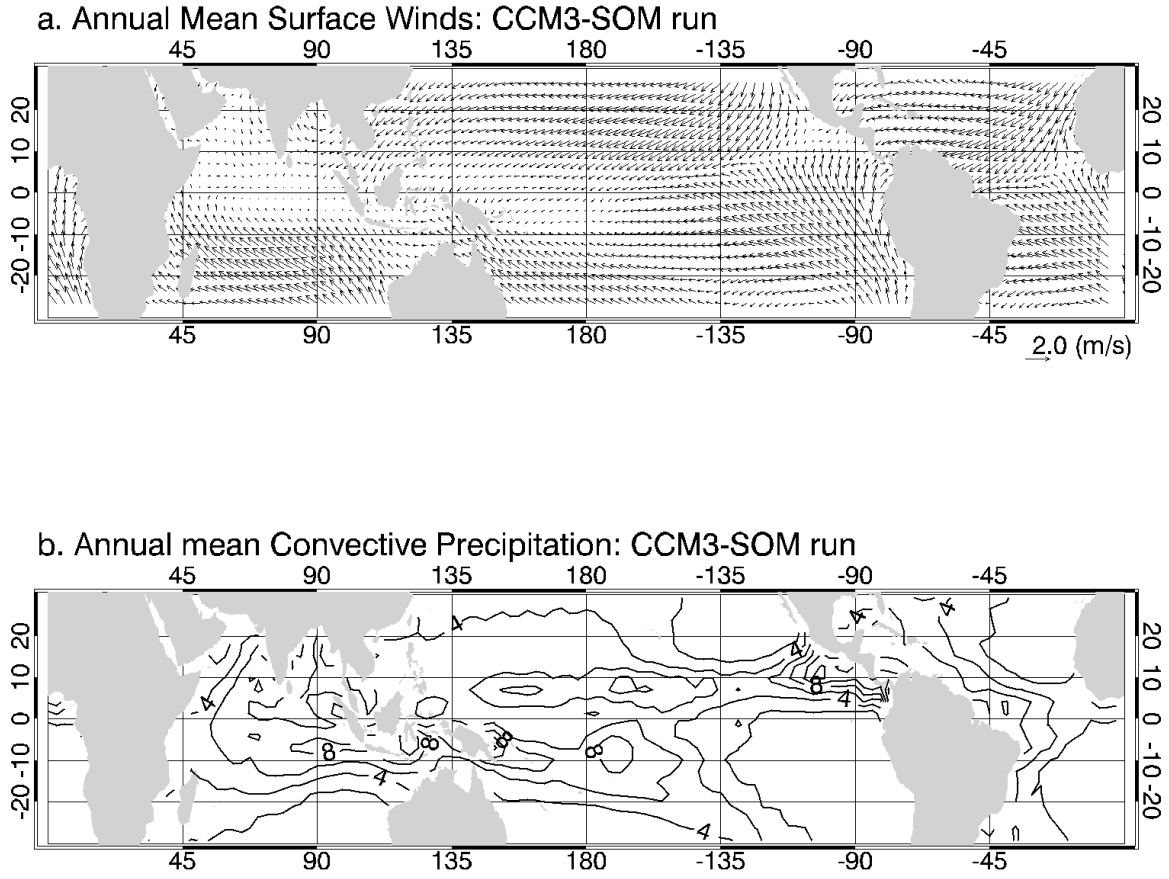

Fig. 5. Annual mean (a) surface winds and (b) convective precipitation (contour interval: 2 mm/day) as simulated in CCM3-SOM.

CCM3-SOM run are then computed using this climatology of surface fluxes to balance out to the control run CCM3-SOM SST climatology. Figure 6a shows the difference in the annual mean SST field between the control run and the WES-off-SOM run. Over the deep tropical oceans the SST fields between the two runs is about the same between 10°S to 10°N. Small warm biases of 0.6-0.8 K, probably arising from sampling errors, are seen in the eastern tropical Pacific, and southern tropical Indian ocean off the coast of west Australia in all seasons. Cold biases in the WES-off-SOM simulation are seen in the eastern tropical north Pacific off the coast of China, of about 0.2-0.4 K. The tropical Atlantic is essentially bias-free, with the climatology of the two simulations matching closely. Warm biases are also observed in the mid-latitudes (not-shown), but these are of little concern as they are likely to have little impact on the tropics.

Similarity in the Q_{lh} of the two integrations is also noted, as seen in Figure 6b, with a maximum difference of about 10 W/m^2. However, the same is not true for the mean winds. Figure 7a shows the change in the mean winds in the WES-off-SOM integration as compared to the control run for the winter season. Significant changes are observed in the deep tropical Pacific and the Indian oceans. The wind fields in the Atlantic ocean are found to behave similarly in the two integrations. A cross-equatorial C-shape profile of the difference in the wind fields is curiously suggestive of the role of the cross-equatorial WES feedback in the northern hemispheric winter and spring seasons, with weaker trade winds in the northern equatorial western Pacific and Indian oceans and stronger trade winds in the southern equatorial oceans in the WES-off-SOM experiment.

The substantial changes in the wind field in the WES-off-SOM run are puzzling, as the mild changes in the SST field could not cause such large changes in the mean field. A CCM3 integration forced with the climatological SST's obtained from the

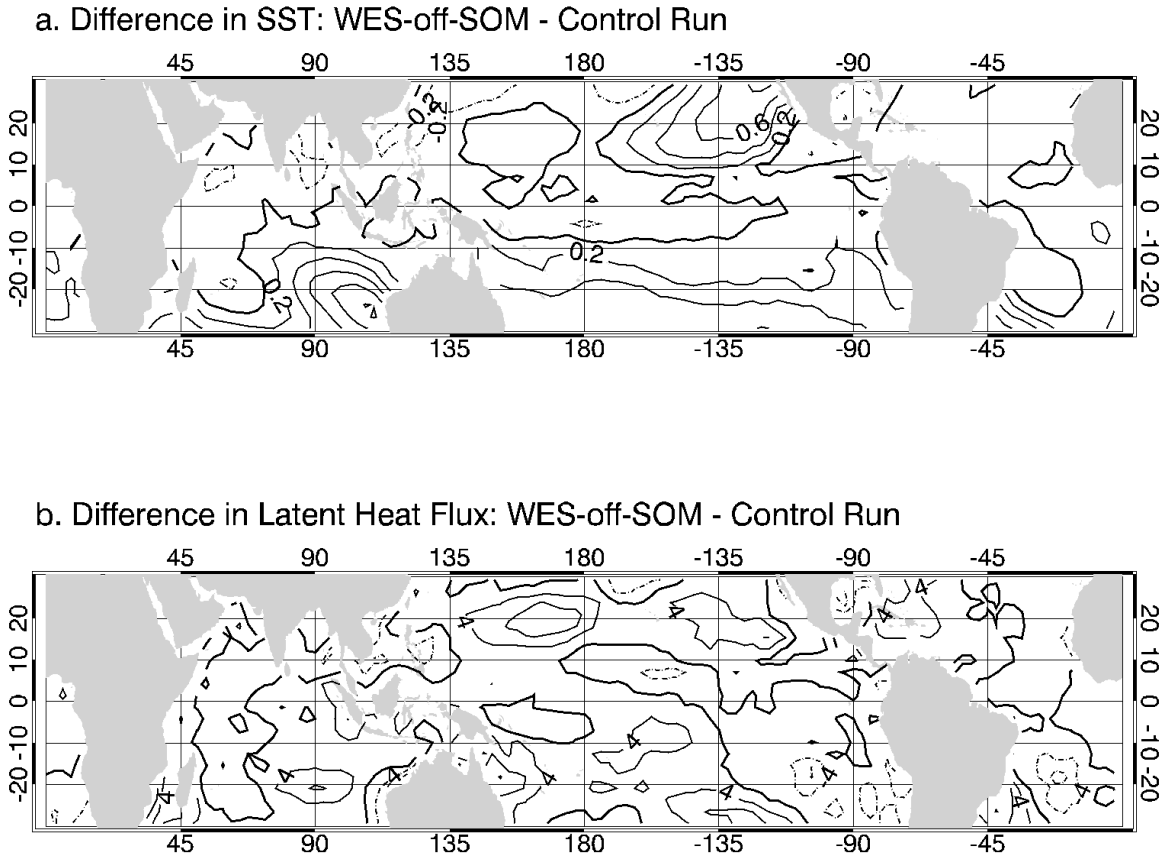

Fig. 6. Difference in annual mean **(a)** SST (contour interval: 0.2 K): WES-off-SOM - CCM3-SOM and **(b)** Q_{lh} (contour interval: 4 W/m^2): WES-off-SOM - CCM3-SOM.

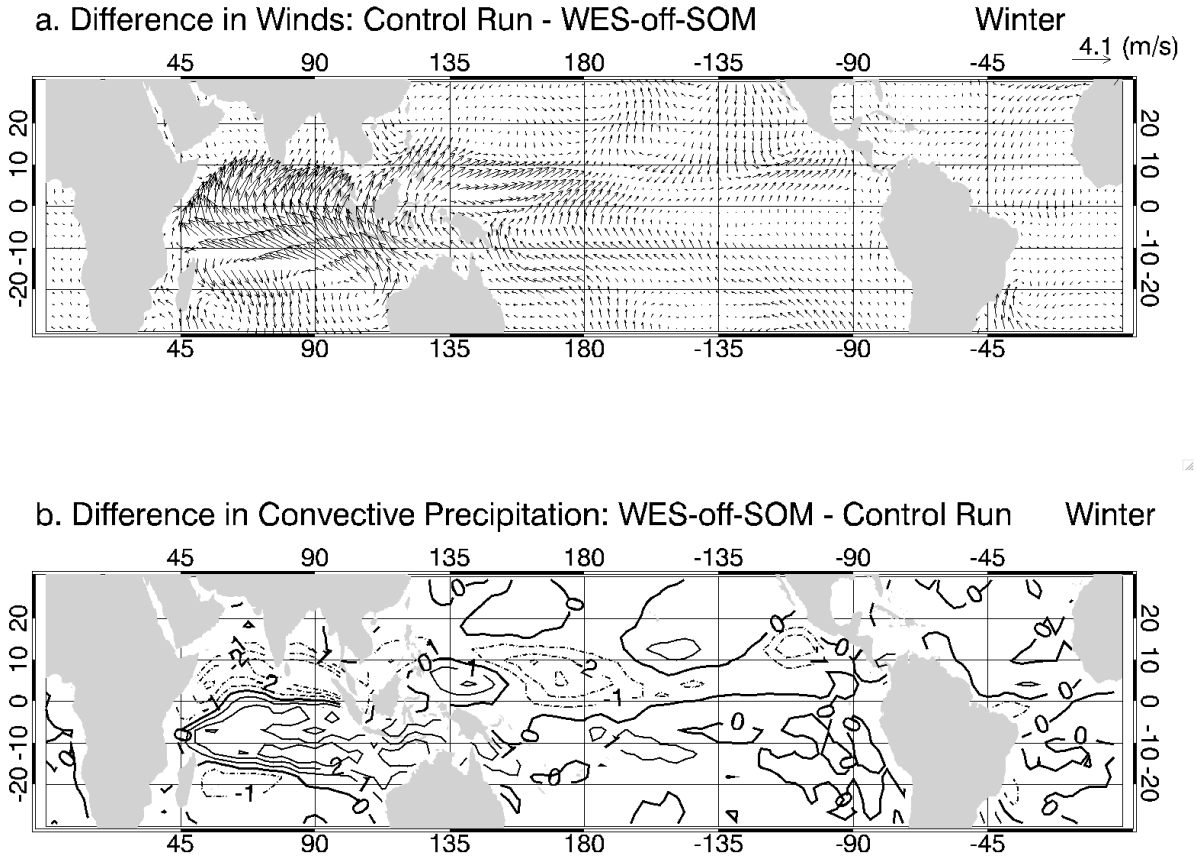

Fig. 7. Difference in mean boreal winter (December to February) **(a)** winds (m/s): CCM3-SOM - WES-off-SOM and **(b)** convective precipitation (contour interval: 1 mm/day): WES-off-SOM - CCM3-SOM.

WES-off-SOM integration supports that argument, where the response of winds do not match those seen in the WES-off-SOM runs (not shown). This demonstrates that the change in the winds is not due to any change in the SST climatology. Limiting the effect of the change of the wind speed on Q_{lh} by prescribing climatological u^* is somehow causing a change in the mean wind fields. The strong change in the response of the variability of various fields (section 3.B) could be a possible cause. However, a direct link between a change in variability to a change in the mean fields is not clear, and suggests non-linear behavior of winds in response to change in variability of other variables. Tropical winds are dominated by the regions of deep convection located on the ITCZ, where near surface convergence occurs. A change in the winds could hence be caused by changes to the ITCZ. However, the ITCZ does not simply force the winds, but also responds to the winds forming a feedback mechanism, hence making it difficult to identify the forcing mechanism for the observed change in the mean state.

Convective precipitation associated with the ITCZ demonstrates a change in the mean state too, being more symmetric in the WES-off-SOM integration in the winter (Figure 7b) and spring seasons over the Pacific and the Indian ocean, and in the summer season over the Atlantic ocean. While part of the change in the mean state of convective precipitation can be caused by the mild SST biases in the WES-off-SOM run as compared to the control run, the WES feedback also appears to be responsible. The change in the mean state of the winds associated with the lack of WES feedback prevents strong convergence from occurring north of the equator in the WES-off-SOM integration, reducing precipitation in the northern equatorial oceans and increasing precipitation in the southern equatorial oceans in the winter and spring seasons. The non-linear dependence of precipitation on SST is well known, with deep convection occurring beyond a certain SST threshold. Reduction of the variability of SST can

thus be a reason for a change in the mean of convective precipitation over the deep tropics as shown in section 3.3. A detailed analysis of the above is beyond the scope of this study and will be a subject of future investigations.

CHAPTER III

FREE TROPICAL VARIABILITY

Integrations of CCM3 coupled to a SOM are analyzed to explicitly identify the role of the WES feedback in the natural low-frequency variability of tropical oceans. After assessing the influence of winds, and hence potentially of the WES feedback, in tropical ocean climate variability in sections III.A and III.B, results of investigations of the proposed role of the WES feedback specifically in the equatorial annual cycle and the unforced meridional mode of the Atlantic are presented in sections III.C and III.D respectively.

A. Influence of Winds and Humidity on Surface Heat Fluxes

The bulk formulations in the GCM's of Q_{lh} and Q_{sh} involve not only the winds, but also humidity and temperature. The relative effect of winds on the heat fluxes can be compared by looking at the correlation between monthly mean fields of u^* and heat fluxes. Figure 8a displays the correlation between u^* and Q_{lh} after removal of the annual cycle from both the terms. A strong correlation (>0.8) observed over most of tropical oceans, particularly over the equatorial oceans, supports the possibility of the presence of WES feedback over most of the deep tropics, as hypothesized in other studies. Eastern equatorial Pacific and the eastern tropical Atlantic regions are however indicative of a lower correlation, suggesting a strong dependence of Q_{lh} on Δq in those regions. Figure 8b displays the correlation between Δq and Q_{lh} for the control CCM3-SOM integration. Not surprisingly, the plot indicates high negative correlations (<-0.6) between Δq and Q_{lh} over regions where u^* demonstrates low correlations with Q_{lh}. Over the central and western equatorial Pacific, western tropical Atlantic and equatorial Indian ocean, however, a positive correlation between

Δq and Q_{lh} is observed. An increase in Δq should cause a decrease in the release of latent heat flux from the ocean surface resulting from the sign convention of equation 1, suggesting negative correlations between the two, if Δq is the controlling term. Positive correlations between Δq and Q_{lh} are thus counter-intuitive, implying that u^* is the dominant term influencing the latent heat flux over those regions.

A positive correlation between u^* and Δq observed over all of the tropical oceans (Figure 9) suggests that while the terms oppose each other's effects on Q_{lh} in the region, they are not independent. While an increase in u^* causes an increase in Q_{lh}, associated increase in Δq causes a decrease in Q_{lh}, indicating that the two terms are damping each other's influence and introducing non-linearities in the system. Stronger correlations (>0.6) are observed in the Indian ocean, and western Pacific and Atlantic oceans, where Q_{lh} is controlled by u^*, and the damping by Δq is over-powered by the WES feedback. In the eastern Pacific and the Atlantic oceans, where the two terms have comparable influence on Q_{lh}, the correlations between the two are weaker indicating possible independent influences on Q_{lh}.

Figures 10a and b display the correlations of monthly mean fields of u^* and Q_{sh} and of ΔT and Q_{sh} respectively. High negative correlations (<-0.6) are observed between ΔT and Q_{sh} over the tropical oceans. Low positive correlations are observed between u^* and Q_{sh} in the deep tropical eastern and western Atlantic, while negative correlations are observed over most of the rest of the deep tropical oceans. The negative correlations between u^* and Q_{sh} are counter-intuitive as increase in wind speed should increase the sensible heat flux release from the ocean surface suggesting a positive correlation. The above correlations imply that u^* mostly impacts the Q_{lh} over the deep tropics, whereas temperature terms control Q_{sh}. Thus, the WES feedback is mainly governed by the impact of winds on the latent heat flux. High positive correlations between u^* and ΔT (Figure 11), which have opposing effects on Q_{sh},

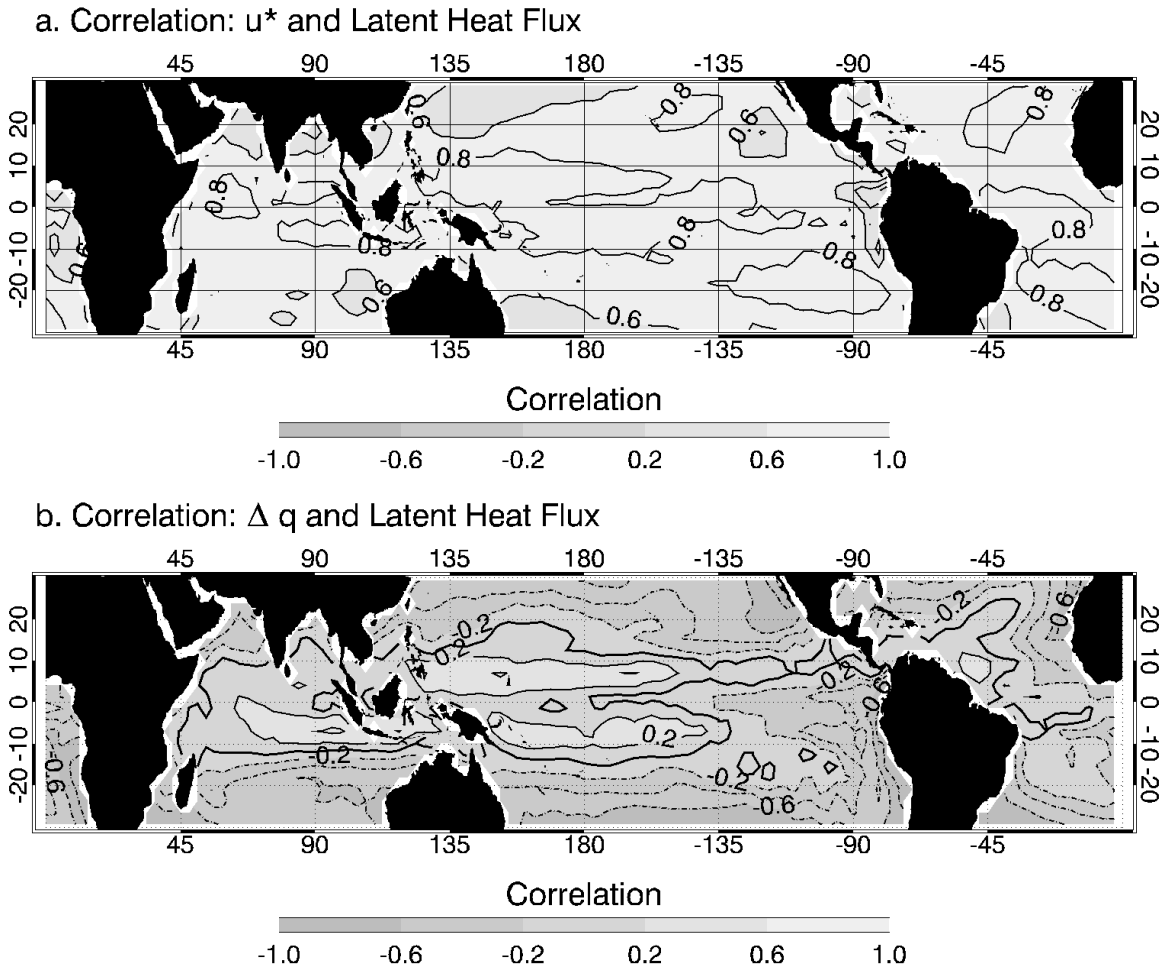

Fig. 8. Correlation (contour interval: 0.2) between monthly **(a)** u^* and Q_{lh} and **(b)** Δq and Q_{lh} for the control CCM3-SOM integration.

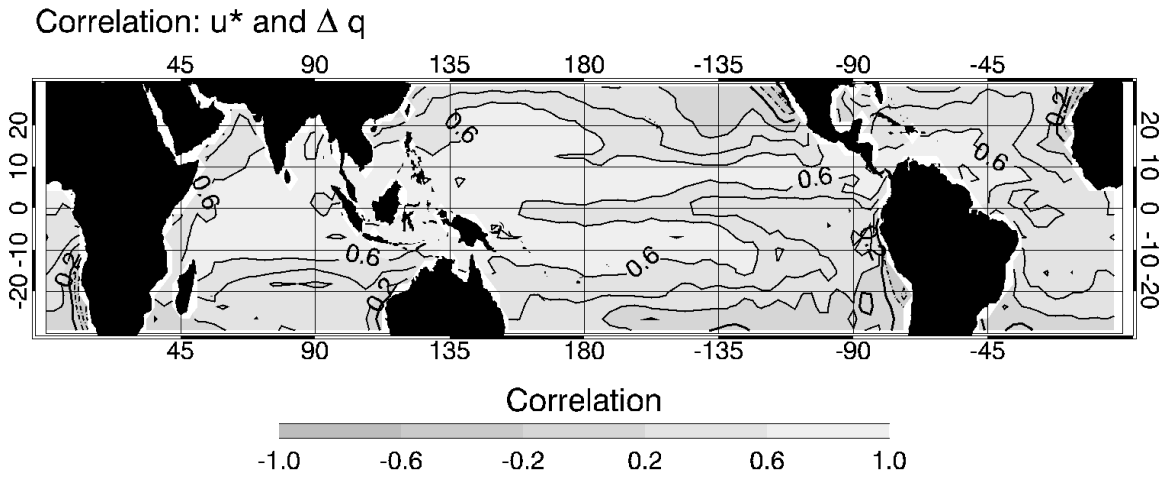

Fig. 9. Correlation (contour interval: 0.2) between monthly u^* and Δq for the control CCM3-SOM integration.

suggest a damping effect of winds on SST via Q_{sh} in the deep tropics. Weaker negative correlations between u^* and ΔT in subtropical north-eastern Pacific ocean off the north American coast and in the northern mid-latitude oceans suggest the presence of weak positive feedback mechanisms in the regions, where Q_{sh} is dominated by air-sea temperature differences (Figure 10a and Halliwell and Mayer, 1996; Alexander and Scott, 2002). The above results are consistent with the study of Alexander and Scott (1997) who found greater impact of humidity and temperature difference variations in the northern mid-latitudes than wind speed on the ocean-atmosphere latent and sensible heat flux anomalies respectively in a GFDL atmospheric GCM simulation. They conducted a partitioning of the contributions of individual anomalous components $u^{*'}$, $\Delta q'$, and $\Delta T'$ on the heat flux anomalies based on regression analysis in the northern oceans using daily output.

The correlation between Q_{lh} and Δq, and u^* and Δq indicates a non-linearity in the relationship between winds, Q_{lh} and SST via humidity affecting the WES feedback. This is only implicit in other studies (Xie, 1996; Chang et al., 1997). Consider the development of an anomalous cross-equatorial northward SST gradient. Along with generating a southward pressure gradient in the region, there would also be an increase (decrease) in the surface saturation humidity in the northern (southern) side. The increase in q_s increases the evaporation in the region, assuming that the specific humidity of the boundary layer does not change, causing greater release of latent heat from the ocean surface, cooling the SST, thus acting as a damping to the anomalous SST development and working as a negative feedback. The development of the anomalous pressure gradient drives cross-equatorial northward winds that turn right in the southern side and left on the northern side due to Coriolis force diminishing (enhancing) on to the background trade winds on the northern(southern) side. One of these two effects dominates, leading to either a positive or negative feedback.

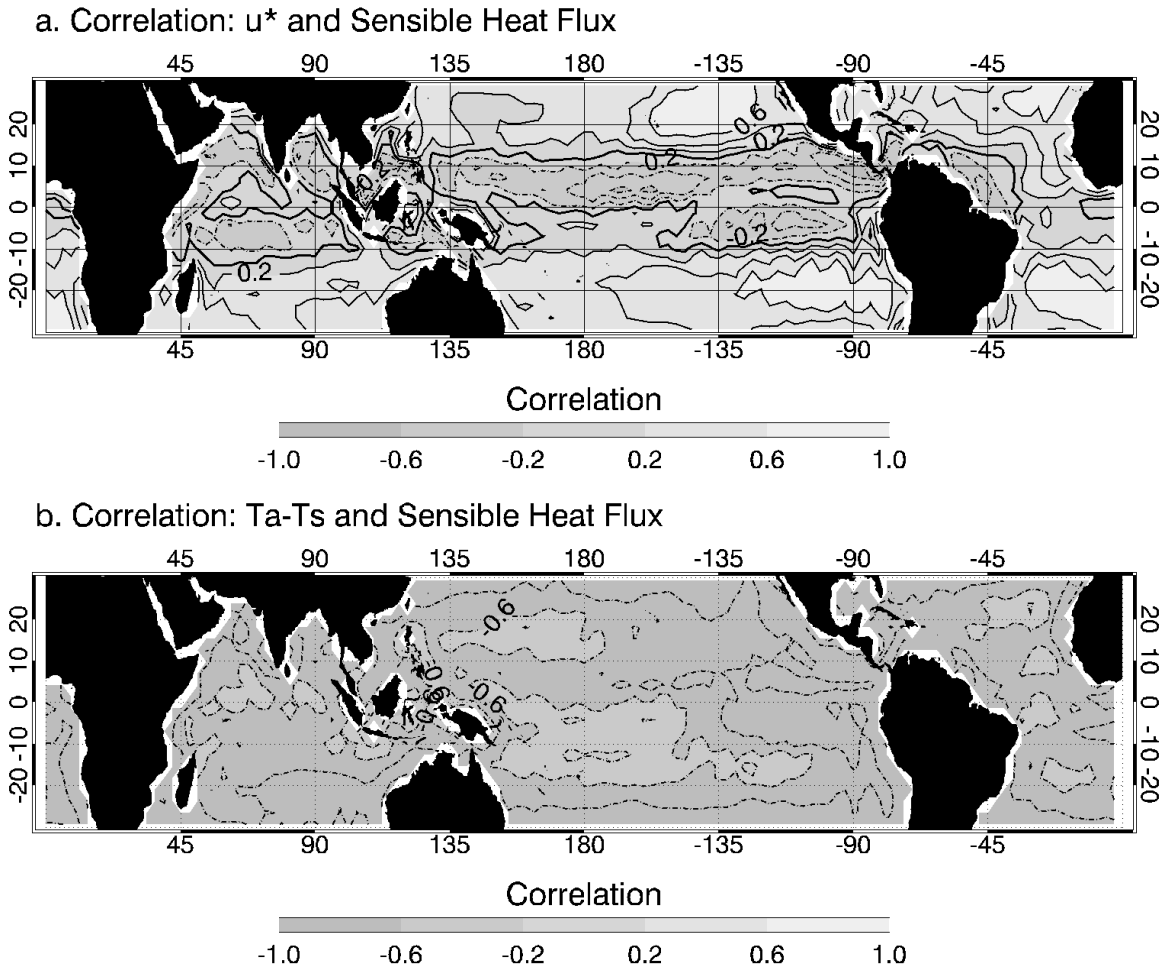

Fig. 10. Correlation (contour interval: 0.2) between monthly **(a)** u^* and Q_{sh} and **(b)** $T_a - T_s$ and Q_{sh} for the control CCM3-SOM integration.

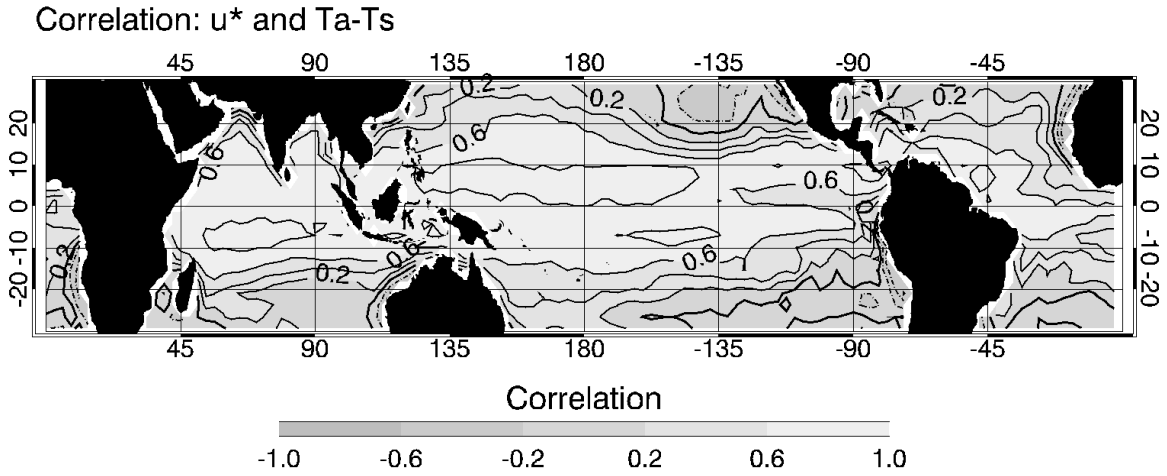

Fig. 11. Correlation (contour interval: 0.2) between monthly u^* and $T_a - T_s$ for the control CCM3-SOM integration.

The magnitude of each of these terms depends on the mean state and their anomalies. The anomalous Q_{lh} could be partitioned as:

$$Q_{lh}^{'} = -(u^{*'}(\overline{\Delta q}) + \overline{u^{*}}(\Delta q)^{'} + (u^{*'}(\Delta q)^{'} - \overline{u^{*'}(\Delta q)^{'}}))\ B \tag{3.1}$$

where, the primes denote the monthly anomalies and the bars denote climatological means and B represents the climatological values of $C_e \rho L_{vap}$. The terms $u^{*'}(\Delta q)^{'}$ and $\overline{u^{*'}(\Delta q)^{'}}$ are found to have much smaller magnitudes as compared to the other two terms over the tropics. The same was found for the north Atlantic by Alexander and Scott (1997). Neglecting those terms yields:

$$Q_{lh}^{'} \approx -(u^{*'}(\overline{\Delta q}) + \overline{u^{*}}(\Delta q)^{'})\ B \tag{3.2}$$

For the WES feedback to be active in a region, the term $u^{*'}(\overline{\Delta q})$ needs to be dominant. In such a region, an initial development of, say, positive SST anomalies, causes negative $u^{*'}$, reducing the Q_{lh} and resulting in an increase in the anomalous SST. The anomalous SST also causes an exponential increase in anomalous q_s via the Clausius-Clapeyron equation, while the relation between u^* and SST is broadly linear (Lindzen and Nigam, 1987). While $u^{*'}(\overline{\Delta q})$ dominates, $q_s^{'}$ grows with the SST, causing the damping to also grow exponentially, ultimately over-powering the wind anomaly term, breaking the WES feedback. Figure 12 shows the regression of the two terms in equation (4) against normalized changes in $Q_{lh}^{'}$. In agreement with the correlations (Figure 8), a dominance of fluctuations of u^* is observed over the tropical central and western Pacific, Indian Ocean and the western Atlantic, suggesting a strong WES feedback in these regions. Over the eastern tropical Pacific and Atlantic, the two terms have comparable magnitudes, suggesting a stronger damping by humidity and hence a weaker WES feedback.

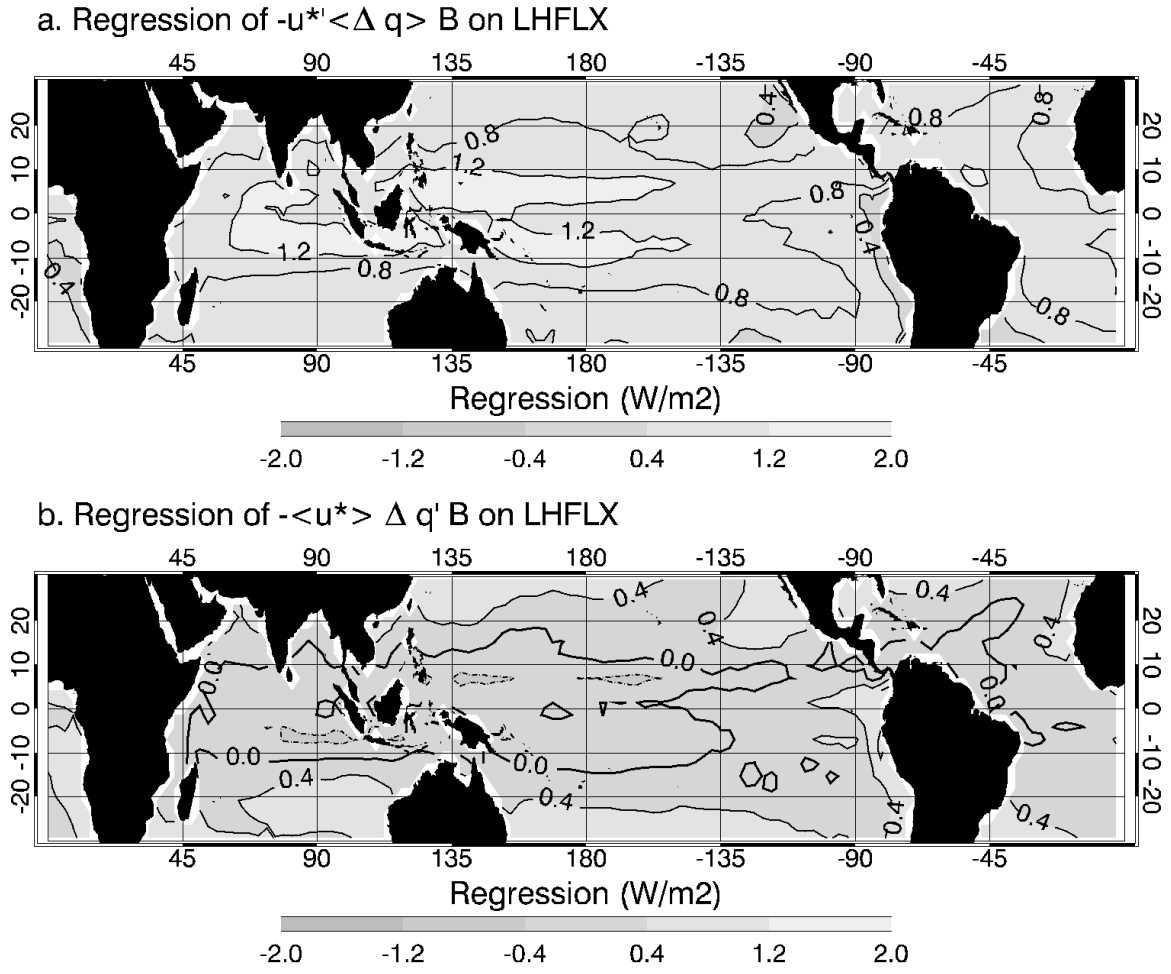

Fig. 12. Regression of (contour interval: 0.4 W/m^2) terms **(a)** $-u^{*'}\overline{\Delta q}B$ and **(b)** $-\overline{u^*}\Delta q^{'}B$ against per unit change in $Q^{'}_{lh}$ for the control CCM3-SOM integration.

B. Winds Stimulated Variability

The set up of the WES-off-SOM run ensures that the winds do not influence Q_{lh} directly, however, indirect effects of winds, such as advection of moist air would still be present. A comparison of the variability of the SST, surface heat fluxes and winds between the control run and the WES-off-SOM run would reveal the thermodynamic variability associated with all the wind-induced feedbacks, although it is likely to be influenced heavily by the WES feedback, as it is the dominant thermodynamic feedback mechanism over the deep tropical oceans.

Figure 13 shows the inter-annual standard deviation of SST and Q_{lh} in the control simulation and Figure 14 shows the change of the same in the WES-off-SOM run. Over the deep tropics, a reduction in the standard deviation of around 60% is observed in the WES-off run as compared to the control run. While the winds affect the SSTs via surface heat fluxes, the SSTs also influence the winds via the WES feedback mechanism by the development of anomalous pressure gradients. Figure 15 shows the standard deviation of the zonal and meridional winds of the control run and their change in the WES-off-SOM run. A reduction in the variability of winds observed in the WES-off-SOM run indicates that winds are indeed influenced by a change in the SST variability, conclusively establishing the presence of the WES feedback. The magnitude of the reduction of the winds, however, does not reflect that of Q_{lh} or the SST, with the reduction in the wind variability being only a fraction of that of Q_{lh} and SST. The remaining reduction in the SST and Q_{lh} can thus only be a result of the influence of Δq. Figure 16b shows about a 50% reduction in the variability of Δq in the WES-off-SOM run as compared to the control run. A perturbed reduction in the variance of wind-induced Q_{lh} thus causes a reduction in the variance of a spectrum of variables, connected via feedback mechanisms as proposed in section 3.1, involving

the winds, q_s, Q_{lh} and SST. A reduction in the variance of Q_{lh} causes a reduction in the variance of SST, which causes a reduction in the variability of winds as well as q_s, which further reduces the variability of Q_{lh}.

Figure 16a shows the reduction in the variability of convective precipitation by about 50% in the WES-off-SOM simulation as compared to the control run over the deep tropics. The ITCZ is known to be forced by SSTs. A reduction in the SST variability thus manifests itself in the ITCZ, reducing the variability of convective precipitation over the region. A striking change in the mean-state of the convective precipitation is observed (Figure 7b). There is a reduction in the precipitation in the northern equatorial Pacific and Atlantic and an increase in precipitation over the southern equatorial oceans, in the winter and spring season causing the ITCZ to be more symmetric in the WES-off-SOM run as seen in Figure 7b. While the variability of surface fields is reduced in the WES-off-SOM integration, the mean state of variables influencing the ITCZ is the same as in the control run. Hence, the change in the mean state of the ITCZ is thus possibly a result of the different variance of surface fields in WES-off-SOM integration. The SSTs in the WES-off-SOM run are not able to stray far from the mean SST, as their variability is constrained by a lack of feedback mechanisms. This prevents the spikes in SST to states where SSTs in the northern equatorial oceans cross the deep convective threshold generating strong CESG in the control run. The lack of strong CESG in the WES-off-SOM integration hence causes a reduction (increase) in the convective precipitation in the northern (southern) side.

This reduction of the inter-annual variability of SST is not surprising, as hierarchical modeling studies (e.g. Carton et al., 1996; Wu and Liu, 2002) reveal similar results. For example, in a partially-coupled modeling study carried out by Wu and Liu (2002), where the overlying north tropical Atlantic atmosphere is decoupled from

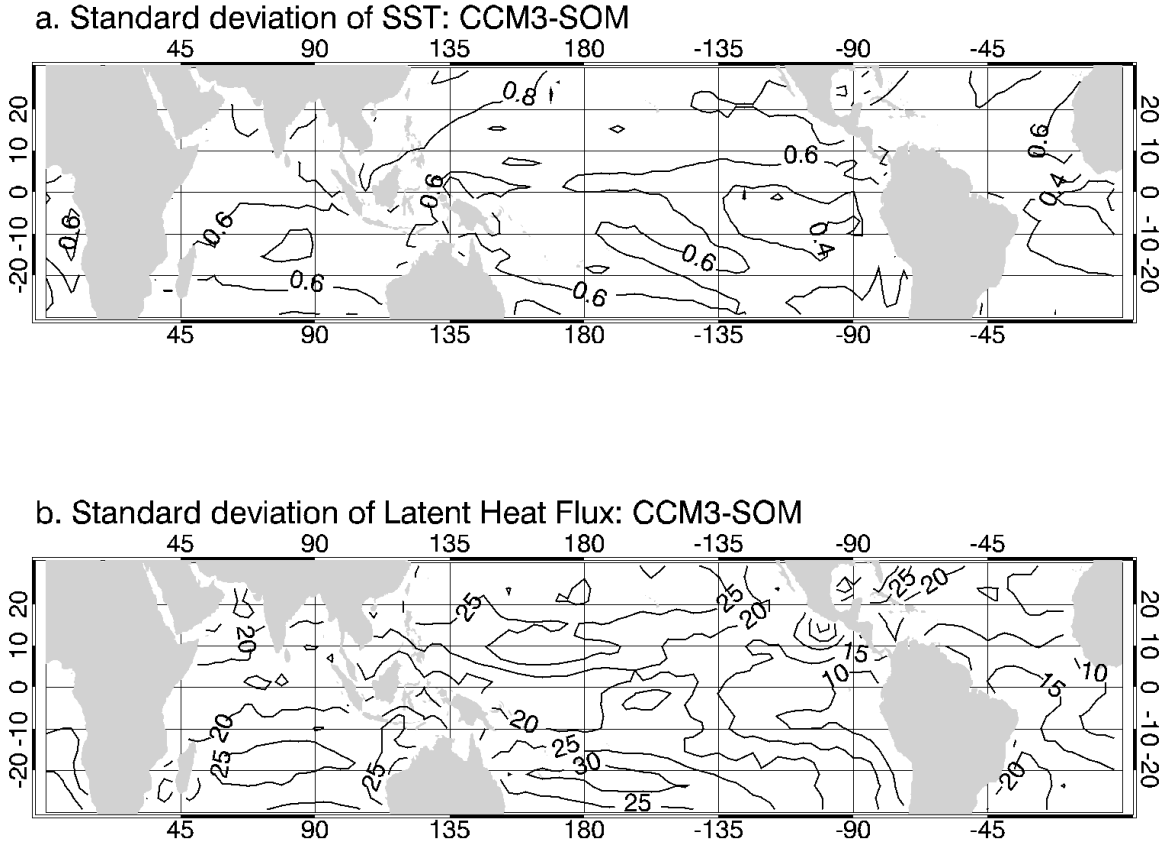

Fig. 13. Inter-annual standard deviation of **(a)** SST (contour interval: 0.2 K) and **(b)** Q_{lh} (contour interval: 5 W/m^2) in CCM3-SOM run.

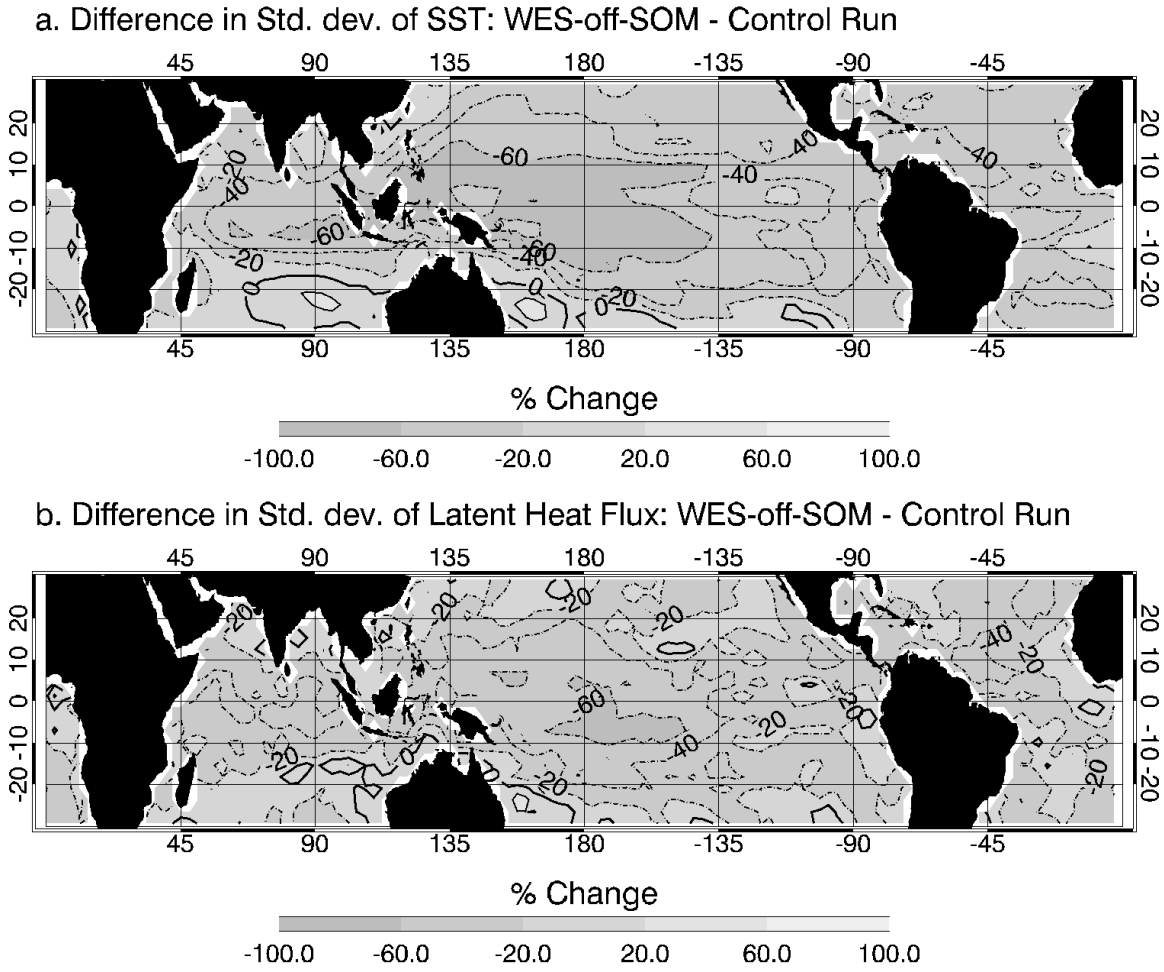

Fig. 14. Percentage change (contour interval: 20%) of the inter-annual standard deviation of **(a)** SST (K) and **(b)** Q_{lh} (W/m^2) in the WES-off-SOM run as compared to the CCM3-SOM run.

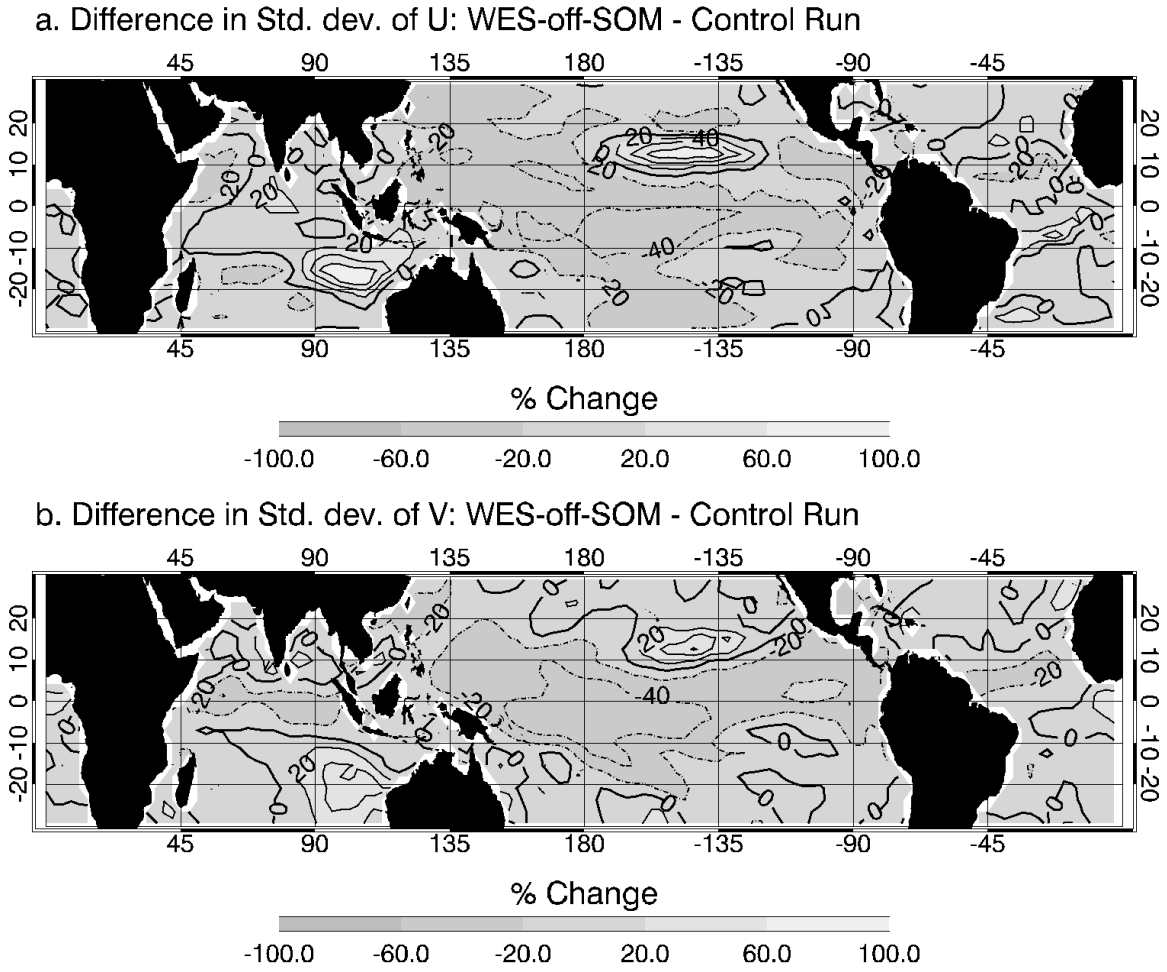

Fig. 15. Percentage change (contour interval: 20%) of the inter-annual standard deviation of **(a)** zonal and **(b)** meridional winds (m/s) in the WES-off-SOM run as compared to the CCM3-SOM run.

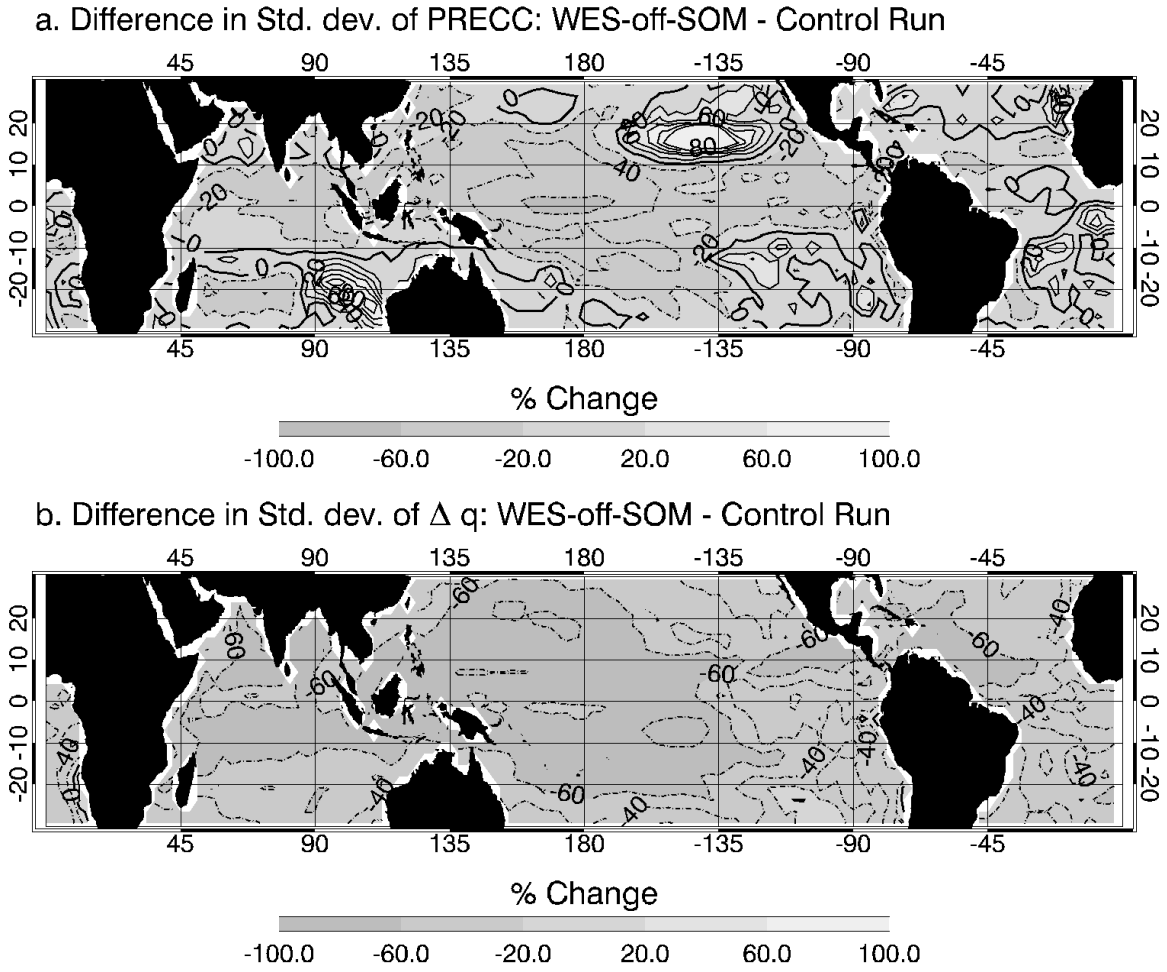

Fig. 16. Percentage change (contour interval: 20%) of the inter-annual standard deviation of **(a)** convective precipitation (mm/day) and **(b)** Δq (mg/kg) in the WES-off-SOM run as compared to the CCM3-SOM run.

the oceans while the ocean is still forced with atmospheric model variability, a substantial reduction of 80% in the variability of SST is observed. A reduction in the inter-annual atmospheric variability as well in this study confirms that variability over the tropical oceans is indeed caused by the feedbacks of the winds, namely the WES feedback. In an experiment design similar to the one here, but applied to a fully coupled atmosphere-ocean model and focusing on the Atlantic, Carton et al. (1996) report a reduction in the variability of the SST only over the off-equatorial tropical Atlantic, as the equatorial variability is a result of dynamical coupling. Since the SOM lacks ocean dynamics, SSTs are only influenced by surface fluxes. A reduction in the variability of the equatorial regions as well in the experiment here emphasizes the role of surface fluxes in the equatorial region in the absence of ocean dynamics.

C. WES Feedback and the Equatorial Annual Cycle

A westward zonal propagation of SST and atmospheric anomalies over the equatorial Pacific as seen in observations (Horel, 1982; Philander and Chao, 1991) is observed in the control run (Figure 17). Latent heat fluctuations over the region in phase with the winds are seen over the Pacific. The SST field responds to these changes in the latent heat fluxes. As seen in observations, the eastern Pacific displays an annual cycle in each of the fields, whereas the western Pacific shows a semi-annual cycle. A westward propagation of departure from the annual means generated in the eastern Pacific are observed until 200°E. Similar behavior is seen over the equatorial Atlantic ocean.

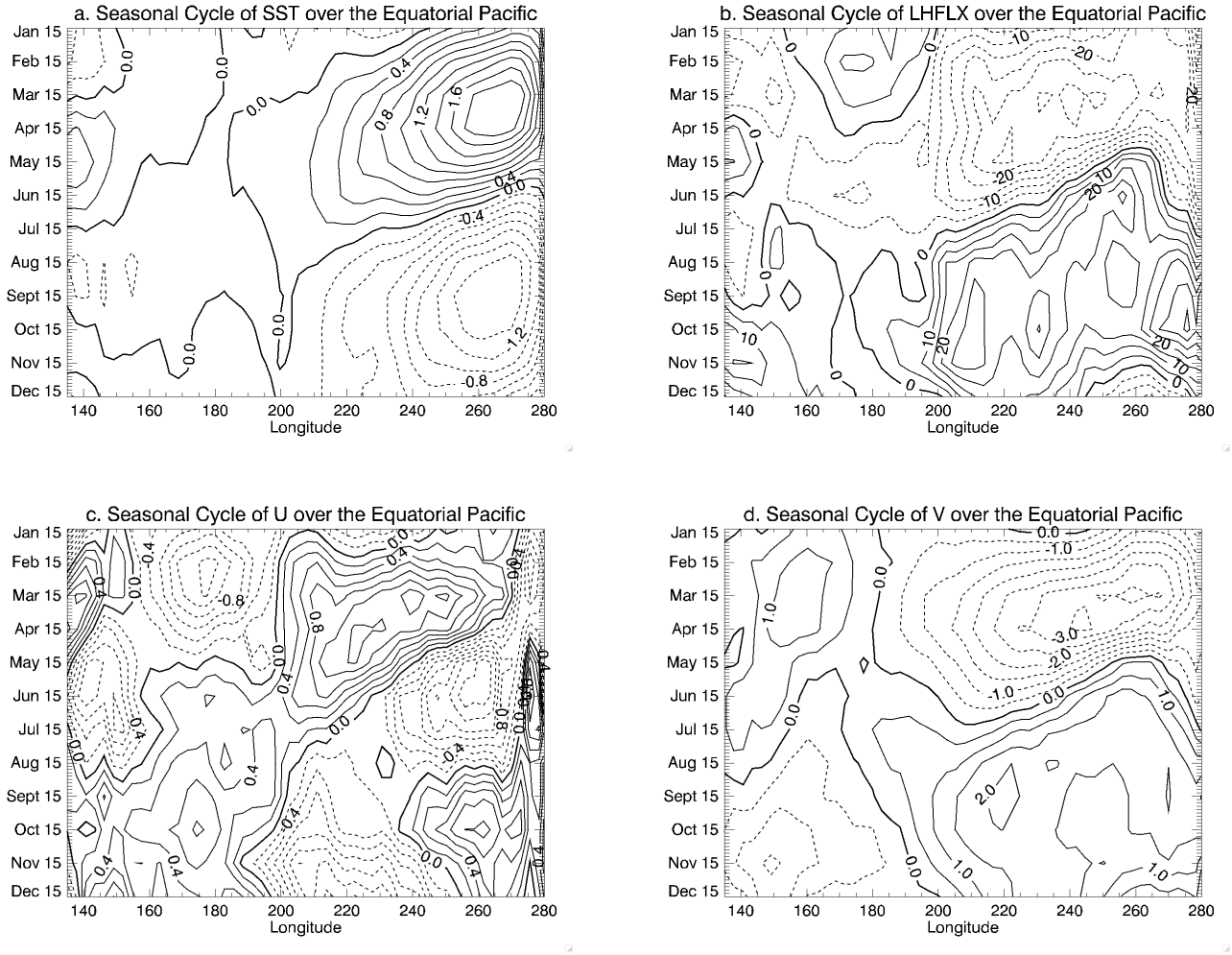

Fig. 17. Annual cycle over the equatorial Pacific (4°S-4°N) of climatological **(a)** SST (contour interval: 0.2 K), **(b)** Q_{lh} (contour interval: 5 W/m^2), **(c)** zonal winds (contour interval: 0.2 m/s) and **(d)** meridional winds (contour interval: 0.5 m/s) for the control run. Note the westward propagation of anomalies of each of the fields.

1. Experimental Set-up

Another CCM3-SOM experiment is conducted to islolate the role of the WES feedback in the generation of the annual cycle of SST over the eastern equatorial Pacific and the zonal propagation of the seasonal anomalies. The experiment, named WES-off-NoAnn, is similar to WES-off-SOM experiment, and only differs in the prescribed values of u^*. Instead of prescribing u^* to model climatological values, as in the WES-off-SOM integration, which exhibits the seasonal cycle of u^*, an annual mean value of u^* is prescribed in the bulk formulations of surface heat fluxes, so that Q_{lh} and Q_{sh} do not respond to the seasonal fluctuations of boundary layer winds. The Q-flux is kept the same in both integrations, because it is sought to figure out how the annual cycle of SST is modified by the lack of the WES feedback. The experimental design thus ensures that the direct influence of winds and their seasonal cycle is removed from surface fluxes.

2. Role of the WES Feedback

Figure 18 shows the annual cycle of the SST, Q_{lh}, U, and V fields as simulated in the WES-off-NoANN experiment. The western Pacific, which is governed by the solar cycle, demonstrates a semi-annual SST cycle similar to the control run. The eastern Pacific, however, still demonstrates an annual cycle of SST and Q_{lh}, implying that winds converging in the ITCZ in the northern hemisphere are not solely responsible for the annual cycle of Q_{lh} that forces an annual cycle of SST in the eastern equatorial Pacific region, dominating over the semi-annual equatorial solar forcing. In fact, the whole of the eastern Pacific and central Pacific exhibit a coherent annual cycle peaking in March and reaching a minimum in July-August. The shift in the phase of the annual cycle in the WES-off-NoANN run is probably because of the weak

annual cycle of Q_{lh} in the simulation, allowing a stronger influence of semi-annual solar forcing on the net surface fluxes. The weaker amplitude of the annual cycle in the eastern Pacific is due to the weaker fluctuations of Q_{lh} in the WES-off-NoANN experiment. The demonstration of an annual cycle by Q_{lh} implies a role for Δq in the equatorial annual cycle. Figure 19 shows the Hovmoeller plot of Δq for the control run and WES-off-NoANN run. Q_{lh} clearly follows Δq in the WES-off-NoANN run. In the control simulation humidity seems to play a secondary role, having smaller amplitudes as compared to the WES-off-NoANN integration. The magnitudes of Δq probably differ because of the different mean states of the two models. It should be noted that ocean dynamics are not simulated in the SOM and hence the air-sea interaction is purely thermodynamic in these simulations.

The secondary role of Δq in the equatorial annual cycle in the control run, in the presence of the annual cycle of winds, is highlighted in the eastern Pacific, where the annual cycle of Δq acts to oppose the effect of the annual cycle of winds on Q_{lh}, but with the influence of winds being dominant. For example, in March while the reduction in background trade winds tends to warm the surface, the decrease in Δq induces an opposite effect, increasing Q_{lh} and damping the warming caused by the winds. The opposing annual cycle of Δq appears to be a response of the enhanced annual cycle of SST over the eastern Pacific in the control run, which increases q_s, whereby decreasing Δq. The argument is supported by a lack of an opposing annual cycle of Δq in the WES-off-NoANN experiment, where the SST annual cycle is small in magnitude. In the WES-off-NoANN experiment, while u^* does not decrease during the spring season, the positive phase of Δq causes Q_{lh} to maintain the same sign as the control run. The presence of an annual cycle in the WES-off-NoANN experiment in the SST field thus indicates that while the amplitude of the Q_{lh} annual cycle is enhanced by the winds, it is also influenced by Δq, which can potentially generate a

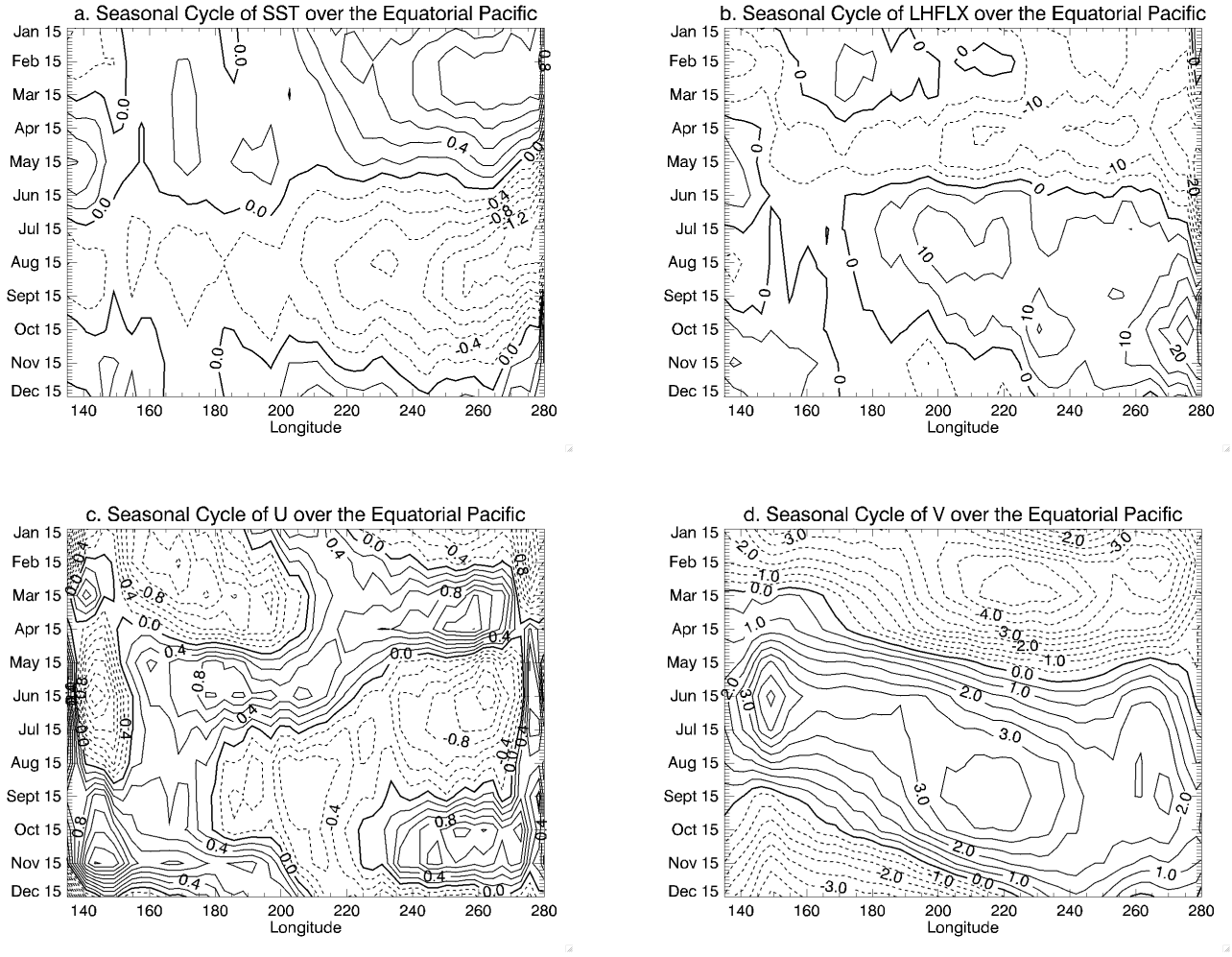

Fig. 18. Annual cycle over the equatorial Pacific (4°S-4°N) of climatological **(a)** SST (contour interval: 0.2 K), **(b)** Q_{lh} (contour interval: 5 W/m^2), **(c)** zonal winds (contour interval: 0.2 m/s) and **(d)** meridional winds (contour interval: 0.5 m/s) for the WES-off-NoANN run. Note the lack of westward propagation of anomalies.

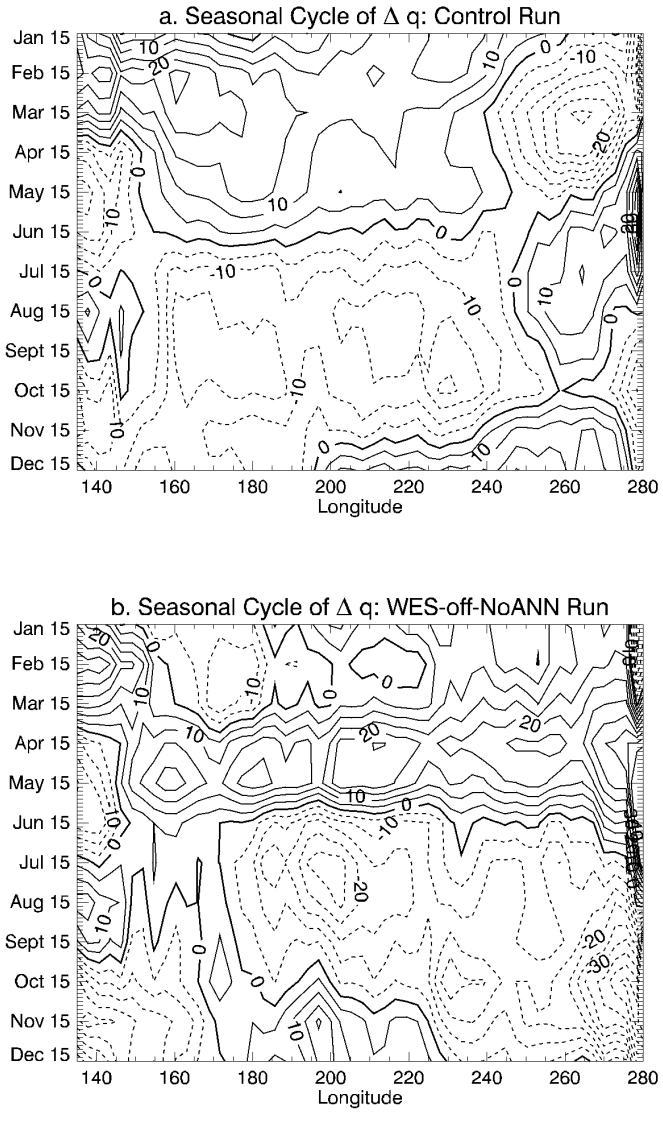

Fig. 19. Annual cycle over the equatorial Pacific (4°S-4°N) of climatological Δq (contour interval: 5 mg/kg) for the **(a)** control run and **(b)** WES-off-NoANN run. Note the lack of westward propagation of anomalies in both runs.

strong enough annual cycle of Q_{lh}, even in the absence of the annual cycle of winds, to dominate over the semi-annual solar forcing.

The westward propagation of seasonal anomalies is weaker in the WES-off-NoANN experiment indicating a role of the WES feedback in the westward propagation of the equatorial annual cycle. In the control experiment a westward propagation of SST anomalies causes a change in the phase of the equatorial annual cycle westwards. A westward reduction of the amplitude of the annual cycle is also seen due to the increasing mixed layer ocean depth westwards. While the SST anomalies peak in March over the eastern equatorial Pacific, they peak in May at about 220°E. The lack of westward propagation in the WES-off-NoANN experiment causes all of the eastern and central Pacific equatorial ocean to exhibit the same phase, peaking in March and reaching a minimum in August. A westward reduction in the amplitude is seen, again caused by the increasing ocean mixed layer depth westwards. The westward propagation of Q_{lh} seen in the control experiment is also missing in the WES-off-NoANN experiment, where the westward propagation of Q_{lh} is driven by Δq. Westward propagation of Δq is neither seen in the WES-off-NoANN run nor in the control run, implying that westward propagation of Q_{lh} is caused by the influence of winds.

The role of the WES feedback is further identified in the westward propagation of seasonal zonal wind anomalies seen in Figure 17c in the control run, supporting Xie's (1996) hypothesis. A stronger warming in the eastern equatorial Pacific causes a westward zonal pressure gradient, causing westerly anomalies along the equator, which weaken the background trade winds and hence reduce Q_{lh}, further warming the western oceans. The westward propagation is caused by the delayed warming of the ocean mixed layer in response to a reduction of Q_{lh} (Xie, 1996). The absence of the WES feedback in the WES-off-NoANN experiment does not allow anomalies to

propagate and hence the anomalies generated in March decay. A stronger warming in the eastern oceans also produces anomalous westerly zonal wind anomalies in the WES-off-NoANN experiment as seen in Figure 18c. But due the absence of the WES feedback, these anomalous winds are not able to influence the SST westwards, preventing the propagation of both the zonal wind and the SST anomalies, supporting the hypothesis that the WES feedback is essential for the westward propagation of SST anomalies. The westward propagation of zonal winds, although weaker, is still observed in the WES-off-NoANN run, which could suggest that other large scale phenomena are causing a westward propagation in the zonal winds, which could then force the SST anomalies to propagate westwards.

Westward propagation of meridional winds is also seen in the control run (Figure 17d), unlike observations (Philander and Chao, 1991) where the annual cycle at the equator is in phase basin-wide. It is also absent in the WES-off-NoANN run. The presence of the westward propagation of the annual cycle in the control run is probably due to the westward propagating air-sea coupled cross-equatorial WES mode waves which propagate as equatorial Rossby waves carrying equatorial asymmetry, including cross-equatorial meridional winds, westwards from the eastern oceans. The absence of such a propagation of meridional winds in the WES-off-NoANN run supports the existence of WES waves over the tropical oceans in CCM3-SOM. However, the absence of these waves in observations possibly indicates a stronger WES coupling in CCM3-SOM as compared to observations.

3. Discussion

The westward propagation of the equatorial annual cycle observed in various studies (Horel, 1982; Mitchell and Wallace, 1992; Philander and Chao, 1991) is explained by equatorially symmetric coupled air-sea modes of variability (Chang and Philander,

1994; Xie, 1994) while the generation of the annual cycle in the eastern equatorial oceans is governed by the asymmetric mode due to the presence of a northward asymmetric ITCZ (Li and Philander, 1996; Wang, 1994; Xie, 1994) as mentioned in the introduction. Both the asymmetric and the symmetric modes involve dynamic coupling, which involves the seasonally varying mixed layer depth, as well as thermodynamic coupling. The SOM has a fixed mixed layer depth and is independent of ocean dynamics. These characteristics are important for the correct simulation of the equatorial annual cycle (Chen et al., 1994). The lack of ocean dynamics in the SOM is compensated by Q-flux adjustments that emulate climatological oceanic heat transport, while allowing us to focus completely on the thermodynamic air-sea interactions.

While we find that thermodynamic interactions are capable of simulating a realistic westward propagating equatorial annual cycle, the generation of the equatorial annual cycle over the eastern oceans is not found to be solely dependent on the winds - the focus of previous studies. Even in the absence of the effects of seasonal changes in winds on the latent heat fluxes in an experiment, a credible annual cycle in the eastern oceans is generated in the latent heat fluxes and the SST forced by the annual cycle of humidity. In the presence of the effects of wind variability on latent heat fluxes, humidity changes act to dampen the effects of winds. Independently, it generates a similar, though weaker, annual cycle of Q_{lh}. The role of humidity however in generating westward propagating equatorial seasonal anomalies is negligible, as a basin-wide same phase annual cycle of the humidity field is seen in the equatorial oceans in the experiment here. Whether the actual mechanism for the equatorial annual cycle is through the symmetric mode or by the equatorward propagation of the off-equatorial annual cycle (Liu, 1996), the results here show that the westward propagation of anomalies in the equatorial oceans are indeed caused by the WES

feedback, in the absence of which little propagation is seen in a GCM setting.

D. WES Feedback and the Free Tropical Atlantic Meridional Mode

1. Atlantic Meridional Mode in CCM3-SOM

The thermodynamic coupled variability of the tropical Atlantic is analyzed by performing a singular value decomposition (SVD) analysis (Bretherton et al., 1992). SVD allows for identification of leading patterns of co-variability of two spatio-temporal fields. Figure 20a shows the spatial patterns of SST and Q_{lh} obtained from the first leading SVD mode of variability over the tropical Atlantic in the CCM3-SOM integration. The spatial patterns resemble the coupled meridional mode of variability, as was also found by Chang et al. (1997). SVD analysis was performed on the cross-covariance matrix of SST and Q_{lh}. A regression of zonal and meridional winds on the principal component of SST of the SVD mode is also shown. In the absence of any coupled dynamical modes, namely the Atlantic-Niño, in an AGCM coupled to a SOM, the appearance of the meridional mode as the leading pattern is not surprising as the thermodynamic interactions are expected to be dominant. A cross-equatorial dipole pattern is observed in the SST field with basin wide northern and southern poles extending from the equator to about 20° latitudes. A dipole in Q_{lh} is also observed, however, the spatial extent of its poles are limited to the deep tropics from the equator to about 10° latitudes.

The co-location of Q_{lh} and SST centers of variability indicates a positive feedback between the two, with warming and cooling by Q_{lh} occuring where the SSTs are warm and cold respectively, over the deep tropics (e.g. Carton et al., 1996). Polewards of 10° latitudes, Q_{lh} variability is small and in fact seems to oppose the development of SST anomalies in those regions, indicative of either a weak relation with SST or a

negative feedback. The response of the wind field to the leading mode of variability of SST and Q_{lh} is suggestive of the existence of the WES feedback, with south-easterlies (southerlies, south-westerlies) appearing over the southern (northern) deep tropics enhancing (weakening) the trade winds in the regions where the SSTs are cold (warm) and Q_{lh} has a cooling (warming) effect.

2. Role of the WES Feedback

The role of the WES feedback over the deep tropics is further elucidated by comparing the modes of variability of the control run to that of the WES-off-SOM run. Figure 20b shows the spatial pattern of the SST and Q_{lh} of the leading SVD mode of SST and Q_{lh} for the WES-off-SOM run. A substantial weakening of the variability of the dipole pattern in the SST mode, particularly over the deep tropics between the equator to 10° latitudes is observed. A simultaneous substantial reduction in the dipole pattern of Q_{lh} is also observed. Curiously, however, the response of the winds to the leading mode of variability, although weaker, resembles that of the control run, indicating that even in the absence of the WES feedback the winds are able to respond to the SST with little change in amplitude. The above results imply that while the WES feedback amplifies the meridional mode in the deep tropics, it is not solely responsible for the generation of the meridional mode.

A non-linear behavior of the wind fields is also indicated. The residual SST dipole pattern in the WES-off-SOM run appears to be enough to generate a response in the winds which is similar to that of the amplified dipole mode in the control simulation. So, while the influence of winds are important in the enhancement of the SST dipole, the magnitude of the winds are not amplified as dramatically as the SST in the presence of the WES feedback. This could also suggest that winds in the tropical Atlantic are not completely driven by tropical SSTs, but other mechanisms like the

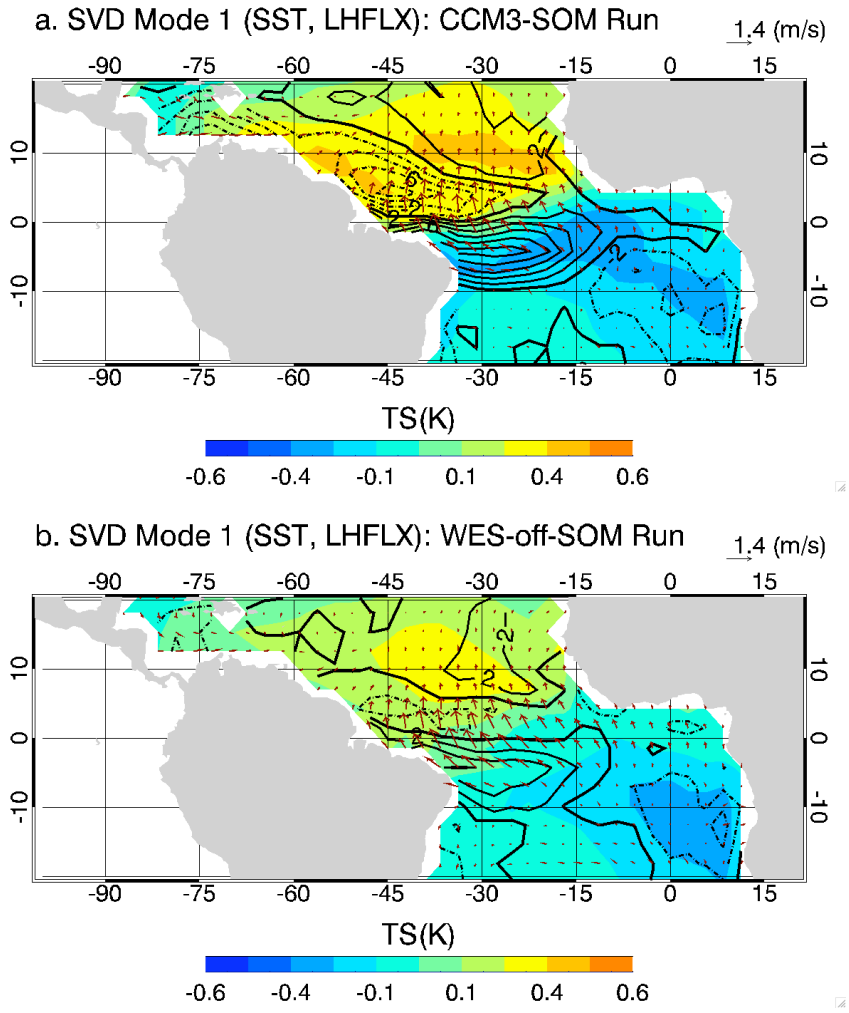

Fig. 20. Spatial pattern of the leading SVD mode of SST and Q_{lh} over the tropical Atlantic for **(a)** CCM3-SOM run and **(b)** WES-off-SOM run. SVD is performed on the cross-covariance matrix of SST and Q_{lh}. The wind pattern is obtained by regressing the normalized time-series of the leading principal component of SST on the zonal and meridional winds. The colors indicate SSTs, and the contours represent Q_{lh} (contour interval: 2 W/m^2). Negative contours indicate warming of the ocean mixed layer. The arrows indicate the change in winds per standard deviation change of the principal component of SST of the leading SVD mode.

influence of land masses, which are exactly similar in the two simulations, might also have a significant role to play in their variability. The reduction in the variability of the meridional mode in the absence of WES feedback is also elucidated in the spectrum of the time-series of the principal components of SST of the leading modes (Figure 21). A sharp reduction in the variability of the meridional mode is observed in the WES-off-SOM run on the inter-annual time-scales, indicating that wind-induced variability is responsible for the low frequency variability of the meridional mode.

3. Discussion

A coherent residual dipole structure is still seen in the deep tropics even in the absence of the WES feedback, as seen in the SST and Q_{lh} pattern in the WES-off-SOM run. What causes this residual dipole pattern? To answer this question we partition Q_{lh} anomalies associated with the dipole mode. Figure 22a shows the regression of Q_{lh} against a SST dipole index for the CCM3-SOM run. The dipole index is defined as the difference in the monthly area-averaged SST over 5°N-15°N, 50°W-20°W and 5°S-15°S, 35°W-10°W. The phase of the dipole index is considered to be positive when the northern side is warmer than the southern side. We revert to a regression on the dipole index here as opposed to time-series of the principal component of the leading SVD mode for a more intuitive analysis. The two poles for computing the dipole index are selected based on the dipole SST pattern observed in the SVD analysis. Similar indices have also been used in other studies. A dipole pattern is seen in the Q_{lh} anomalies, similar to that observed in the SVD analysis, with poles in the deep tropical Atlantic extending from the equator to about 10° latitudes. Q_{lh} anomalies if linearly partitioned appear to come from two terms as follows:

$$Q'_{lh} = -(u^{*'}(\overline{\Delta q}) + \overline{u^*}(\Delta q)')\ B \tag{3.3}$$

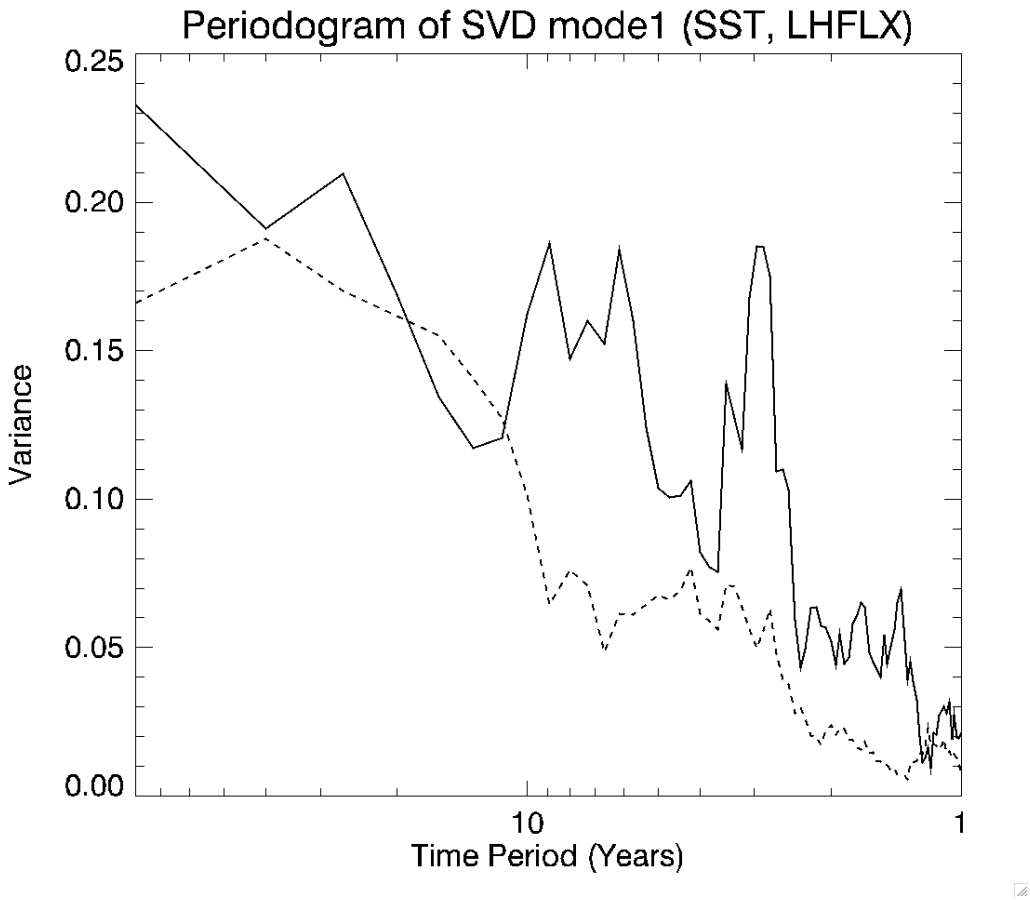

Fig. 21. Spectral density of the principal component of SST of the leading SVD mode of SST and Q_{lh} over the tropical Atlantic for CCM3-SOM (solid) and WES-off-SOM (dashed) runs. The spectrum is smoothed using a moving window with a band width of 6. The horizontal axis is in log-scale.

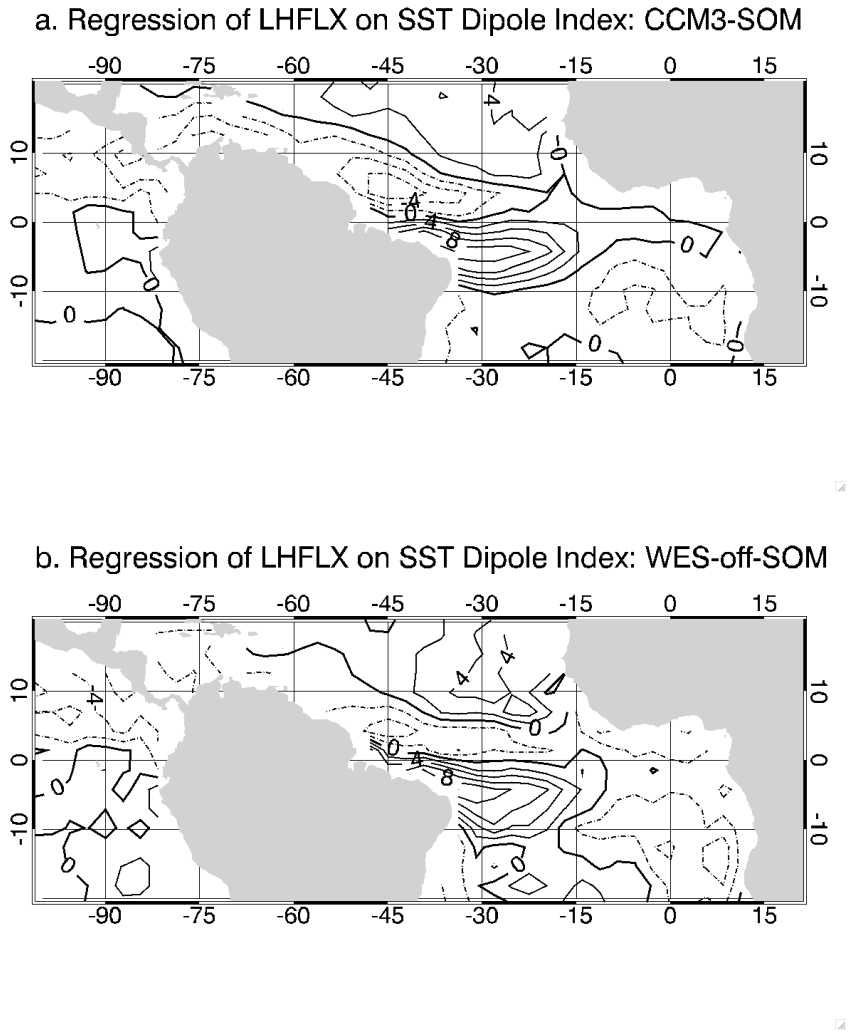

Fig. 22. Regression of Q_{lh} (contour interval: 2 W/m^2) against the Atlantic SST dipole index for **(a)** CCM3-SOM and **(b)** WES-off-SOM run.

where, the primes denote the monthly anomalies and the bars denote climatological means. The contribution of each of these terms is shown in Figure 23, where the terms are individually regressed on the SST dipole index. A dipole pattern analogous to that observed in Q_{lh} is observed for the $u^{*'}(\overline{\Delta q})$ term. A dipole pattern, albeit with opposite polarity to that of Q_{lh} pattern, is observed for the $\overline{u^*}(\Delta q)'$ term. The coherence of the pattern of $u^{*'}(\overline{\Delta q})$ term with Q_{lh} anomalies over the deep tropics indicates that the term dominates in contribution to Q_{lh} with $\overline{u^*}(\Delta q)'$ acts to damp the anomalies consistent with the result of Breugem et al. (2007). So, while the wind anomalies work to increase the SST on the northern side during the positive phase of the dipole mode, the anomalous development of Δq acts to cool down the SST, caused probably by the increase in saturation specific humidity above the ocean surface, which is linked to SST via the Clausius-Clapeyron equation.

In the absence of the WES feedback in the WES-off-SOM integration, the contribution of the first term to Q_{lh} anomalies disappears. Figure 22b shows the regression of Q_{lh} against the SST dipole index for the WES-off-SOM run. The dipole structure is still seen, with a comparable magnitude to that of CCM3-SOM run. The strength of the dipole pattern appears to be stronger in the dipole analysis as compared to the SVD analysis of WES-off-SOM run. This is because SVD accounts for the reduction in the variability of the mode in the WES-off-SOM run (Figure 21), while the regression analysis, which simply represents the change in Q_{lh} per degree change in the SST dipole index, does not. The anomalies in Q_{lh} in the WES-off-SOM are caused only by the second term, and hence all of the fluctuations of the Q_{lh} are brought about by changes in Δq. Figure 24a shows the regression of Δq against the dipole index for the CCM3-SOM integration. A dipole pattern coherent with the contribution of the $\overline{u^*}(\Delta q)'$ term as per the sign convention in equation 1 is observed. However, in the WES-off-SOM run opposite polarities of the Δq pattern are observed as compared to

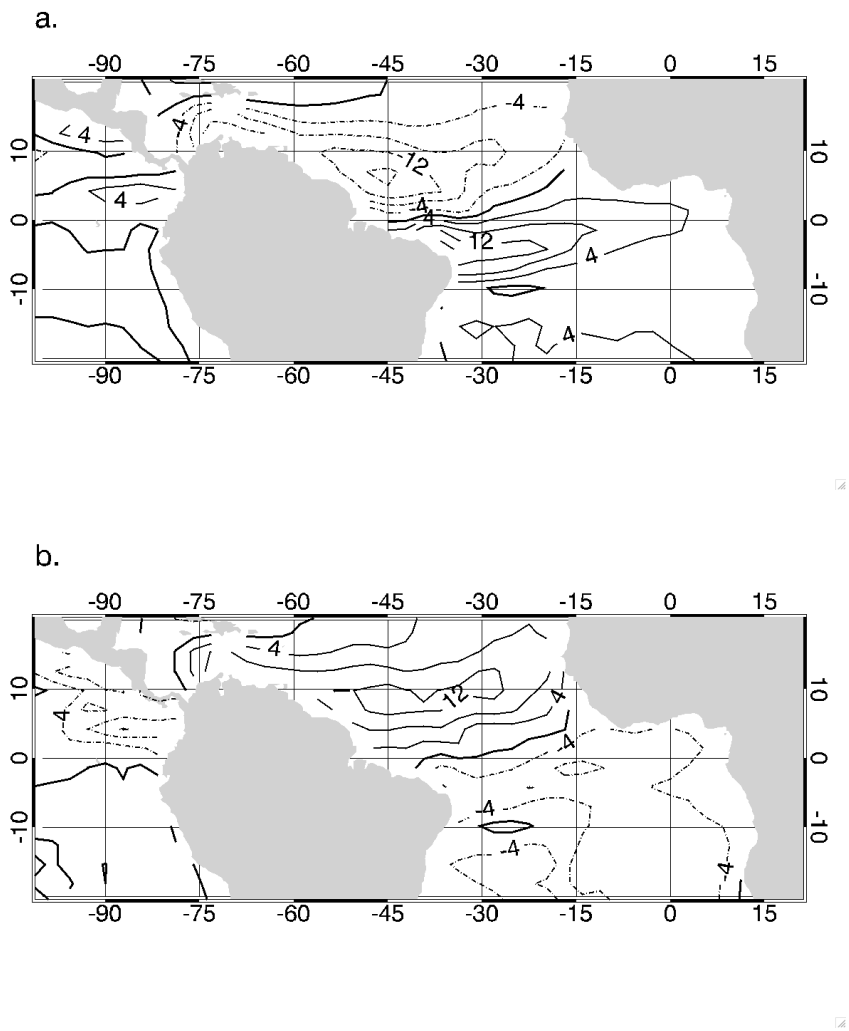

Fig. 23. Regression of terms **(a)** $u^{*'}(\overline{\Delta q})\ B$ and **(b)** $\overline{u^*}(\Delta q)'\ B$ of the linearized partition of Q_{lh} (contour interval: 4 W/m^2) against the Atlantic SST dipole index.

the control run (Figure 24b).

The polarity of Δq in the WES-off-SOM run is thus in accord with Q_{lh} pattern seen in Figure 22b. The co-located dipole pattern of Q_{lh} with SST in the WES-off-SOM run, indicative of the presence of a positive feedback, hence appears to be caused by the effect of Δq. In the absence of the wind-induced warming, the role of humidity changes from being a damping agent, as in the CCM3-SOM run, to that of a positive feedback, with an increase in Δq associated with an increase in SST. The dipole in Δq during the warm phase, in the absence of the WES feedback, is probably caused by the anomalous advection of air from the southern side to the northern side by the winds increasing q in the northern side and decreasing it in the southern side. The mean specific humidity pattern over the tropical Atlantic (Figure 25) supports the argument, with the maximum specific humidity being exhibited near the equator under the ITCZ (Figure 5b). An anomalous northward advection would thus lead to an increase in q in the northern side. Over the tropical Atlantic in the WES-off-SOM run q_s does not change as much as in the CCM3-SOM run since the amplification of the SST dipole is limited in the WES-off-SOM run. The dipole in Δq causes a dipole of Q_{lh} which warms (cools) the SST in the northern (southern) side of the equator. The SST dipole then generates anomalous cross-equatorial southerly winds that further advect air from the south to the north. The meridional mode can also be generated by humidity in the absence of the influence of winds on surface heat fluxes, albeit with a weaker amplitude. The proposed feedback mechanism above is illustrated in a schematic in Figure 26.

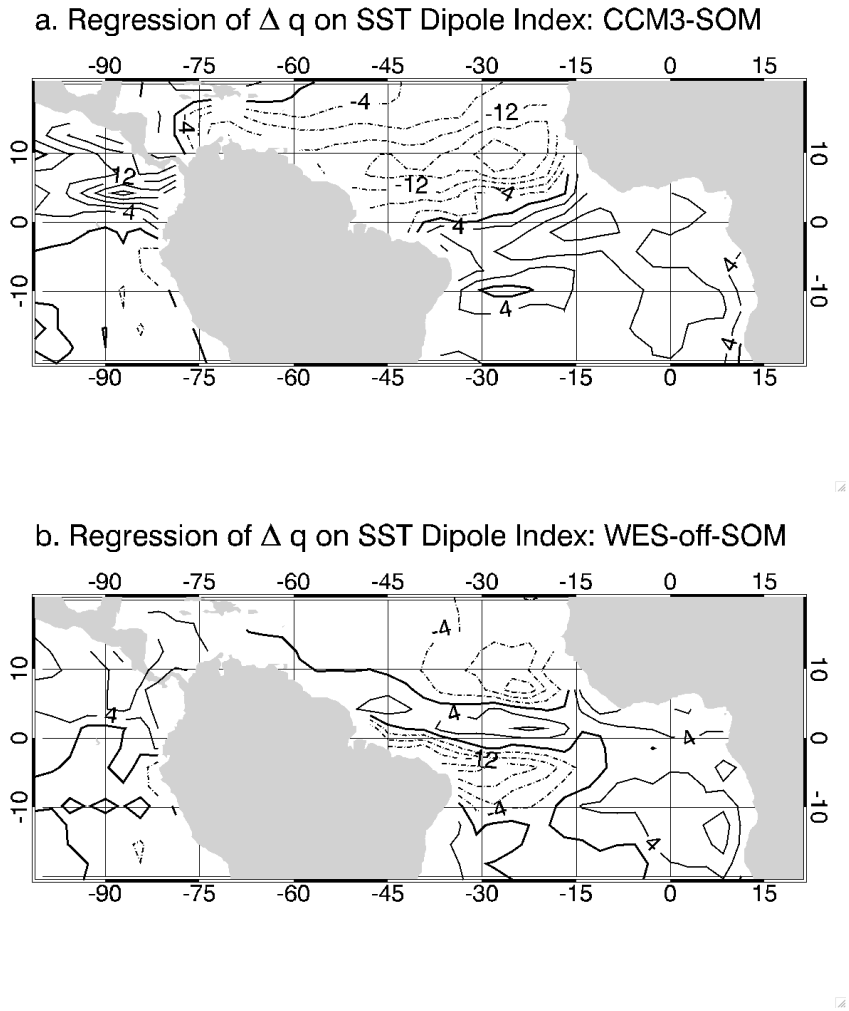

Fig. 24. Regression of Δq (contour interval: 4 mg/kg) against the Atlantic SST dipole index for **(a)** CCM3-SOM and **(b)** WES-off-SOM run.

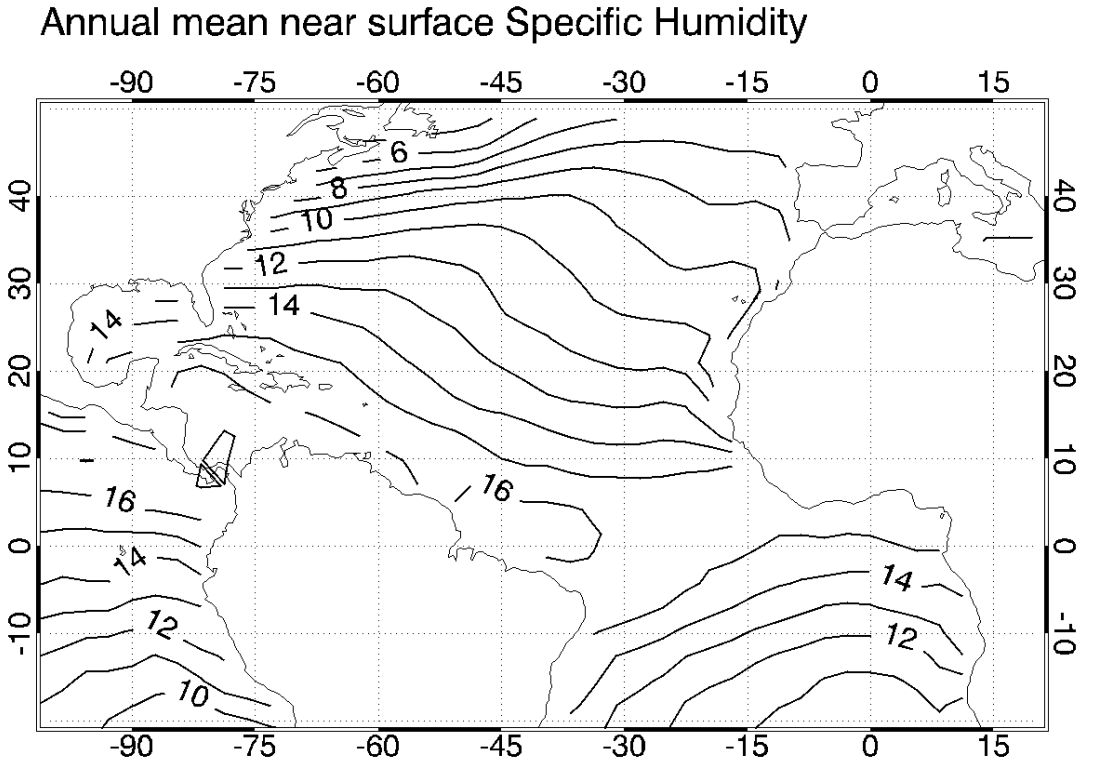

Fig. 25. Annual mean near surface specific humidity over the tropical Atlantic in CCM3-SOM integration.

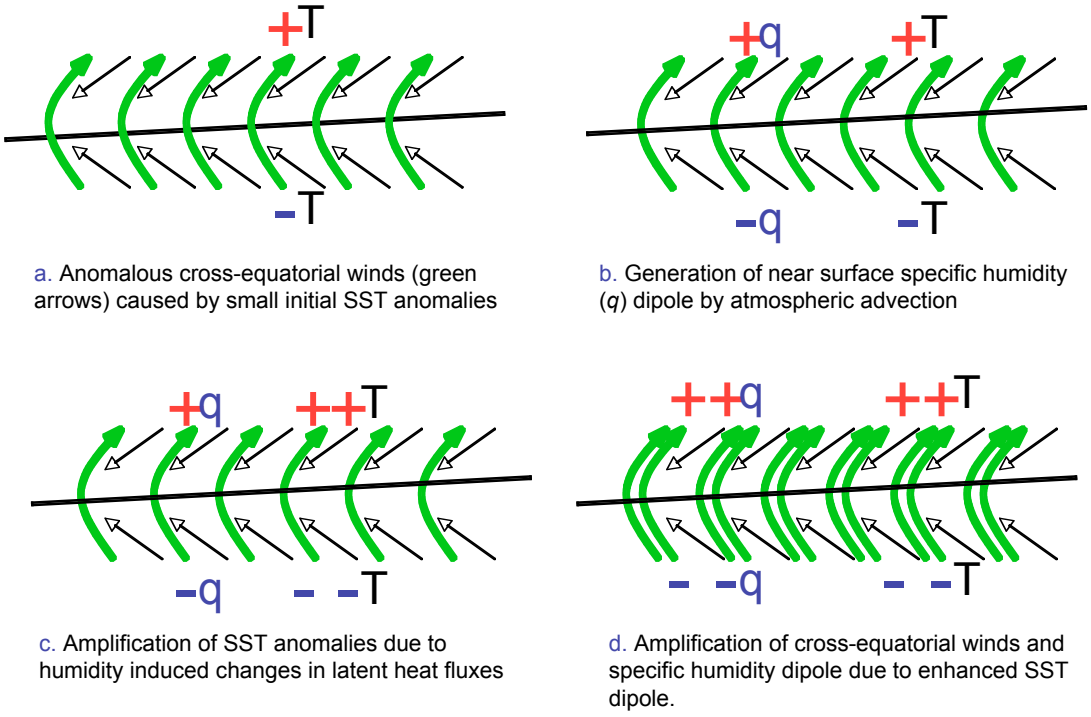

Fig. 26. Schematic of the near surface specific humidity induced positive feedback mechanism in the deep tropics in the absence of the WES feedback. The black line represents the line of maximum mean specific humidity, and the black arrows indicate trade winds.

CHAPTER IV

FORCED TROPICAL VARIABILITY

The tropical response of CCM3 coupled to a SOM to two forcings external to the local tropical system are studied. The first study focuses on the response of the Atlantic ocean to ENSO, while the other addresses the response of the global tropical oceans to abrupt high latitude cooling. Both of these forcings have been proposed to generate tropical responses by tele-connection mechanisms where the WES feedback plays a dominant role. The following sections reveal the results of investigations to isolate the WES feedback mechanism using experimental set-ups that distinctly emulate these remote forcings.

A. ENSO Forced Tropical Atlantic Ocean

1. Experimental Set-up

In order to understand the influence of ENSO on the Atlantic, separate runs with a forced ENSO-like SST cycle in the tropical Pacific are carried out. To isolate the analysis from ENSO multi-year variability, an idealized four-year ENSO-like SST cycle is prescribed over the tropical Pacific. An artificial ENSO cycle is generated by adding a weighted cosine function, with an amplitude equal to one standard deviation of the observed Niño 3 index and a time period of four years, to observed SST climatology over each grid point of CCM3 over the tropical Pacific. The weights of the cosine functions are taken to be the loadings of the first EOF of observed SSTs over the tropical Pacific derived from Carton-Geise Simple Ocean Data Assimilation (SODA) data-set available at the International Research Institute for Climate and Society (IRI) data library (Carton et al., 2000). The prescribed tropical SSTs are hence

generated as:

$$T_{i,t} = \hat{T}_{i,j} + e_i \; A \; cos(\frac{2\pi t}{48} - m) \tag{4.1}$$

where, $T_{i,t}$ is the SST at grid point, i and time, t in months, such that $t = 0$ corresponds to January of the first year of simulation, $\hat{T}_{i,j}$ is the climatology of SST at point i for month, $j = t \; MOD \; 12$. e_i is the loading of the first EOF at grid point i, A is the amplitude of the cosine function, i.e. of the artificial ENSO cycle, and m is the phase of the cosine function, whereby $m = 11$ implies that ENSO peaks in December, as applied in this study.

SST anomalies prescribed in the above manner ensure a spatial pattern of ENSO forcing for CCM3 that are similar to the real world ENSO pattern. Integrations are carried out for the control CCM3-SOM model as well as for the modified WES-off model forced with the prescribed ENSO cycle. The control ENSO forced integration is termed as CCM3-SOM-ENSO integration, whereas the modified integration is termed as WES-off-ENSO integration. All integrations are run for 75 years. The analyses presented here are based on 70 years of integrations after discarding the first five years as spin-up time.

2. SVD Analysis

The meridional mode of variability has been hypothesized to be the chosen mode for the response of the tropical Atlantic to ENSO forcing (e.g. Ruiz-Barradas et al., 2000). Figure 27a shows the spatial pattern of the leading SVD mode of SST and Q_{lh} over the tropical Atlantic for the CCM3-SOM-ENSO experiment. Regression of winds on the principal component of SST of the leading mode are also shown. A coherent dipole pattern of SST and Q_{lh} and winds similar to that of CCM3-SOM

integration is observed but with a stronger northern and a weaker southern SST pole. The Q_{lh} northern pole is also found to be weaker. The reduction in the co-variability of SST and Q_{lh} indicates that other surface fluxes also have a part to play in the response of the Atlantic to changes in the Pacific. The coherent structure of SST, Q_{lh}, and winds in the CCM3-SOM-ENSO experiment nonetheless supports the role of WES feedback in the response of the tropical Atlantic to the Pacific and confirm that the dipole pattern is the chosen mode of response.

In the absence of the WES feedback, the response of the Atlantic is found to exhibit little cross-equatorial structure, as seen in the spatial pattern of the leading SVD mode of SST and Q_{lh} and the regression on winds (Figure 27b). No coherence is observed between SST and Q_{lh}. The dipole pattern, which is a free mode of variability even in the absence of WES feedback, ceases to exist in the WES-off-ENSO experiment indicating that the WES feedback is the leading mechanism in the generation of the dipole mode of variability in response to Pacific forcings. The role of humidity, capable of generating a dipole mode in the absence of forcings, appears to be over-shadowed by the effects of ENSO forcing like tropospheric subsidence that causes drying of the boundary layer over the equatorial Atlantic (Klein et al., 1999). The mechanisms and the role of the WES feedback in the response of the Atlantic, to ENSO are further discussed in the following sections.

3. Tropical Atlantic Response to ENSO in CCM3-SOM

The mechanism of the meridional mode response of the tropical Atlantic to ENSO events is studied using lagged regression analysis of SST and atmospheric variables against the model Niño 3 index. The extra-tropical Atlantic response to ENSO events is also examined. A regression of Atlantic SST averaged against the Niño 3 index for January shows statistically significant warm responses in all of the northern tropical

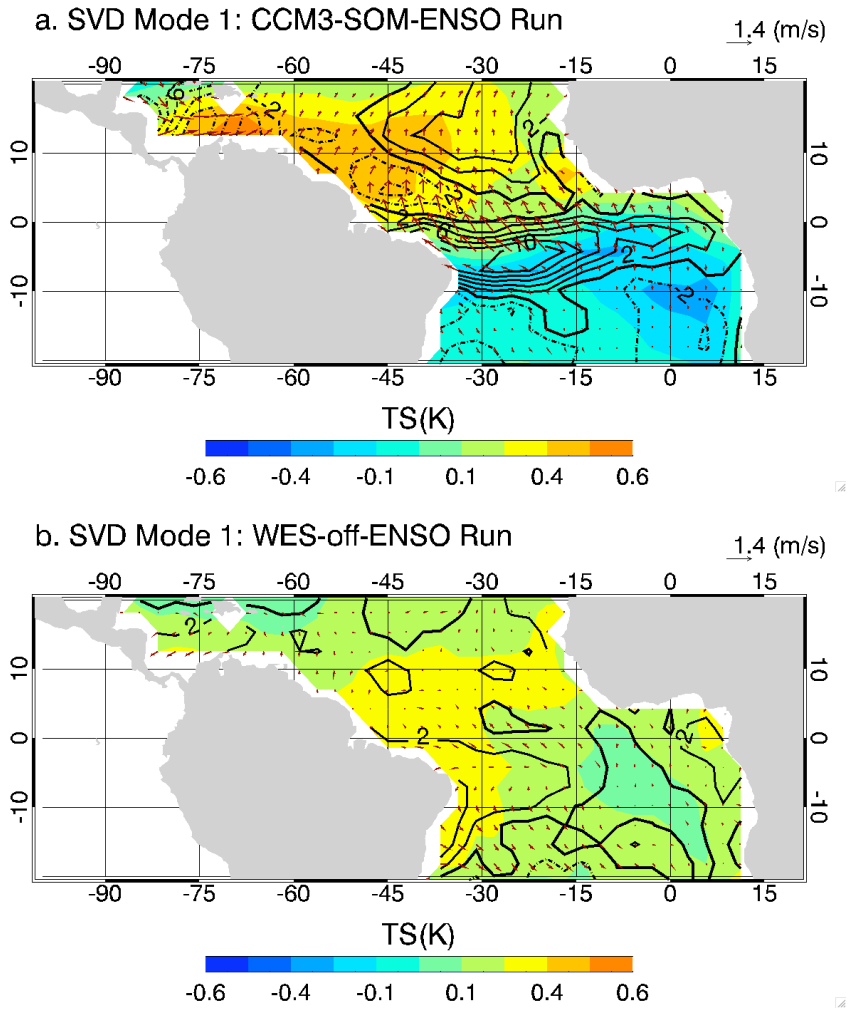

Fig. 27. Spatial pattern of the leading SVD mode of SST and Q_{lh} over the tropical Atlantic for **(a)** CCM3-SOM-ENSO run and **(b)** WES-off-ENSO run. SVD is performed on the cross-covariance matrix of SST and Q_{lh}. The wind pattern is obtained by regressing the normalized time-series of the leading principal component of SST on the zonal and meridional winds. The colors indicate SSTs, and the contours represent Q_{lh} (contour interval: 2 W/m^2). Negative contours indicate warming of the ocean mixed layer. The arrows indicate the change in winds per standard deviation change of the principal component of SST of the leading SVD mode.

Atlantic up to 20° N, and off the Canadian coast in the extra-tropics centered around 40° N and 60° W, strengthening progressively and displaying a maximum response in April-June, peaking at about 0.4 K off the coast of west Africa between the equator and 10° N, and about a 0.6 K off the Canadian coast (Figure 28a). Cooling is seen in the Caribbean Sea, and off the south-eastern coast of the US. This tri-banded response in the Atlantic in response to ENSO has been reported in observational studies (Lau and Nath, 2001; Wallace et al., 1990; Deser and Blackmon, 1993) as well as modeling studies (Lau and Nath, 2001). While the warming in the north tropical Atlantic and cooling in the Caribbean and off the south eastern coast of the US in response to ENSO is consistent among all studies focusing on the Atlantic, the warming off the Canadian coast is not always evident. Lau and Nath (2001) analyzing COADS data and GFDL MLM simulations find a warming of about 0.3° K off the coast of Canada in both observations and model output, a few degrees north of the peak CCM3 SOM response shown here. Alexander and Scott (2002), however, do not see such a response in their analysis of NCEP SST, and the same GFDL model, in fact they see a mild cooling in the region (their Figure 1). The difference in those two studies is likely because of the different SST data analyzed, as their methodologies, with Lau and Nath using regression analysis and Alexander and Scott using composite analysis, are similar. An analysis of ERSST dataset, which is derived from COADS data also reveals a tri-band pattern as seen in Figure 29 with milder warming as compared to that seen in CCM3 simulation here and the analysis of Lau and Nath (2001). A cooling in the higher latitudes as seen in the analysis of (Lau and Nath, 2001) is missing in ERSST analysis, which is also not seen in their MLM simulations, indicating the weak influence of ENSO in the region.

While a strong dipole pattern as suggested by the SVD analysis of SST and Q_{lh} is not evident in the regression analysis over the deep tropical Atlantic in SST, a strong

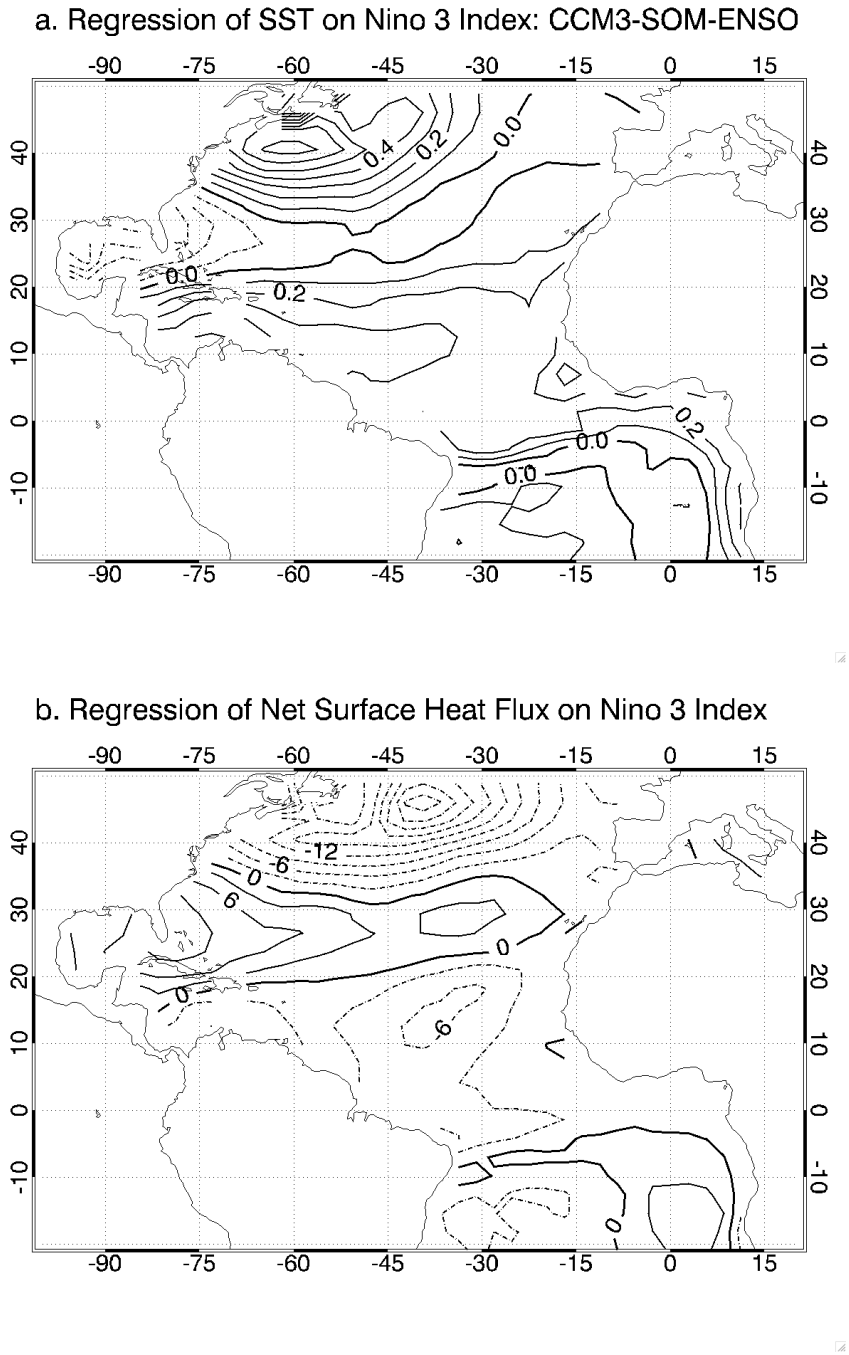

Fig. 28. Regression of **(a)** April to June averaged SST (contour interval: 0.1 K) and **(b)** January to March averaged net surface heat flux (contour interval: 3 W/m^2) against the January Niño 3 index for the CCM3-SOM-ENSO integration.

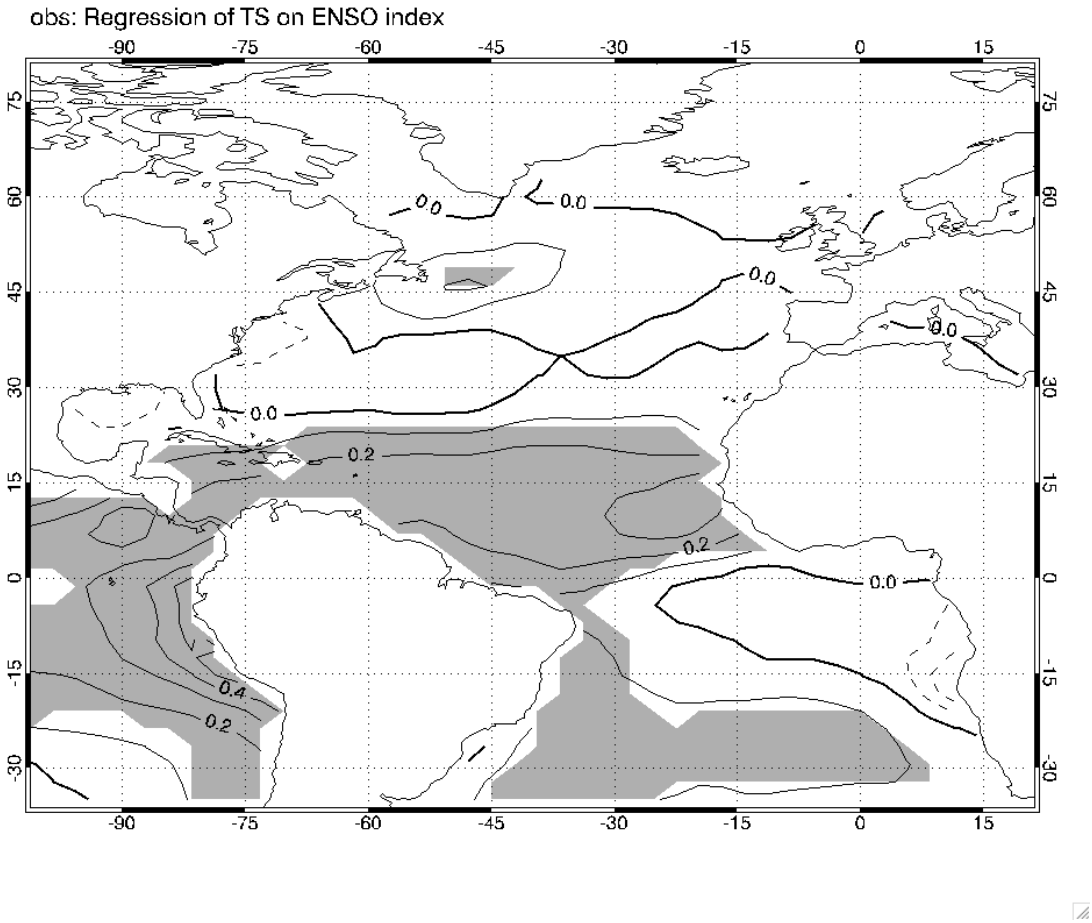

Fig. 29. Regression of observed Atlantic SST (K) averaged over April to June against the January Niño 3 index for the ERSST data-set. Shaded areas represent statistically significant responses at the 95% confidence level based on the two-tailed t-test.

cross-equatorial meridional SST gradient is observed, with warming in the northern equatorial Atlantic and a mild cooling in the southern side. Ocean dynamics such as Ekman pumping do not exist in the SOM. Hence, a change in SST in the Atlantic ocean in the model is a result only of changes in the surface heat fluxes associated with ENSO and is delayed by a few weeks because of the thermal capacity of the mixed layer depth. Figure 28b shows the regression of the net surface heat flux over the Atlantic against the Niño 3 index for the January to March period which results in the SST anomalies in the April to June period (Figure 28a). It should be noted that the lack of local Ekman pumping in the SOM causes biases in the response of the oceans to external forcings. For example, Lau and Nath (2001) in their study using the GFDL-SOM show a weak response in the region off the coast of Africa, caused by the lack of Ekman downwelling associated with reduced winds in the SOM in response to ENSO, and the thicker 50m mixed layer ocean in the region. The response of the CCM3-SOM in the region is close to that of observations, probably because of the shallow mixed layer, at about 10m in the region (Figure 3), responding with stronger temperatures even with weak surface flux anomalies of about 2 W/m^2.

A decomposition of the contribution of individual surface heat flux components during January to March reveals that Q_{lh} is dominant in the tropical Atlantic, with Q_{sh} playing a major role over mid-latitude Atlantic. Q_{sw} and Q_{lw} play a secondary role over the Atlantic during these months except in the south tropical Atlantic, where Q_{sw} anomalies are strong, as shown in Figure 30c and various other studies, probably caused by the reduction in convective clouds in the region forced by the subsidence associated with the change in the walker circulation during El Niño events (Curtis and Hastenrath, 1995; Enfield and Mayer, 1997; Klein et al., 1999; Saravanan and Chang, 2000). A dipole pattern in the Q_{lh} anomalies over the deep tropical Atlantic is observed as suggested by the SVD analysis, but is counter-acted by Q_{sw} to reduce

the magnitude of the pattern in the net surface heat flux anomalies (Figure 28b). Q_{lh}, which is dependent on the surface winds and Δq, can be further partitioned to analyze the influence of winds. ENSO events are associated with the development of high surface-pressure anomalies in mid-latitude Atlantic and south of 15°N, and low surface-pressure anomalies in the subtropical north Atlantic, causing geostrophic anomalous easterlies over the mid-latitudes, south-westerlies in the eastern subtropical Atlantic, north-westerlies in the Gulf of Mexico and the Caribbean sea, and south easterlies over the equatorial Atlantic, where the geostrophic balance does not hold (Figure 31a). The associated anomalous flow decreases surface wind speed over most of the north Atlantic working to reduce the ocean to air latent heat fluxes, and increases the wind speed over the equatorial south Atlantic increasing the ocean to air latent heat fluxes (Figure 30a) suggestive of the existence of the WES feedback.

The onset of an El Niño event also causes widespread changes in the surface specific humidity over the Atlantic (Figure 31b) caused by the transport of moisture from the Pacific through the change in the Walker circulation. The drying in the Gulf region and off the coast of south eastern US is presumably caused by the anomalous north westerlies that bring in dry continental air. And, the increase in the surface specific humidity in the mid-latitude Atlantic is possibly caused by the anomalous easterly flow, which reduces the transport of mean flow dry cold continental air and brings in moist warm maritime air from the central mid-latitude Atlantic (Lau and Nath, 2001). Q_{lh} however depends on Δq, and not just surface specific humidity. An increase in the surface temperatures increases q_{sat}. Thus, the eastern mid-latitude Atlantic and north tropical Atlantic would experience increases, while the Gulf of Mexico and the ocean off the southeastern US face a decrease in q_{sat}. Figure 32 shows the contribution to Q_{lh} anomalies during ENSO events by changes in u^* and Δq. ENSO forced changes in Δq largely oppose the effect of changes in u^* and

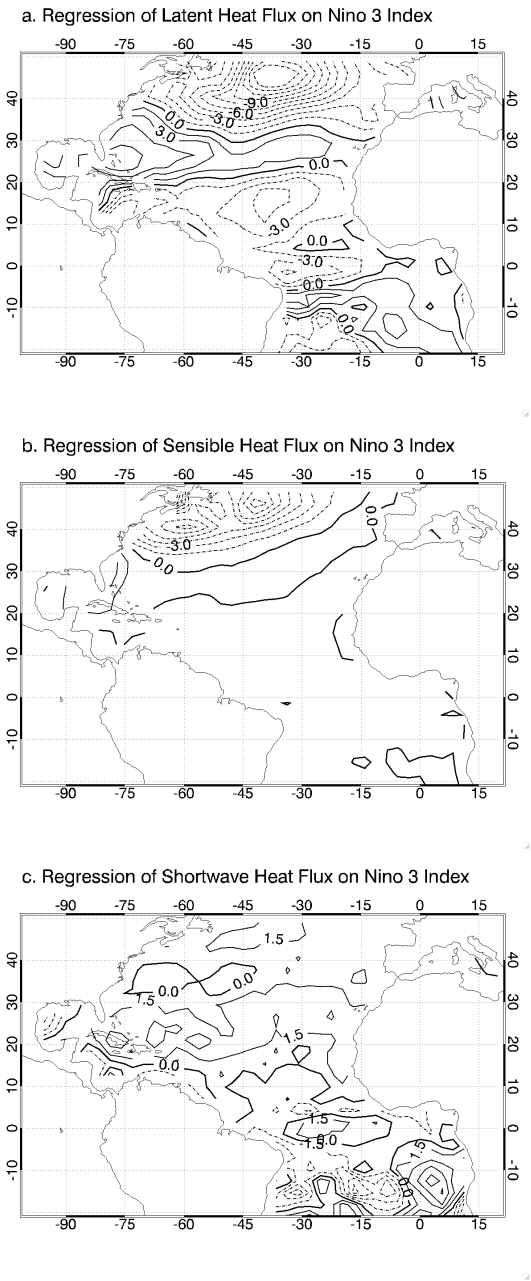

Fig. 30. Regression of January to March averaged **(a)** Q_{lh} (contour interval: 1.5 W/m^2) **(b)** Q_{sh} (contour interval: 1.5 W/m^2) and **(c)** Q_{sw} (contour interval: 1.5 W/m^2) against the January Niño 3 index for the CCM3-SOM-ENSO integration.

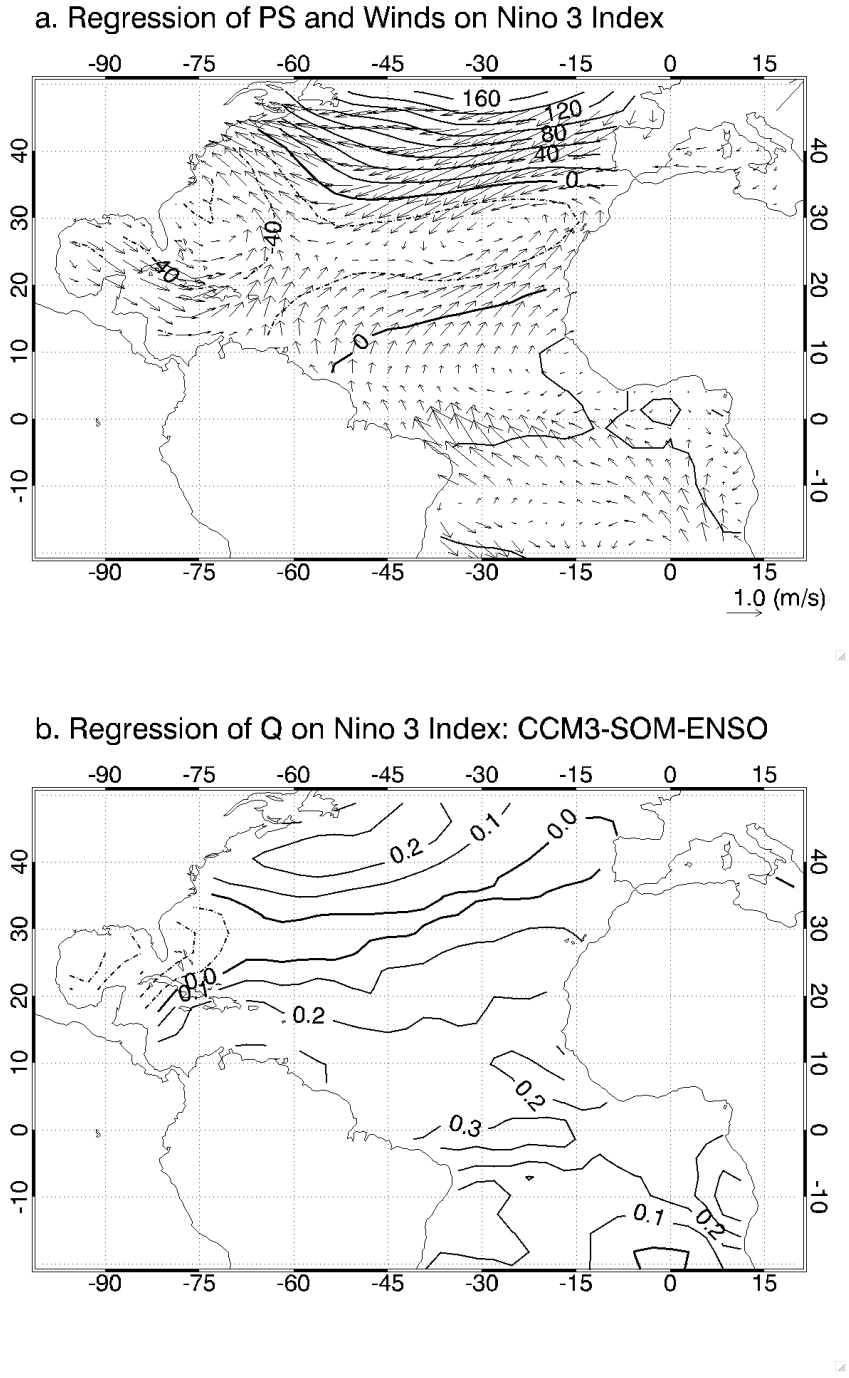

Fig. 31. Regression of January to March averaged **(a)** surface pressure (contour interval: 20 Pa) and winds (arrows) and **(b)** near surface specific humidity (contour interval: 0.1 g/kg) against the January Niño 3 index for the CCM3-SOM-ENSO integration.

hence the WES feedback, on Q_{lh} over tropical Atlantic with the effect of u^* being dominant.Over the central mid-latitude Atlantic ocean both u^* and Δq work to reduce Q_{lh} warming up the oceans. The advected warm maritime air over the ocean off the Canadian coast combined with the reduced wind speeds also causes a reduction of the sensible heat fluxes (Figure 30b), contributing to warming the ocean further.

In the April to June period, when the ENSO associated SST anomalies peak, the net surface heat flux anomalies work to damp the northern Atlantic SST anomalies developed during the previous months as is observed in the SST field over the June to August period (Figure 33). A heat budget analysis reveals that while Q_{lh} is still dominant in these regions, Q_{sw} contributes substantially, particularly to the south equatorial Atlantic ocean net flux (Figure 34), counteracting the cooling effect of Q_{lh}. A further partitioning of Q_{lh} reveals that while in the northern Atlantic changes in Δq govern Q_{lh} (Figure 35b), in the tropical Atlantic Q_{lh} is still governed by winds (Figure 35a). These anomalous northward cross-equatorial winds (Figure 36a) advect moist air from the southern side to the northern side, as seen in the strong northward gradient in the anomalies of q in Figure 36b. Climatologically, the position of the ITCZ displays the largest variation and it travels south of the equator during this period of the year. With the anomalous flow during El Niño events, the convergence shifts northwards. A regression of the simulated convective precipitation against the Niño index (Figure 37) supports these results, showing an increase of precipitation over the north equatorial Atlantic, and a decrease over the southern side, also explaining the change in Q_{sw} caused by the change in the deep convective cloud cover over the tropical Atlantic (Figure 34b). The magnitude of the increase in precipitation on the northern side is less than the decrease seen on the southern side. This anomalous dipole of precipitation and the reduction of precipitation is also seen in observations (Chiang et al., 2002) and noted in other GCM simulation

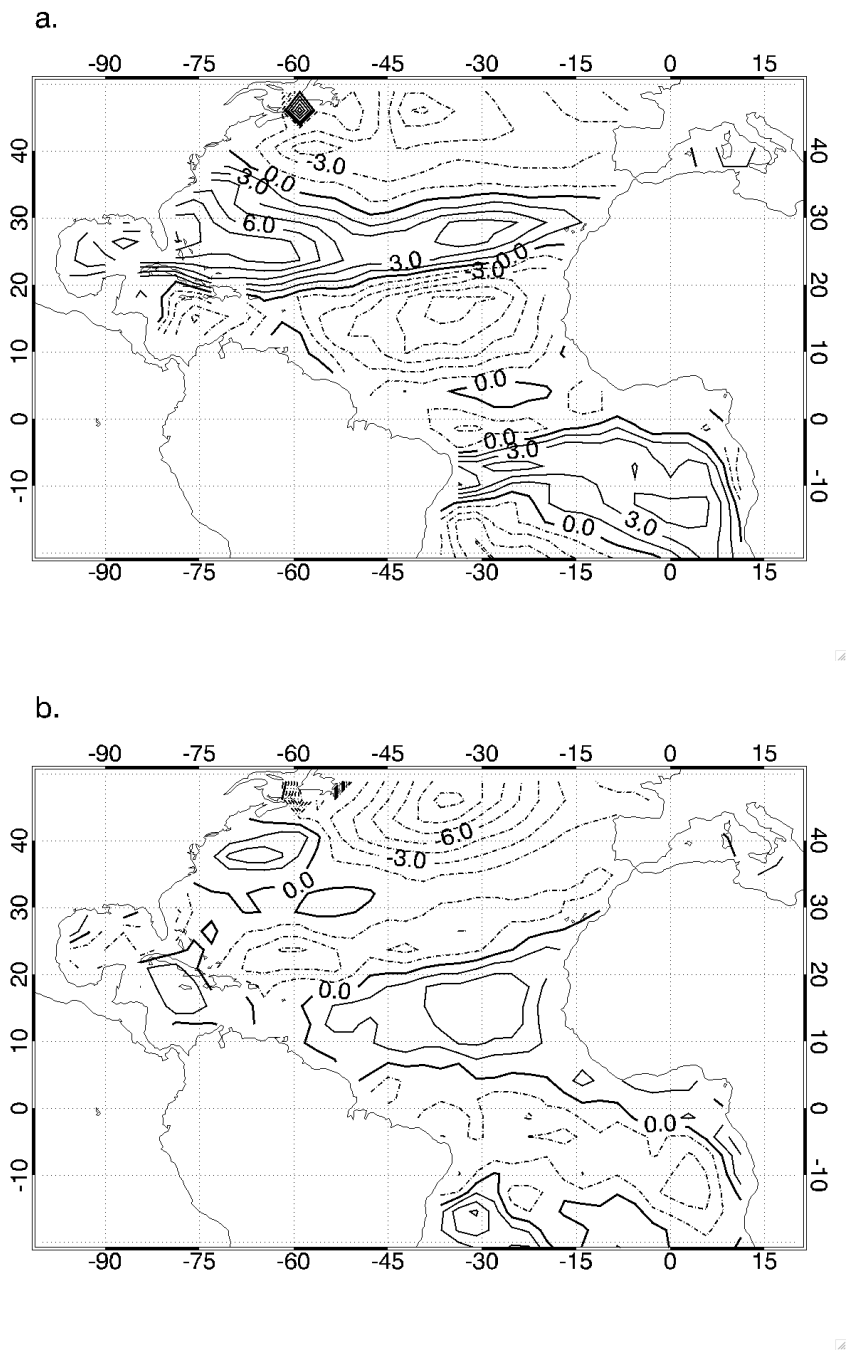

Fig. 32. Q_{lh} anomalies (contour interval: 1.5 W/m^2) caused by fluctuations in **(a)** u^* and **(b)** Δq in the January to March period during ENSO events for the CCM3-SOM-ENSO integration.

studies (Saravanan and Chang, 2000). The reduction in precipitation in the equatorial Atlantic is also associated with the increase in static stability due to the warming of the troposphere over the region and the subsidence associated with the modified Walker circulation during El Niño events (Saravanan and Chang, 2000).

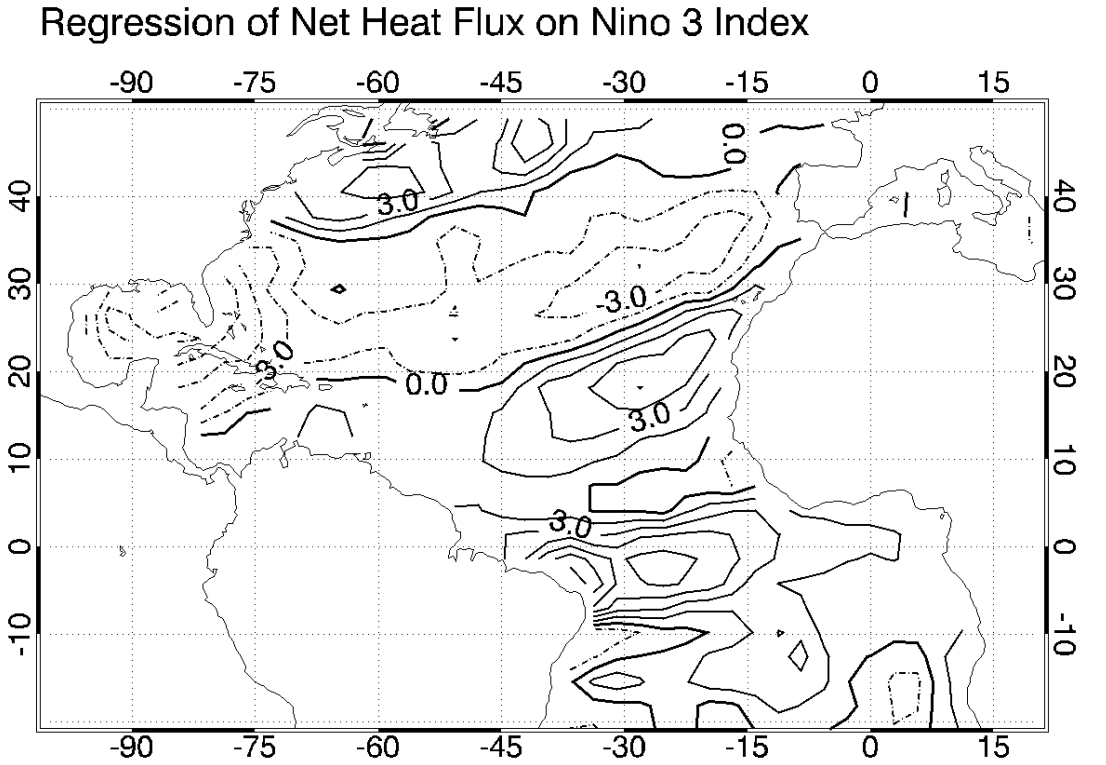

Fig. 33. Regression of April to June averaged net surface heat flux (contour interval: 3 W/m^2) against the January Niño 3 index for the CCM3-SOM-ENSO integration.

The co-location of latent heat fluxes and wind anomalies with SST anomalies developing later in the season, while signifies a cause and effect phenomenon, their

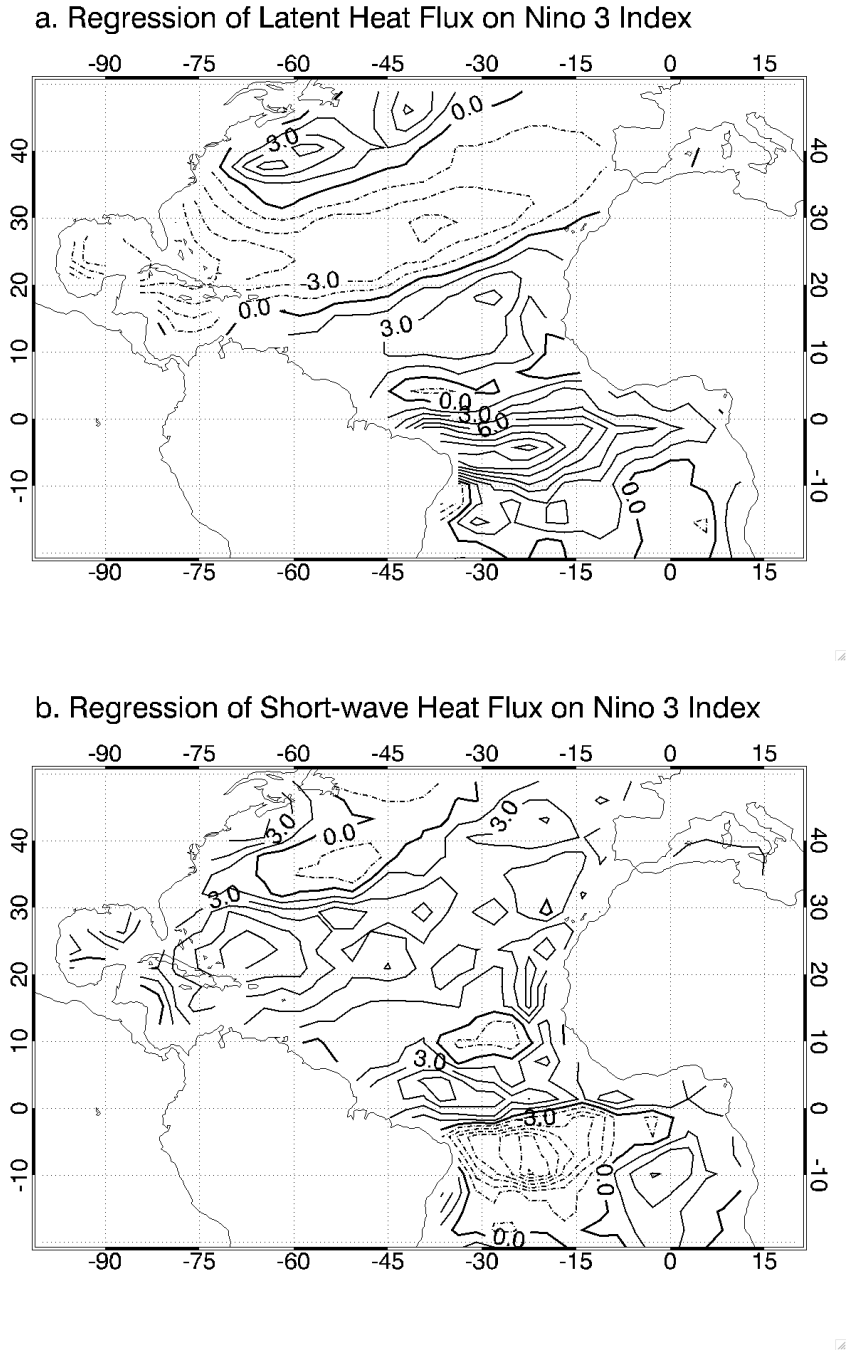

Fig. 34. Regression of April to June averaged **(a)** Q_{lh} (contour interval: 1.5 W/m^2) and **(b)** Q_{sw} (contour interval: 1.5 W/m^2) against the January Niño 3 index for the CCM3-SOM-ENSO integration.

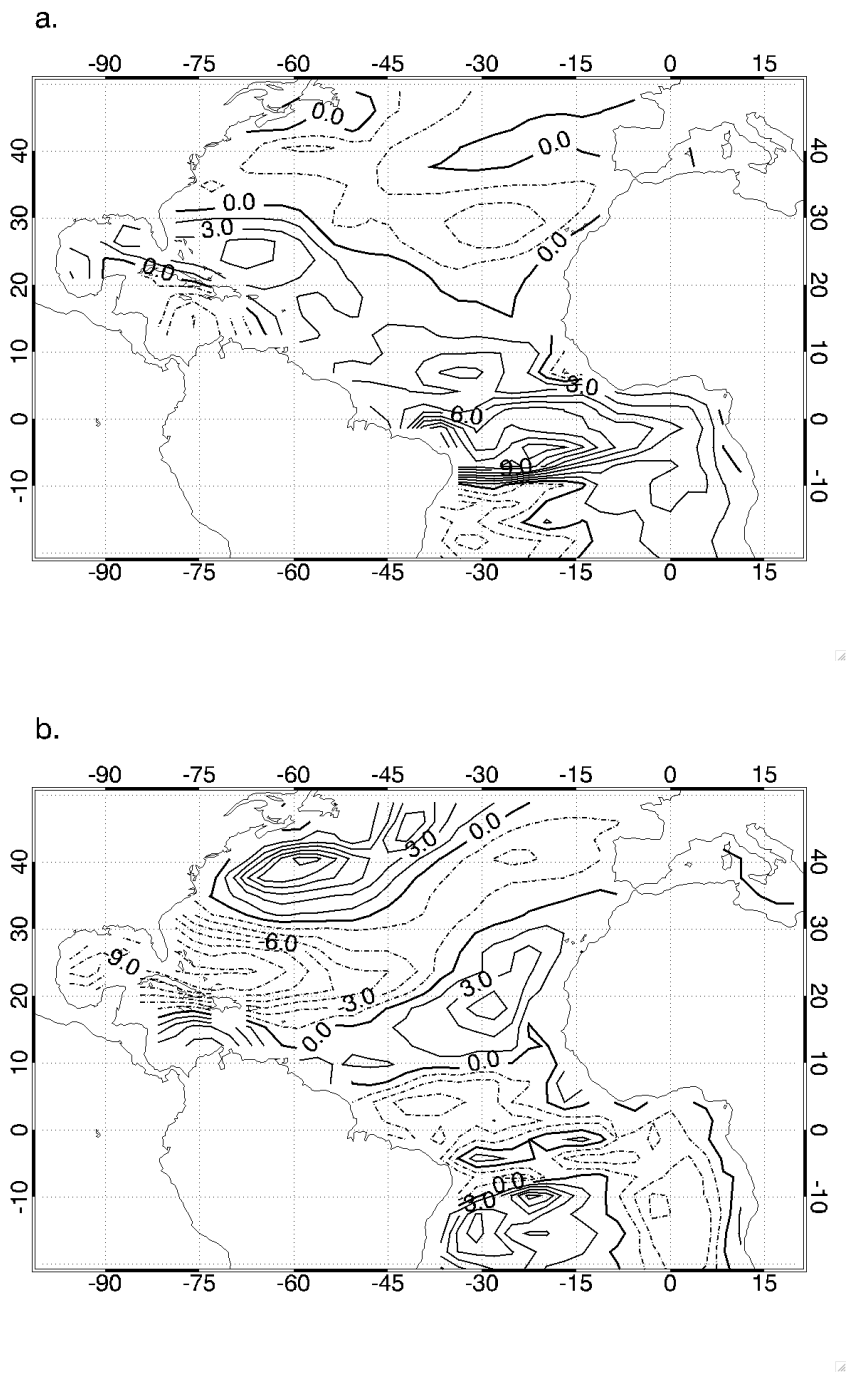

Fig. 35. Q_{lh} anomalies (contour interval: 1.5 W/m^2) caused by fluctuations in **(a)** u^* and **(b)** Δq in the April to June period during ENSO events for the CCM3-SOM-ENSO integration.

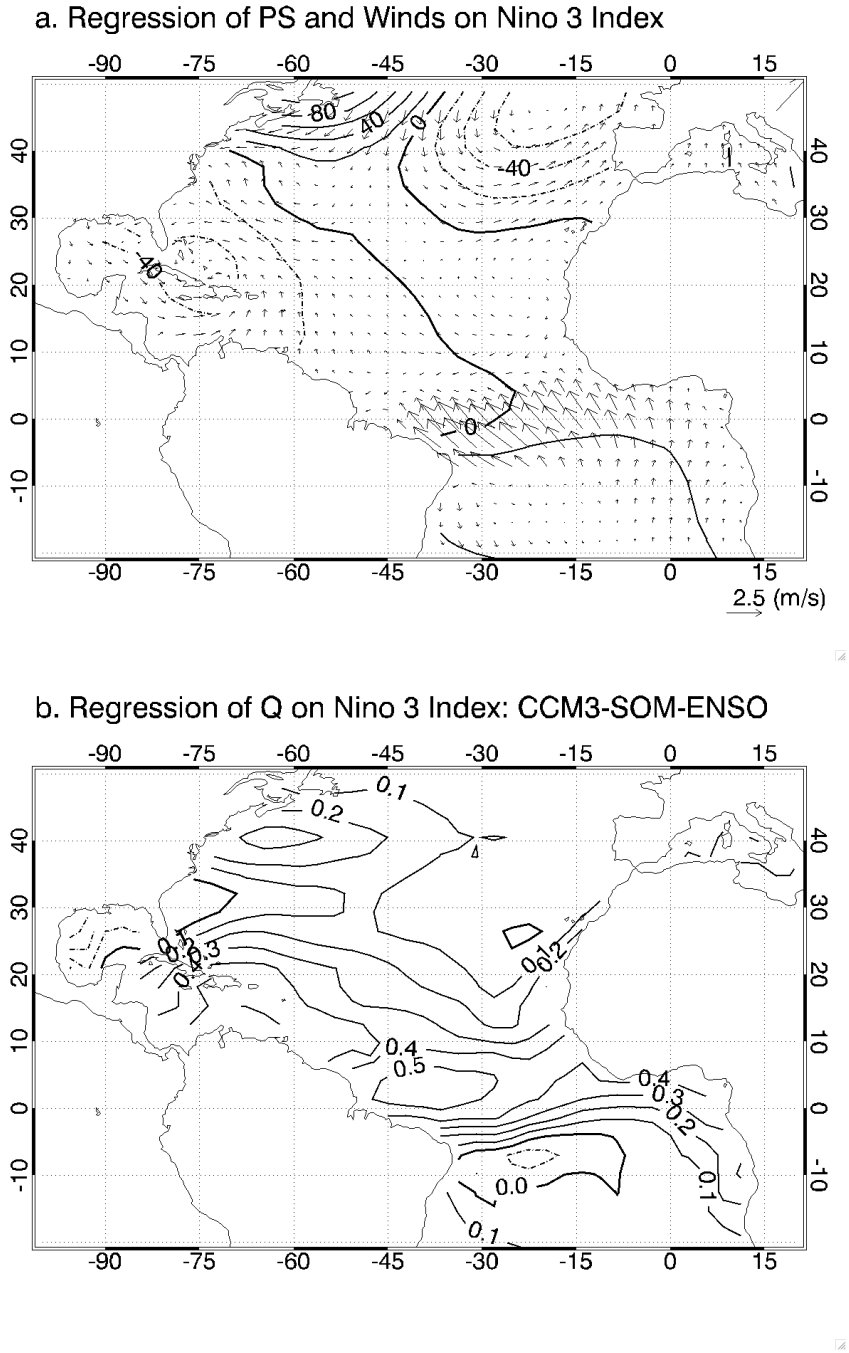

Fig. 36. Regression of April to June averaged **(a)** surface pressure (contour interval: 20 Pa) and winds (arrows) and **(b)** near surface specific humidity (contour interval: 0.1 g/kg) against the January Niño 3 index for the CCM3-SOM-ENSO integration.

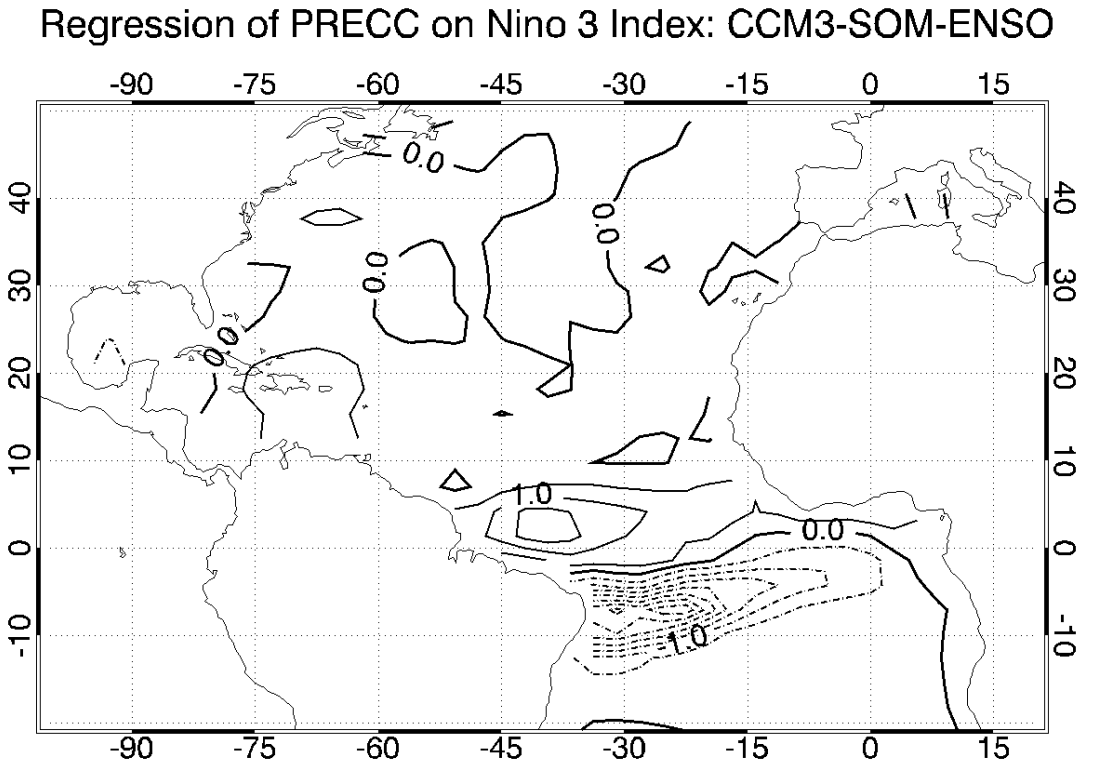

Fig. 37. Regression of April to June averaged convective precipitation (contour interval: 0.5 mm/day) against the January Niño 3 index for the CCM3-SOM-ENSO integration.

amplification is also an indicator of feedback mechanisms like the WES feedback (Chang et al., 1997). From the analysis above, this suggests that the WES feedback is probably active in the western mid-latitude Atlantic, off the coast of Canada, and the north tropical Atlantic, where the reduction in winds cause a reduction in the latent heat release leading to an increase of the SSTs, which in turn cause the winds to reduce further in the January to June period. A potential for an active WES feedback over the south equatorial Atlantic is suggested by the strong wind speed anomalies in the April to June period in response to the anomalous warming north of the equator which cause an increase of Q_{lh} in the south equatorial Atlantic region. But, a response in the SST is not seen, as the increase in Q_{lh} is counteracted upon by Q_{sw} anomalies, caused by reduced convection in the region, reducing the net surface heat flux anomalies. The following analysis of the WES-off-ENSO experiment, elucidates the role of the WES feedback in the above mentioned regions.

4. Tropical Atlantic Response to ENSO in WES-off Experiment

Figure 38a shows the response of the Atlantic ocean SST to the artificial ENSO forcing in the Pacific in the WES-off-ENSO experiment in the April to June period. Anomalous warming of about 0.2 K is observed in tropical and mid-latitude Atlantic. The response is weaker than that observed in the CCM3-SOM-ENSO experiment and observations over the tropical Atlantic. Over the mid-latitude Atlantic, where the CCM3-SOM-ENSO simulation over-estimates the warming of the oceans, SST response in the April to June period is found to be similar to observations. The weak response of SST over the Atlantic is due to the weak surface fluxes in the experiment, as seen in Figure 38b. The strongest net surface flux anomalies are observed over the central mid-latitude Atlantic, where the mixed layer depth is deep, generating modest SST responses. A decomposition of the net surface heat flux indicates that

Q_{sh} and Q_{lw} contribute in relatively small amounts through-out the Atlantic. In the January to March period, however, Q_{sh} contributes considerably over the mid-latitude Atlantic, with its relative contribution being similar to that observed in CCM3-SOM-ENSO integration. The Q_{lh} seems to dominate over other regions of the Atlantic Ocean, with Q_{sw} making little contributions over most of the Atlantic, but, similar to CCM3-SOM-ENSO response, contributing in significant amounts over the south equatorial Atlantic in the April to June period.

Since by experimental design the inter-annual variance of wind speed is disallowed to influence Q_{lh}, a change in the Q_{lh} in response to ENSO events is caused almost completely by the change in Δq. The change in the Q_{lh} and Q_{sh} in the WES-off-ENSO experiment is free of feedback mechanisms associated with the wind speed. However, the winds are free to respond to other forcings. Figure 39a shows the surface pressure field and the associated wind response over the Atlantic to ENSO events for the WES-off-ENSO experiment the April to June period. Differences can be observed in the mid-latitude Atlantic off the coast of Canada from January to June, in the tropical north Atlantic around 15°N from January to March, and equatorial Atlantic during April to June period, where the spatial gradient of the surface pressure anomalies of the WES-off-ENSO experiment are weaker as compared to the CCM3-SOM-ENSO response. These are the regions where the SST and the winds demonstrate strong responses to ENSO in the CCM3-SOM-ENSO integration. In the CCM3-SOM-ENSO integration, warm SSTs in response to El Nino events generate local anomalous low pressure centers in the boundary layer by hydrostatic adjustment (Lindzen and Nigam, 1987), causing increased surface pressure gradients in their neighborhood. The lack of warm anomalies in the WES-off-ENSO experiment prevents the formation of these anomalous pressure systems, and hence causes weaker surface pressure gradients. Hence, the wind anomalies in the WES-off-ENSO experi-

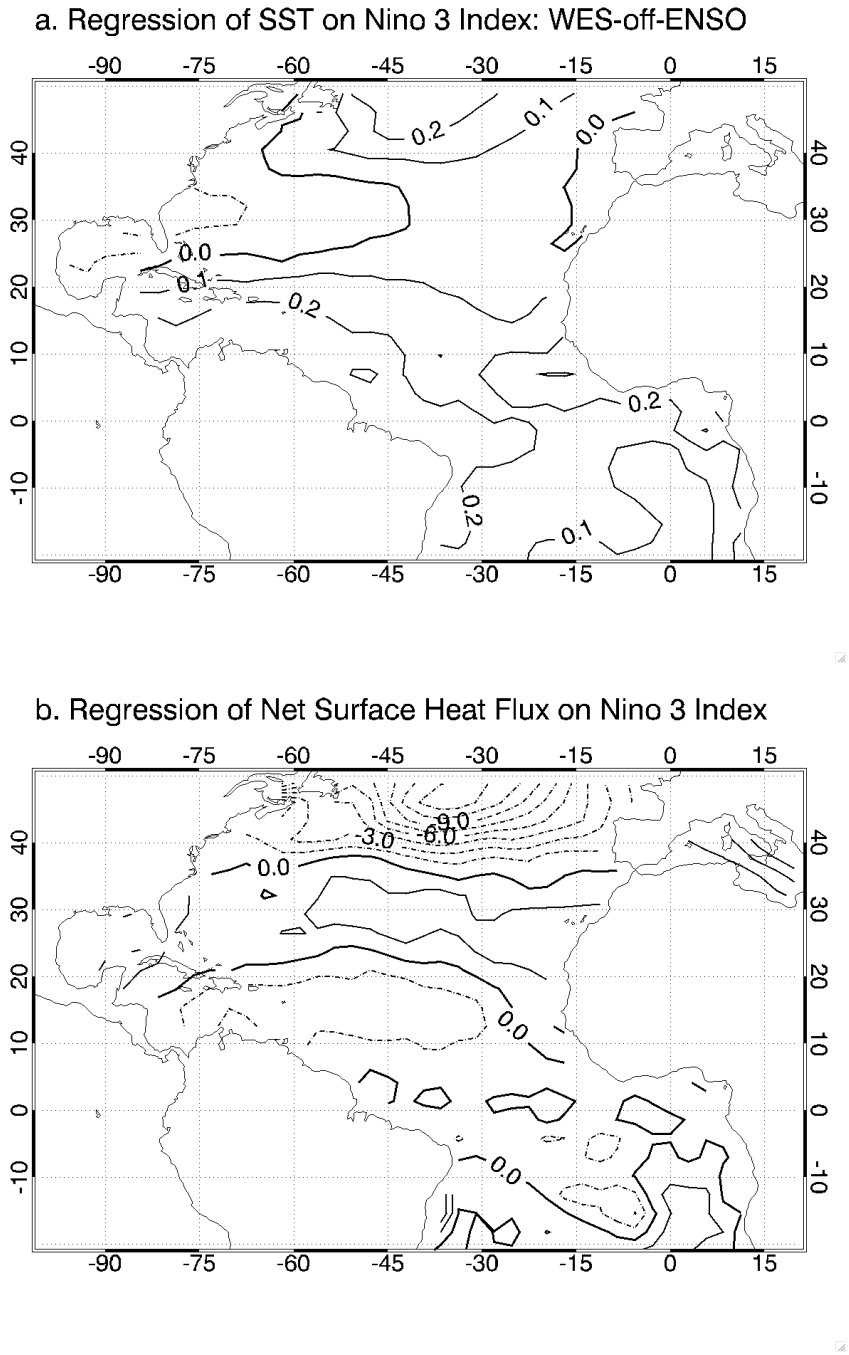

Fig. 38. Regression of April to June averaged **(a)** SST (contour interval: 0.1 K) and **(b)** January to March averaged net surface heat flux (contour interval: 1.5 W/m^2) against the January Niño 3 index for the WES-off-ENSO integration.

ment in these regions in response to weaker anomalous surface pressure gradients are weaker. The wind response to ENSO in these regions in the WES-off-ENSO experiment is found to be weaker by about 50% and more, as can be seen in Figure 39a, as compared to the CCM3-SOM-ENSO run. The weaker response of the winds, Q_{lh}, Q_{sh} and SST to ENSO in the WES-off-ENSO experiment implies that other forcings produce only modest responses in these regions, and strong responses can only be generated in the presence of the WES feedback in CCM3-SOM-ENSO simulations.

The above analysis conclusively indicates that the WES feedback is indeed directly amplifying the SST, latent and sensible heat fluxes and the wind response to ENSO events in the eastern mid-latitude Atlantic off the coast of Canada, and in the northern tropical Atlantic, and equatorial Atlantic in the CCM3-SOM-ENSO simulations by a factor of more than two in the January to June period. The influence of the feedback on wind anomalies also affects the advection of moisture, as can be seen in the regression plot of q against the ENSO index in Figure 39b. Strong gradients of q are seen in the WES feedback impact regions. Off the Canadian coast, the surface air is drier in the WES-off-ENSO experiment as compared to the CCM3-SOM-ENSO simulation, as the wind flow is not amplified in the WES-off-ENSO experiment because of weak advection of maritime air into the region. Over the equatorial Atlantic, the advection of moist surface air from the south equatorial region to the north equatorial Atlantic region is also reduced. A signature of this reduced transport of moisture is also seen in the convective precipitation response in Figure 40 as well as the response of Q_{sw} (not shown). A reduction in the precipitation associated with increased stability and subsidence over the equatorial Atlantic is seen, but the response is weaker as it is not amplified by the transport of moisture associated with the WES feedback from the southern side to the northern side, and hence the positive response of convective precipitation over the north equatorial Atlantic is weak in the

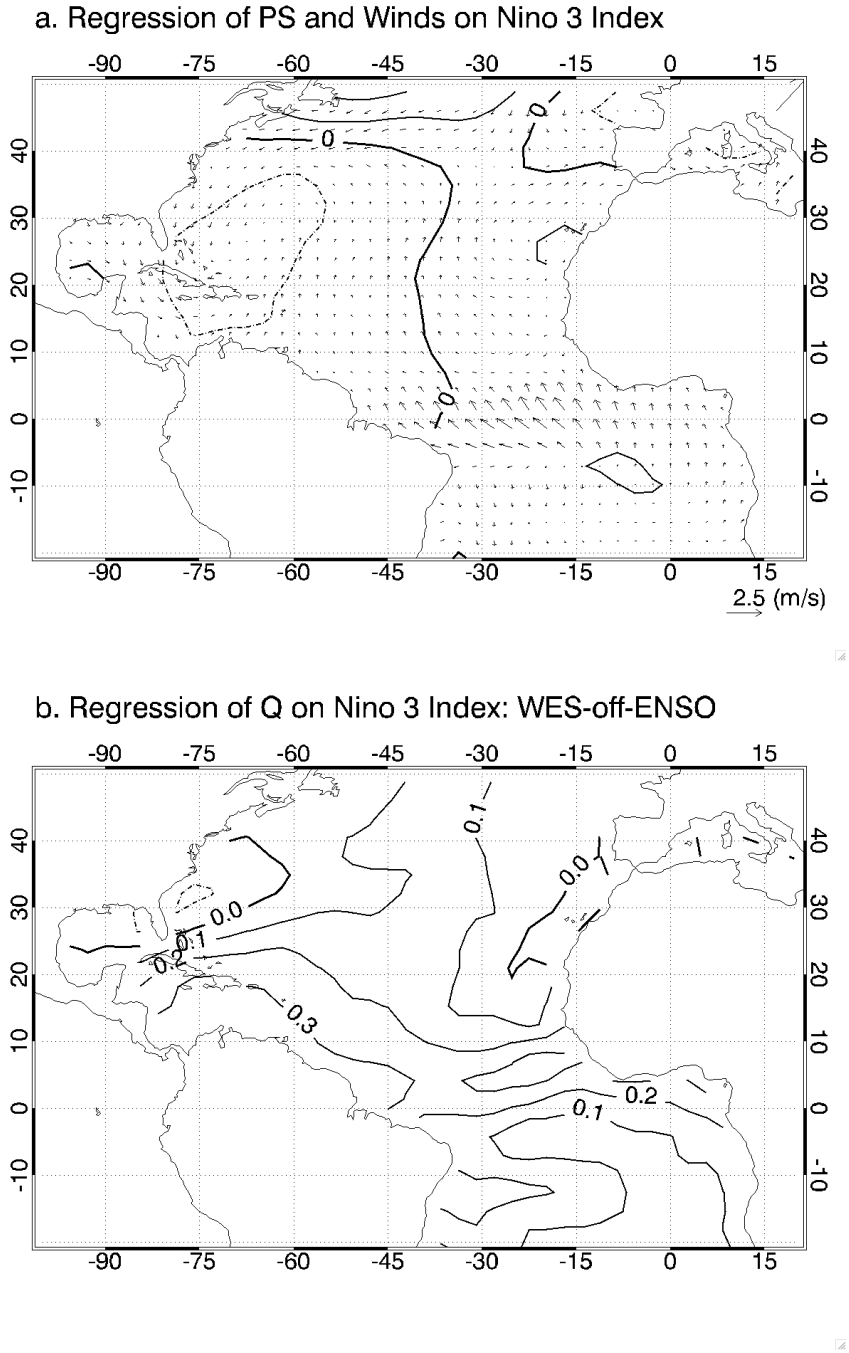

Fig. 39. Regression of April to June averaged **(a)** surface pressure (contour interval: 20 Pa) and winds (arrows) and **(b)** near surface specific humidity (contour interval: 0.1 g/kg) against the January Niño 3 index for the WES-off-ENSO integration.

WES-off-ENSO experiment.

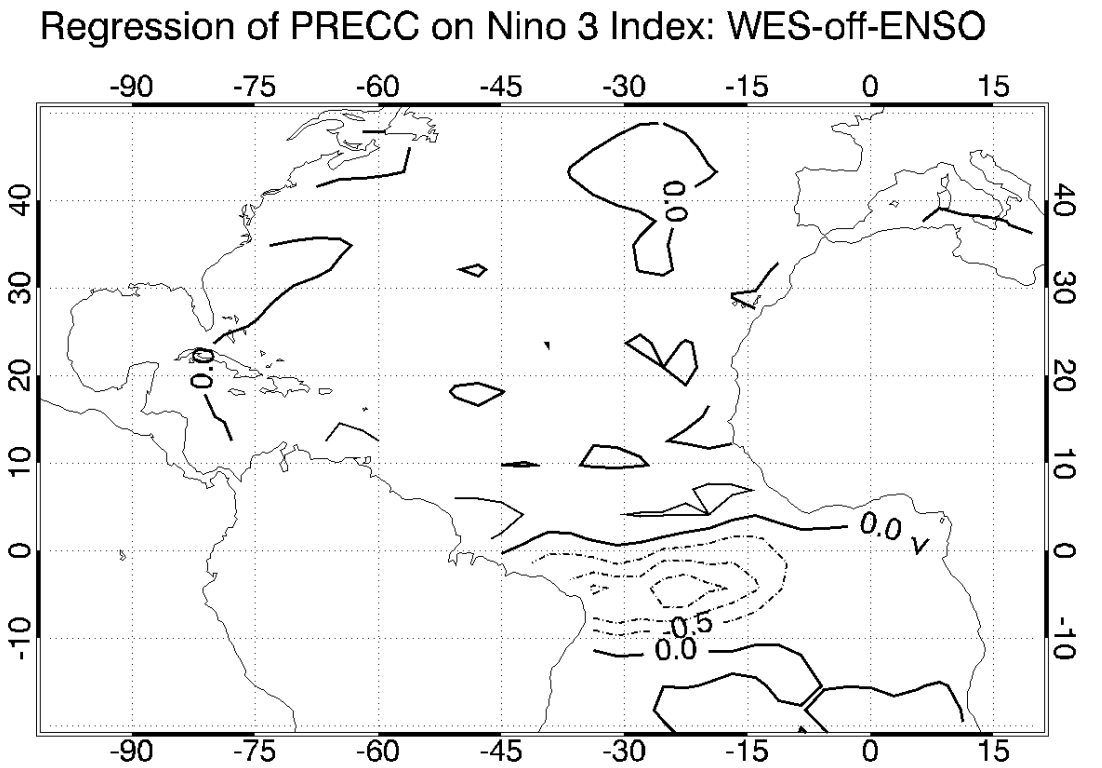

Fig. 40. Regression of April to June averaged convective precipitation (contour interval: 0.5 mm/day) against the January Niño 3 index for the WES-off-ENSO integration.

5. WES feedback in the Boreal Fall Season

Following the January to June period, the developed anomalies decay in the CCM3-SOM-ENSO integration over the Atlantic as is seen in the SST and winds in Figure 41a. Q_{lh} is dominated by Δq instead of u^* over the eastern mid-latitude and the

north tropical Atlantic, causing a reduction of the strength of the WES feedback starting from the month of April. However, the WES feedback seems to be active in the north equatorial Atlantic even in the July to September period, counter-acting the damping caused by humidity, as indicated by the dipole-like collocated anomalies of SST- with a stronger positive polarity on the northern side, and a small negative anomaly of about 0.1 K in the southern side, wind speed and Q_{lh} in response to ENSO events (Figure 41a). The depth of the mixed layer in the region is shallow at about 20m, hence the SST response to surface heat flux anomalies are seen within a few weeks. The mean background trade winds in the region during this period converge at the center of the anomalous dipole, with the south-easterlies flowing on the south side of the dipole and the north-easterlies on the northern side, which along with the dominance of u^* on Q_{lh} (Figure 42) create favorable conditions for the WES feedback to flourish. The wind vector anomalies in response to ENSO in the region resemble the classic cross equatorial WES feedback associated wind anomalies with weaker zonal components as they occur north of the equator. A similar dipole pattern in the WES-off-ENSO experiment is missing, conclusively indicating that the existence of the dipole in the CCM3-SOM-ENSO integration is indeed caused by the WES feedback (Figure 43).

6. Discussion

It should be noted that intrinsic noise variability in simulations here include NAO, which has been found to have its own influence on the tropical Atlantic (Xie and Tanimoto, 1998). This might imply that there is a fair chance that the meridional mode as seen in simulations here might have been generated as a forced response to the NAO rather than being a part of natural tropical Atlantic variability. However, recent studies have shown that the NAO could in fact be influenced by tropical

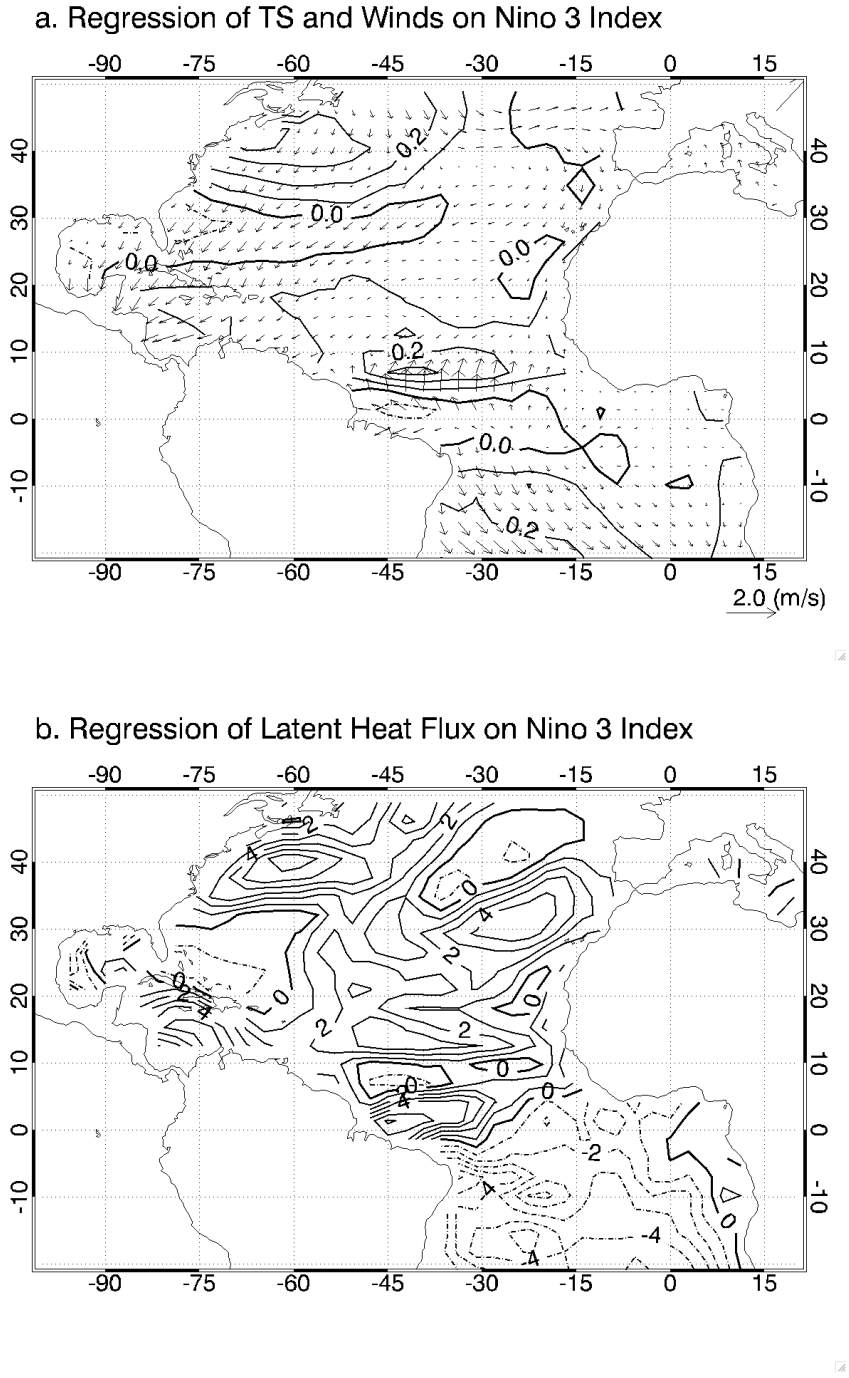

Fig. 41. Regression of July to September averaged **(a)** SST (K) and winds (m/s) and **(b)** Q_{lh} (contour interval: 1 W/m^2)against the January Niño 3 index for the CCM3-SOM-ENSO integration.

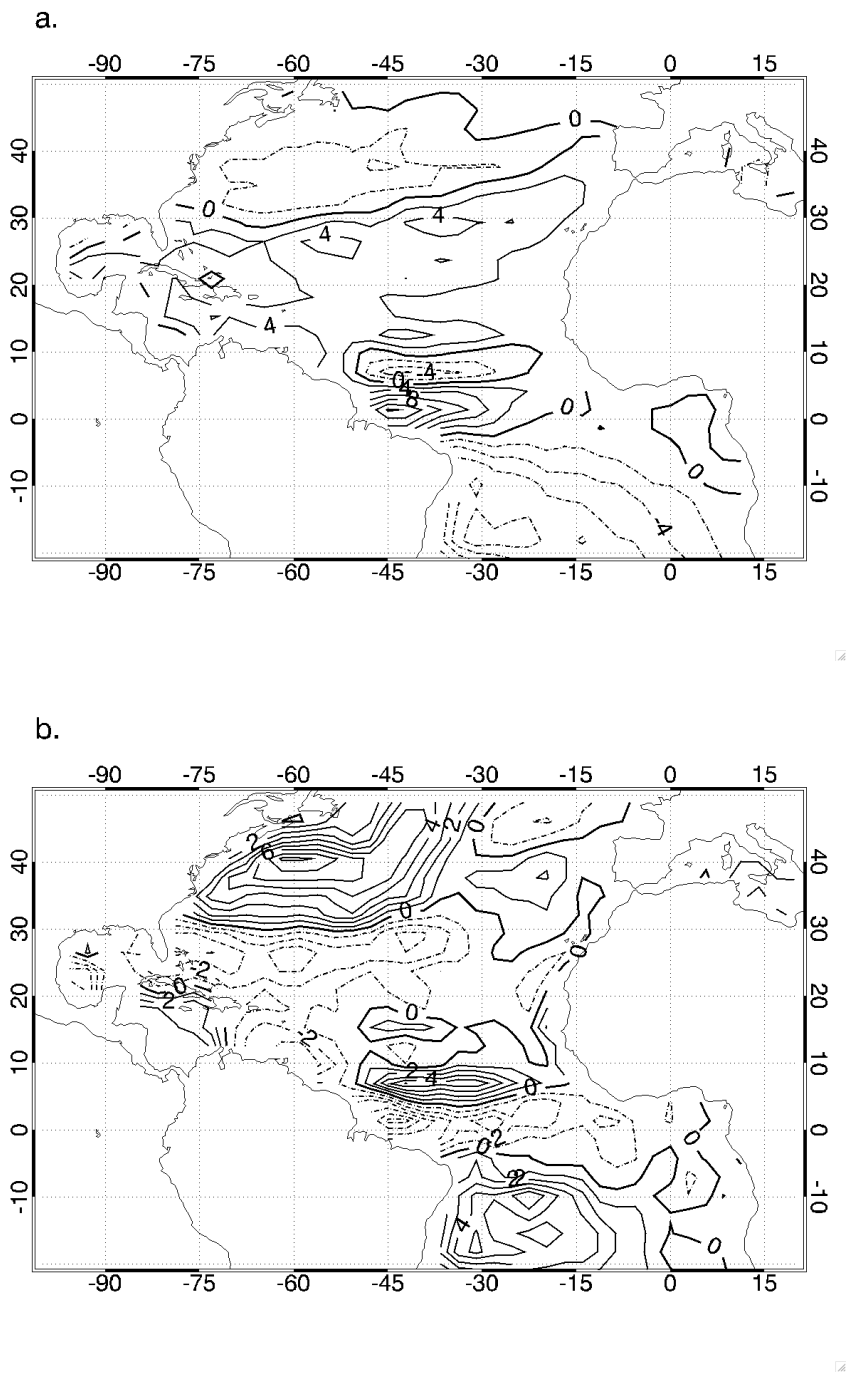

Fig. 42. Q_{lh} anomalies (contour interval: 1.5 W/m^2) caused by fluctuations in **(a)** u^* and **(b)** Δq in the July to September period during ENSO events for the CCM3-SOM-ENSO integration.

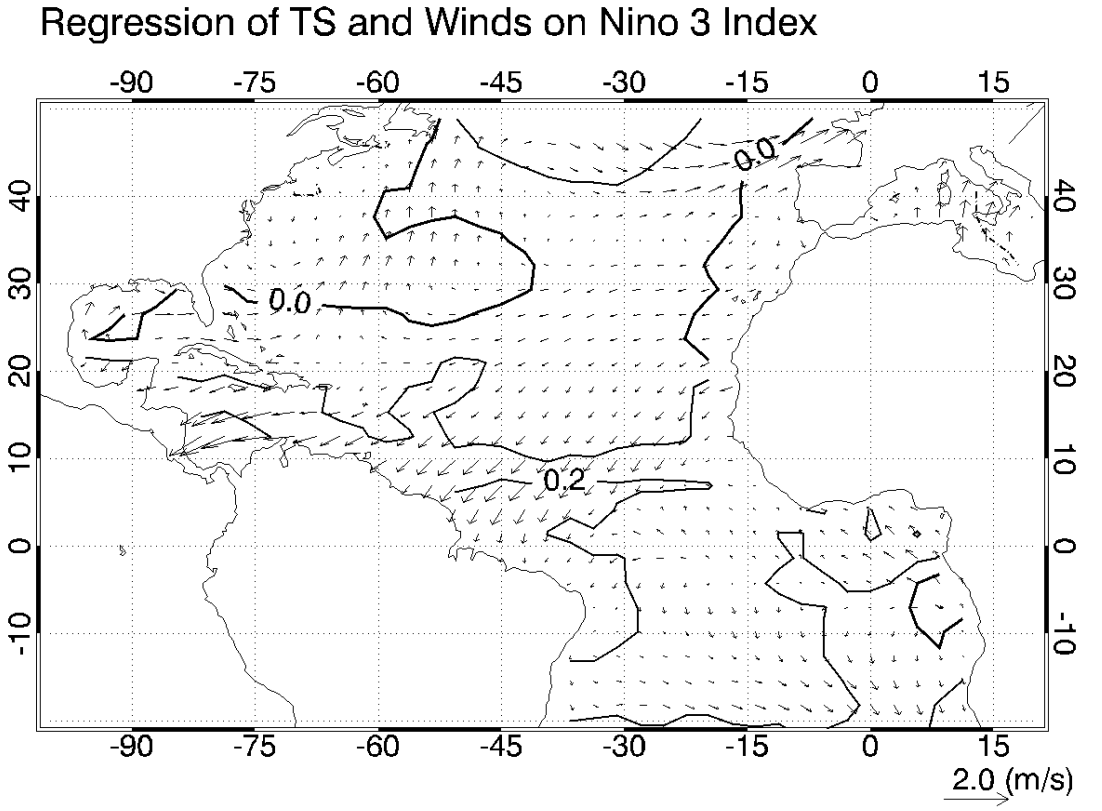

Fig. 43. Regression of July to September averaged SST (contour interval: 0.1 K) and winds against the January Niño 3 index for the WES-off-ENSO integration.

Atlantic variability via tele-connections (Okumura et al., 2001; Rajagopalan et al., 1998). Nonetheless, it is clear that the WES feedback enhances the meridional mode of tropical Atlantic variability, be it free or forced.

Regression of the ENSO index on Atlantic SSTs alone reveals a CESG (Figure 28a) and not a clear meridionally asymmetric response. This result is consistent with the study of Enfield and Mayer (1997) who find only a mild asymmetry in observations of Atlantic SSTs rather than a cross-equatorial dipole. The appearance of a dipole like pattern in coupled variability of free and forced tropical Atlantic climate (e.g. Ruiz-Barradas et al., 2000; Chang et al., 1997) and a lack of the same in independent analysis of SSTs (e.g. Mehta, 1998; Enfield et al., 1999) is consistent with other studies as coupled dipolar configurations only reveal the bivariate relationships between SSTs and atmospheric variables (Enfield et al., 1999). The development of an anomalous CESG in CCM3-SOM-ENSO simulations over the tropical Atlantic in response to ENSO is found to be critically dependent on the WES feedback, in the absence of which CESG is found to be weaker, consistent with the SVD analysis. Without the feedback the response appears to be primarily governed by the change in the static stability of the troposphere caused by global tropospherical changes associated with ENSO events (e.g. Chiang and Sobel, 2002) and subsidence over the tropical Atlantic due to change in the Walker circulation during El Niño events (e.g. Klein et al., 1999).

The changes in the eastern mid-latitude Atlantic off the Canadian coast during ENSO events have not yet been associated specifically to the WES feedback in previous studies, although the existence of feedbacks in the region has been known (Lau and Nath, 2001). While the warming in the region in other modeling and observational studies confirm the active presence of the WES feedback in the mid-latitude Atlantic, the precise location and the magnitude of the response associated with the feedback remains uncertain as suggested by the varied responses among different stud-

ies. From the analysis here, the difference in the response of SST off the Canadian coast to ENSO forcings between the CCM3-SOM-ENSO integration and WES-off-ENSO experiment, with exaggerated SST responses in the CCM3-SOM-ENSO integration and modest observation-like response in the WES-off-ENSO experiment, suggests that the manifestation of WES feedback is probably inflated in this region in CCM3-SOM. The dominant role of the WES feedback in the region in CCM3-SOM could also probably be due to the lack of ocean dynamics in the model, and reduced atmospheric damping of SST in the region by the model. An analysis of dynamically coupled atmospheric-ocean models, proposed for a future study, would be helpful in increasing our understanding. More attention also needs to be paid to the accurate simulation of the thermodynamic WES feedback in climate models for improved climate prediction on seasonal time-scales.

The existence of a dipole in the north equatorial Atlantic in the months of summer and early fall, as seen in the CCM3-SOM-ENSO simulation has also not been reported before. Xie and Carton (2004) in their review study conclude that the WES feedback is weak in the equatorial Atlantic and cannot sustain the cross-equatorial gradients through the summer. While the analysis here reveals the WES feedback as the mechanism behind the dipole, it is probably able to manifest itself in the region because of the lack of water transport by surface currents in the SOM, a counteracting mechanism to the WES feedback, allowing the thermodynamic interaction of atmosphere-ocean system to dominate and generate its own modes of variability.

The atmospheric bridge connection between the tropical Pacific and North Atlantic in the WES-off-Experiment could have been modified due to the absence of WES feedback in the Pacific as well. The role of the WES feedback in the Pacific is worth considering as the presence of air-sea feedbacks in the region have been demonstrated in modeling studies, where the atmospheric anomalies in the presence

of interactive oceans persist longer (e.g. Lau and Nath, 2001; Bladé, 1997). However, the amplitude of the feedback is quite modest (Alexander et al., 2002). If the WES feedback is active in the North Pacific, the atmospheric and SST response of the North Pacific to ENSO events in the WES-off-ENSO experiment are also reduced, changing the atmospheric circulation and possibly impacting the response in the North Atlantic as well. Further study of the WES feedback over the Atlantic, isolated from the remote forcing of the North Pacific is needed.

B. Tropical Response to High Latitude Sea-ice Induced Cooling

1. Experimental Set-up

Two sets of experiments with additional sea-ice in the northern latitudes are performed, where high latitude cooling is achieved by placing additional sea-ice in the higher latitudes, to clearly isolate the proposed roles of the WES feedback mechanisms in the propagation of high latitude signals to the tropics. In the first experiment, a monthly climatology of sea-ice cover in CCM3-SOM over the northern high-latitudes corresponding to the last glacial maximum as interpolated from the February and August reconstructions of LGM sea-ice cover derived from the CLIMAP data (Hostetler and Mix, 1999) as seen in Figure 44 is prescribed. It is noteworthy that most of the additional sea-ice occurs over the north Atlantic Ocean, consistent with the local response of a weakening of AMOC. The prescribed LGM sea-ice run is referred to as the CCM3-SICE run. Following (Chiang et al., 2003), other boundary conditions like orbital parameters, ice-topography and green-house gases are kept the same as the modern climate to study the impact of additional sea-ice in isolation. The second experiment features exactly the same set-up as the first experiment, but with the modified WES-off model, and is termed as WES-off-SICE run. To study

the equilibrium state of the sea-ice forced run, one run of 45 years for each of these experiments is made. In addition, 3 more ensemble runs are carried out, each with a different atmospheric initial condition, of both the experiments to study the transient response of the models. All the runs were prescribed with Q-fluxes in the SOM that force the model to follow present day SST climatology. Most paleoclimate AMOC slowdown experiments use today's climate as the mean state of their models for inter-comparisons, even though the LGM climate might be cooler than the current climate (Stouffer et al., 2006). Since the goal of the study is to isolate a particular thermodynamic mechanism, modest differences of background mean-state are likely to have little impact on the results. Hence, the current climate is considered to be the mean-state for the simulations similar to other AMOC slowdown experiments.

2. Mean-state Response

CCM3-SICE, which was forced with northern high latitude LGM equivalent sea-ice boundary condition reaches a new equilibrium state within a period of 5 years, consistent with that noted by Chiang and Bitz (2005) in a similar study. Figure 45 shows the change in the annual-mean SST averaged over 40 years of simulation of the sea-ice perturbed run after reaching equilibrium, as compared to the mean state of the control run CCM3-SOM. A cooling is observed over all northern hemispheric oceans when sea-ice is imposed at higher latitudes, broadly consistent with other AMOC slowdown experiments (Stouffer et al., 2006). Over the equatorial oceans, the development of an anomalous cross-equatorial SST dipole across global oceans, with cooling (warming) in the northern (southern) side is found, again consistent with other AMOC slowdown experiments (e.g. Vellinga and Wood, 2002; Zhang and Delworth, 2005). Particularly strong cooling of about 1 K in the central Pacific and a strong warming of about 0.5 K in the eastern Pacific ocean is observed, consistent

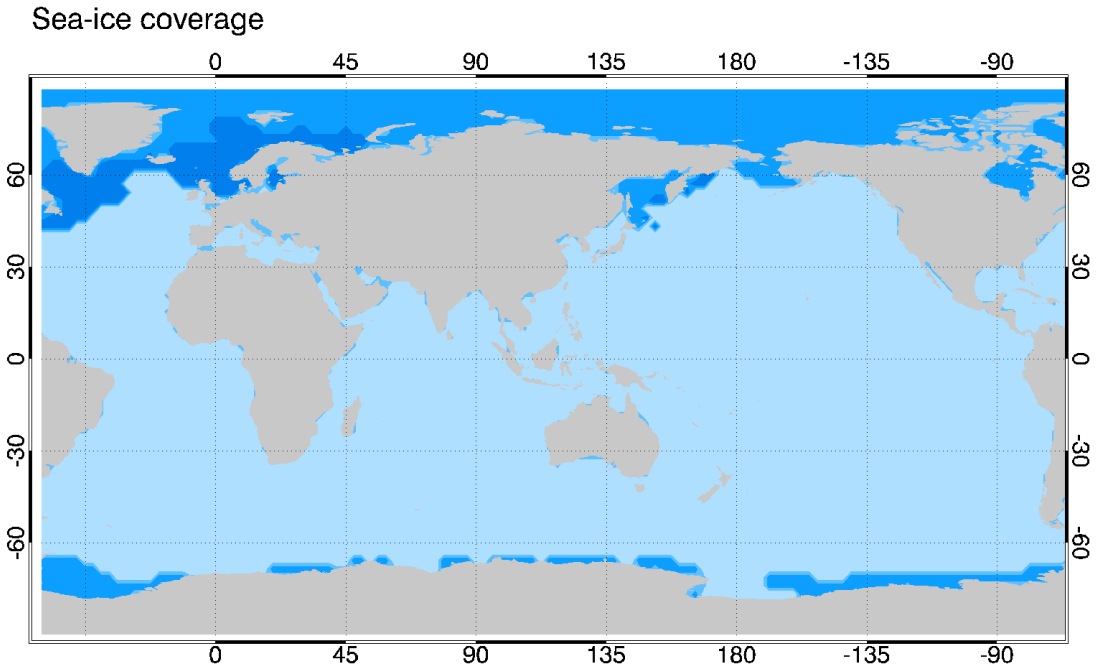

Fig. 44. Prescribed sea ice cover climatology for sea-ice experiments replicating the northern hemisphere Last Glacial Maximum (18 kyr BP) sea-ice cover derived from CLIMAP data for the month of January. The open ocean is represented in light blue color. Darker shade represents additional sea-ice as compared to the modern day sea-ice cover.

with the simulation carried out by Chiang and Bitz (2005).

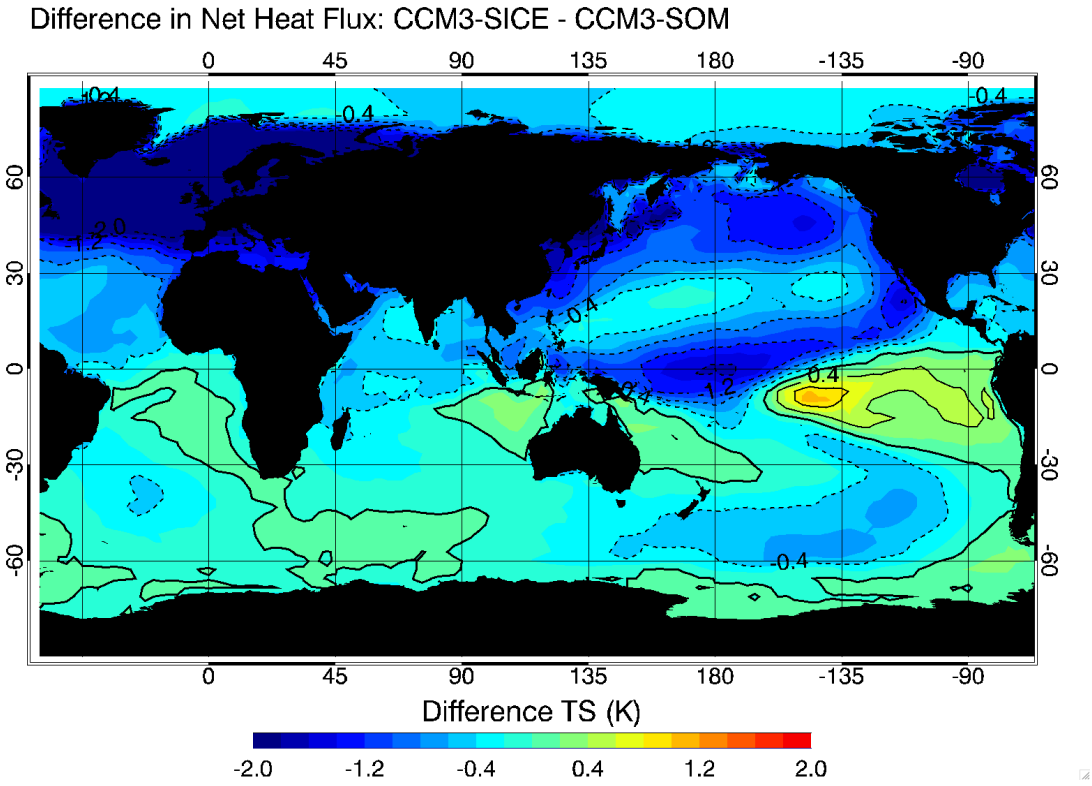

Fig. 45. Difference (CCM3-SICE - CCM3-SOM) in annual mean SST between the equilibrium state of LGM sea-ice forced simulation (CCM3-SICE) and the equilibrium state of the unperturbed control run (CCM3-SOM). Contour intervals are 0.4 K.

The anomalous meridional asymmetry in the eastern tropical Pacific SST is consistent with the result of other similar experiments such as that of Zhang and Delworth (2005), who also find a similar response in the GFDL coupled model, albeit to a shutdown of the AMOC, but which causes cooling in the north Atlantic - a forcing similar in effect to sea-ice prescribed perturbation here. However, when they couple their GFDL AGCM to a SOM (AGCM-SOM), a very weak response is seen in the

tropical Pacific, possibly indicating a weaker thermodynamic air-sea coupling over the eastern Pacific in the GFDL AGCM-SOM as compared to the CCM3-SOM. Also, the warming over the south-equatorial Atlantic in CCM3-SICE is mild, and does not compare well with the warming observed in AMOC shutdown experiments (e.g. Zhang and Delworth, 2005; Vellinga and Wood, 2002), where a warming of about 2 K is observed over the south-tropical Atlantic. The results here are however, consistent with the modeling results of Chiang and Bitz (2005), who also use CCM3 coupled to a SOM. A stronger role for ocean dynamics in the tropical response to high latitude forcings is however not obvious, as in the GFDL AGCM-SOM experiment Zhang and Delworth (2005) still find a strong warming in south equatorial Atlantic. Distinct responses of CCM3-SICE and the GFDL AGCM-SOM indicate different physical and thermodynamical mechanisms at play in different models, a clear understanding of which would require further in-depth comparative studies.

The equilibrium state of CCM3-SICE experiment also exhibits a southward shift of tropical precipitation over global oceans in the CCM3-SICE experiment as compared to the CCM3-SOM run (Figure 46). The southward transition of the ITCZ in response to northern sea-ice anomalies is consistent with the findings of experiments performed by Chiang et al. (2003); Chiang and Bitz (2005) and that of AMOC slowdown experiments (e.g. Vellinga and Wood, 2002; Dahl et al., 2005) and follows the equilibrium state SST anomalies. Cooling of the northern equatorial oceans in the CCM3-SICE experiment reduces the northward preference of the ITCZ, as the SST is prevented from reaching the deep convective threshold in the northern equatorial oceans, thus making the ITCZ more symmetric about the equator. The increased SST in the south equatorial oceans also appears to be conducive to the increased convective precipitation in the region. The strongest response in the shift of tropical convective precipitation is seen in the central Pacific basin where the strongest

cross-equatorial SST response is observed (Figure 45).

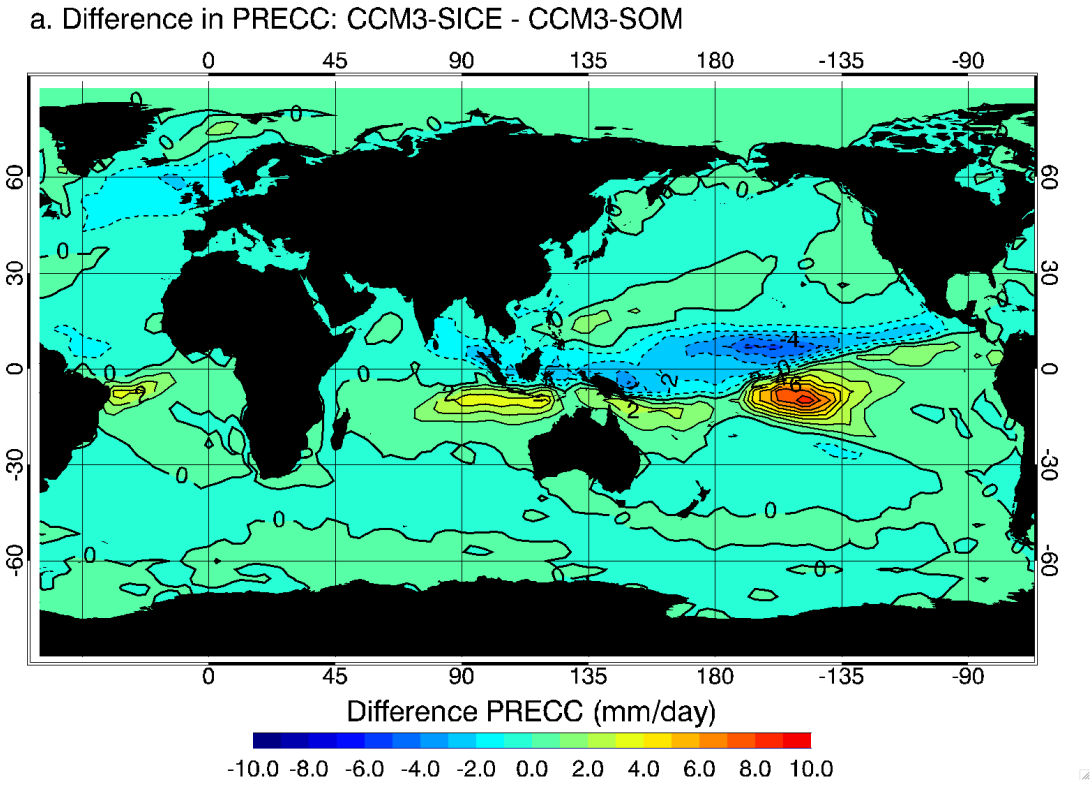

Fig. 46. Difference (CCM3-SICE - CCM3-SOM) in annual mean convective precipitation between the equilibrium state of LGM sea-ice forced simulation (CCM3-SICE) and the equilibrium state of the unperturbed control run (CCM3-SOM). Contour intervals are 1 mm/day.

The southward shift of the ITCZ is also reflected in the trade wind response of the CCM3-SICE experiment. In the equilibrium state, anomalous north-easterlies (north-westerlies) are observed over the northern (southern) equatorial ocean basins, as seen in Figure 47. This C-shaped profile of equatorial trade wind anomalies as discussed in the introduction is suggestive of the participation of the WES feedback in maintaining the equilibrium state of the southward shifted ITCZ in the CCM3-

SICE experiment as proposed by Chiang and Bitz (2005). In addition, the response of the equatorial SST as a dipole, particularly in the central and eastern Pacific also supports the existence of the WES feedback (Figure 45). A cross-equatorial dipole pattern is also observed in the latent heat flux anomalies in the CCM3-SICE experiment over the ocean basins (Figure 48), with increased (decreased) cooling of the ocean mixed layer occurring over the north (south) equatorial oceans, with the strongest response seen over the central Pacific ocean. To isolate the role of the WES feedback in the equilibrium state response of the CCM3-SICE experiment over the equatorial oceans, as only suggested by the co-location of wind response, SST and latent heat fluxes, the response of the WES-off experiments is analyzed.

3. Mean-state Response in the Absence of WES Feedback

In the absence of the WES feedback, the global SST response to high latitude sea-ice perturbations in the WES-off-SICE experiment is shown in Figure 49. The anomalies are computed as departures from the control run WES-off-SOM's equilibrium state. Cooling is observed over all of northern oceans, with a magnitude equal to that of the CCM3-SICE simulation suggesting that it is possible for other mechanisms in the northern tropical oceans to cool it down, attaining the same equilibrium state, even in the absence of the WES feedback. The response in the tropical Atlantic and the Indian oceans is similar to that of CCM3-SICE experiment with cooling in the northern deep tropics and warming in the southern deep tropics. However, the SST dipole pattern seen over the central and eastern Pacific equatorial ocean in the CCM3-SICE experiment is noticeably weaker in the WES-off-SICE response suggesting a strong role of the WES feedback in the region in maintaining the equilibrium state. A strong cooling observed over the central equatorial Pacific in the CCM3-SICE experiment is also absent in the WES-off-SICE experiment, again indicative of a dominant role of

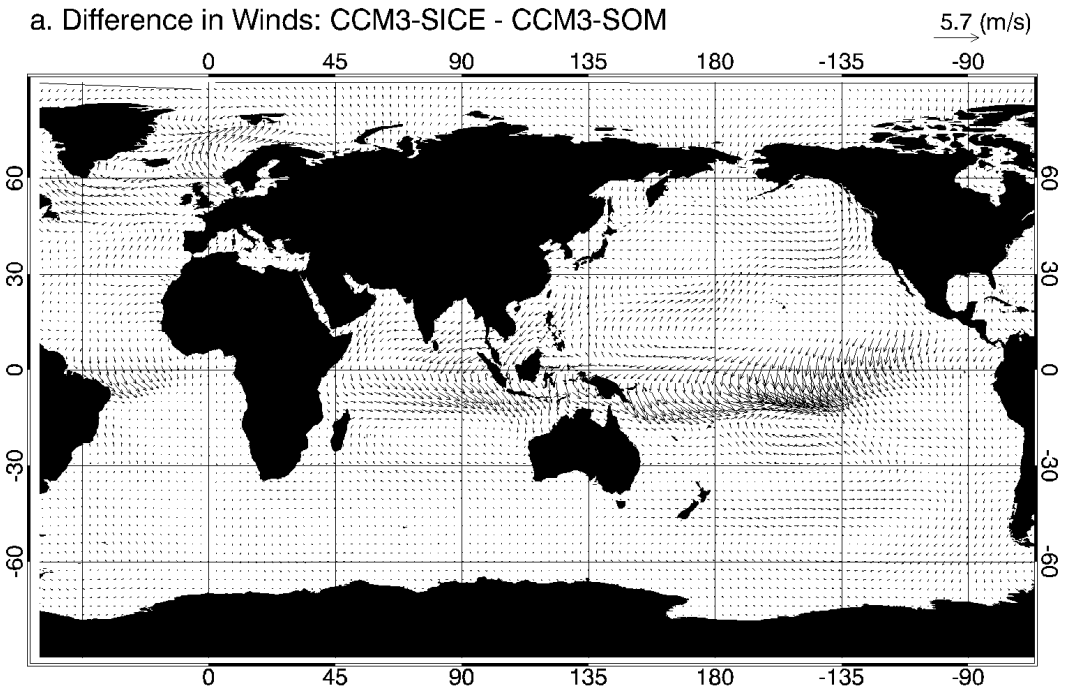

Fig. 47. Difference (CCM3-SICE - CCM3-SOM) in annual mean surface winds between the equilibrium state of LGM sea-ice forced simulation (CCM3-SICE) and the equilibrium state of the unperturbed control run (CCM3-SOM). Note the C-shaped wind anomalies over the equatorial region.

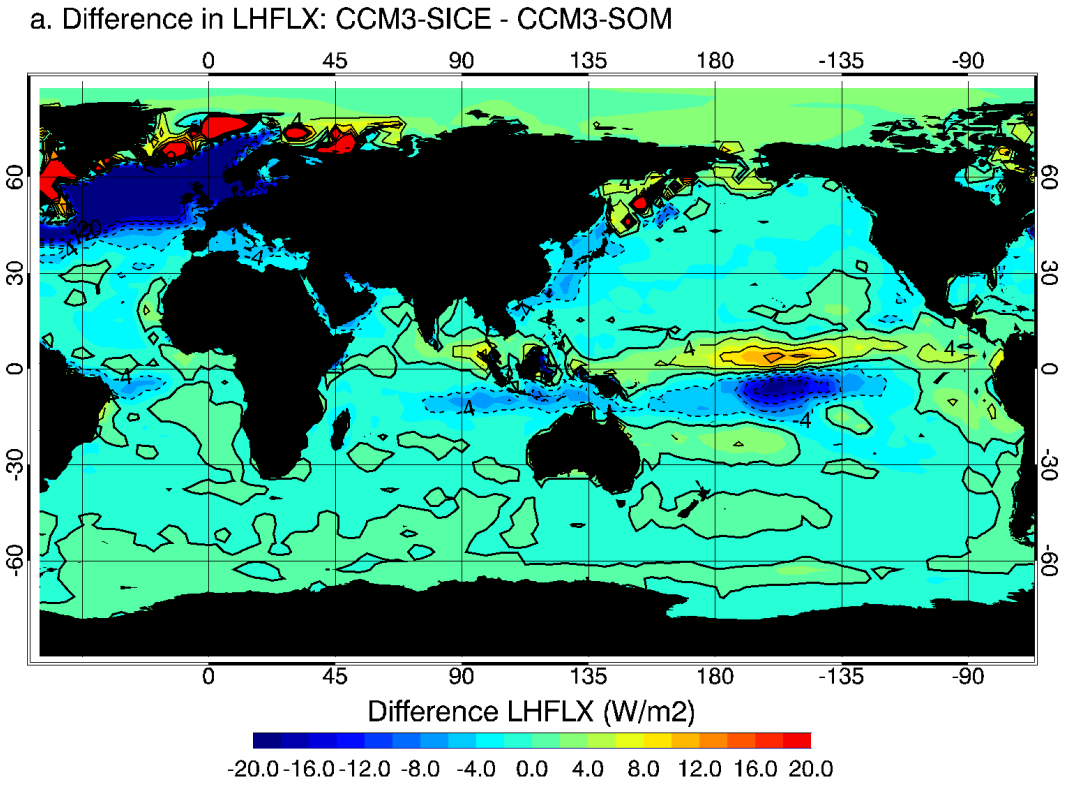

Fig. 48. Difference (CCM3-SICE - CCM3-SOM) in annual mean latent heat flux between the equilibrium state of LGM sea-ice forced simulation (CCM3-SICE) and the equilibrium state of the unperturbed control run (CCM3-SOM). Contour intervals are 4 W/m^2. Positive values indicate ocean to atmosphere upward heat flux.

the WES feedback.

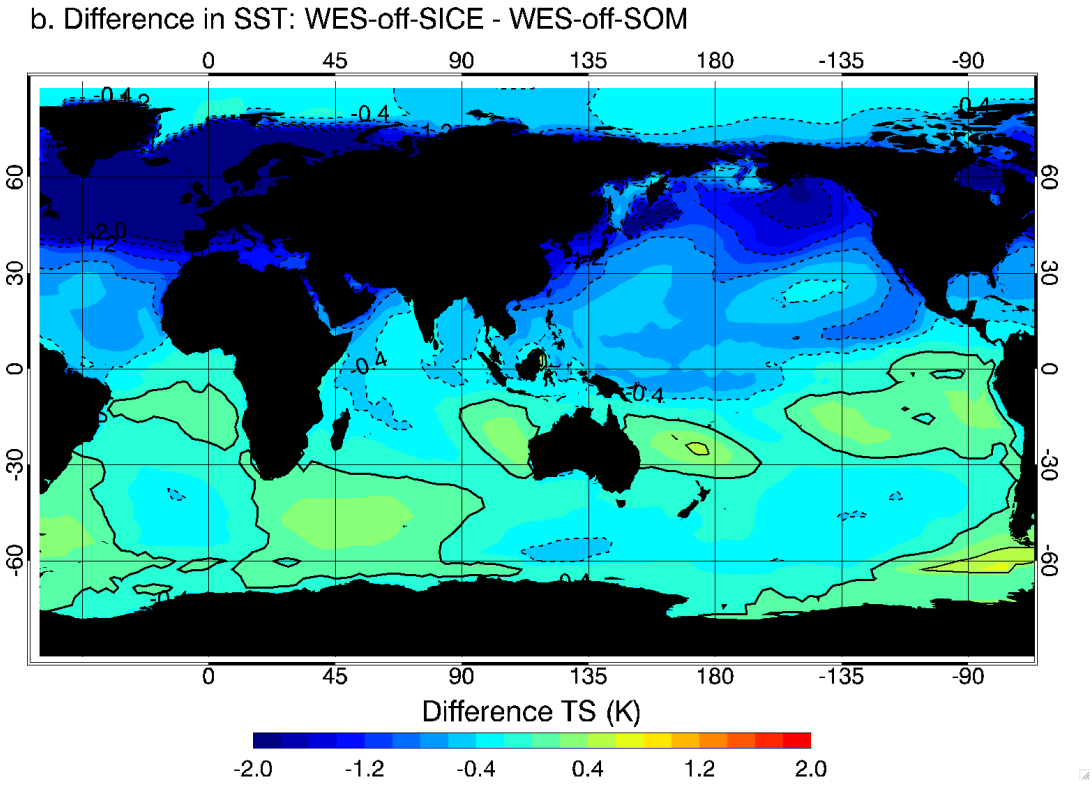

Fig. 49. Difference (WES-off-SICE - WES-off-SOM) in annual mean SST between the equilibrium state of LGM sea-ice forced WES-off simulation (WES-off-SICE) and the equilibrium state of the unperturbed WES-off run (WES-off-SOM). Contour intervals are 0.4 K.

The lack of the amplification of SST anomalies in the WES-off-SICE run is also reflected in the convective precipitation. Figure 50 shows the anomalous convective precipitation over global oceans when an equilibrium state is reached in WES-off-SICE experiment. A southward shift in the ITCZ as also seen in the CCM3-SICE experiment is observed. While the response in the Atlantic and Indian oceans is similar to that of CCM3-SICE experiment, the central and eastern equatorial Pacific

oceans show a much weaker response in the WES-off-SICE experiment following the weak response of SST in the region (Figure 49).

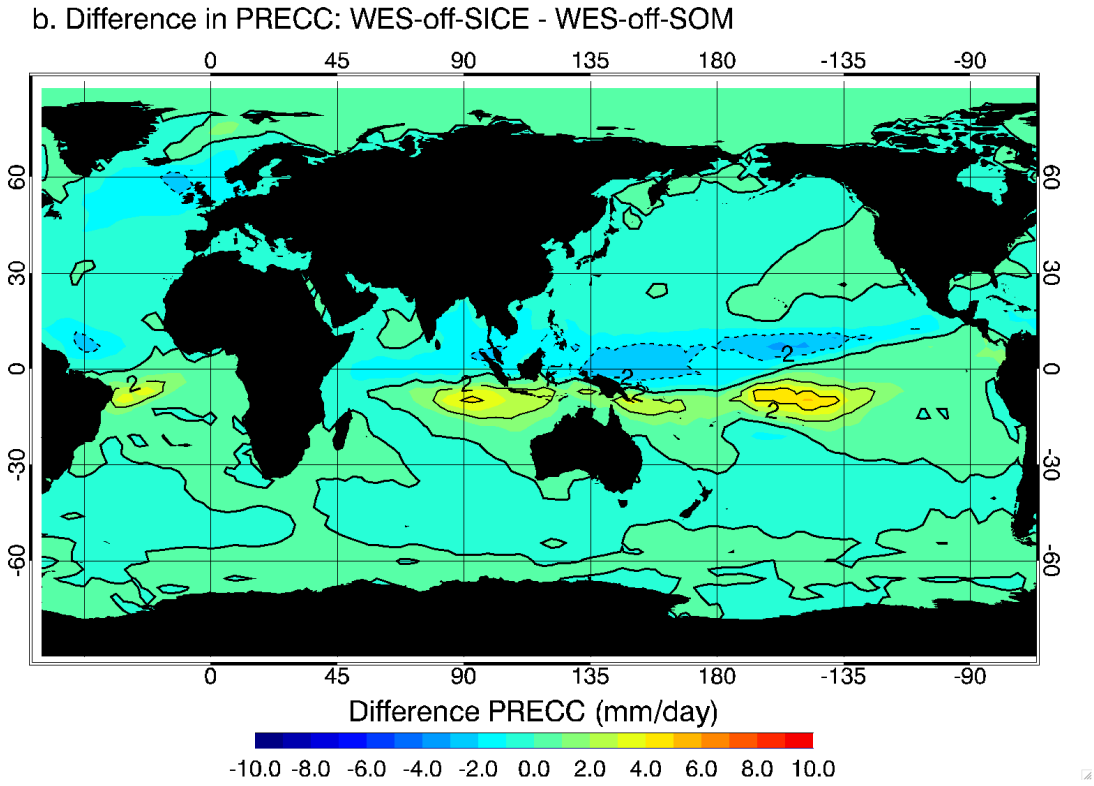

Fig. 50. Difference (WES-off-SICE - WES-off-SOM) in annual mean convective precipitation between the equilibrium state of LGM sea-ice forced WES-off simulation (WES-off-SICE) and the equilibrium state of the unperturbed WES-off run (WES-off-SOM). Contour intervals are 2 mm/day.

A weaker response of the surface winds and latent heat fluxes is also seen in the WES-off-SICE experiment (Figures 51 and 52) over global equatorial oceans, particularly over the central and eastern Pacific oceans. The weak cross-equatorial dipole of SST, winds and the latent heat fluxes in the absence of the WES feedback in the WES-off-SICE run conclusively indicates that the WES feedback is essential for

generating a cross-equatorial dipole response in CCM3-SOM. Over the central and eastern Pacific oceans, the role of the WES feedback appears to be dominant, while over the Atlantic and the Indian oceans, processes other than the WES feedback appear to be active in maintaining the new equilibrium state in the equatorial oceans in response to high latitude cooling. Identifying these other mechanisms requires further investigation and would be a subject of future studies.

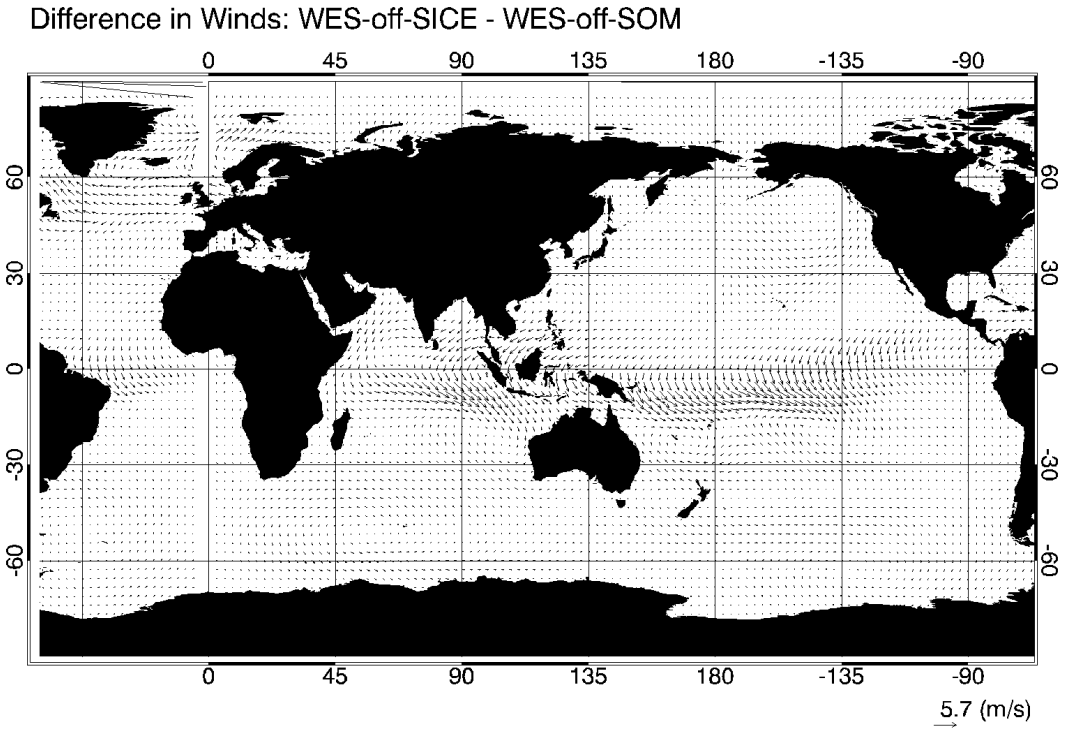

Fig. 51. Difference (WES-off-SICE - WES-off-SOM) in annual mean surface winds between the equilibrium state of LGM sea-ice forced WES-off simulation (WES-off-SICE) and the equilibrium state of the unperturbed WES-off run (WES-off-SOM).

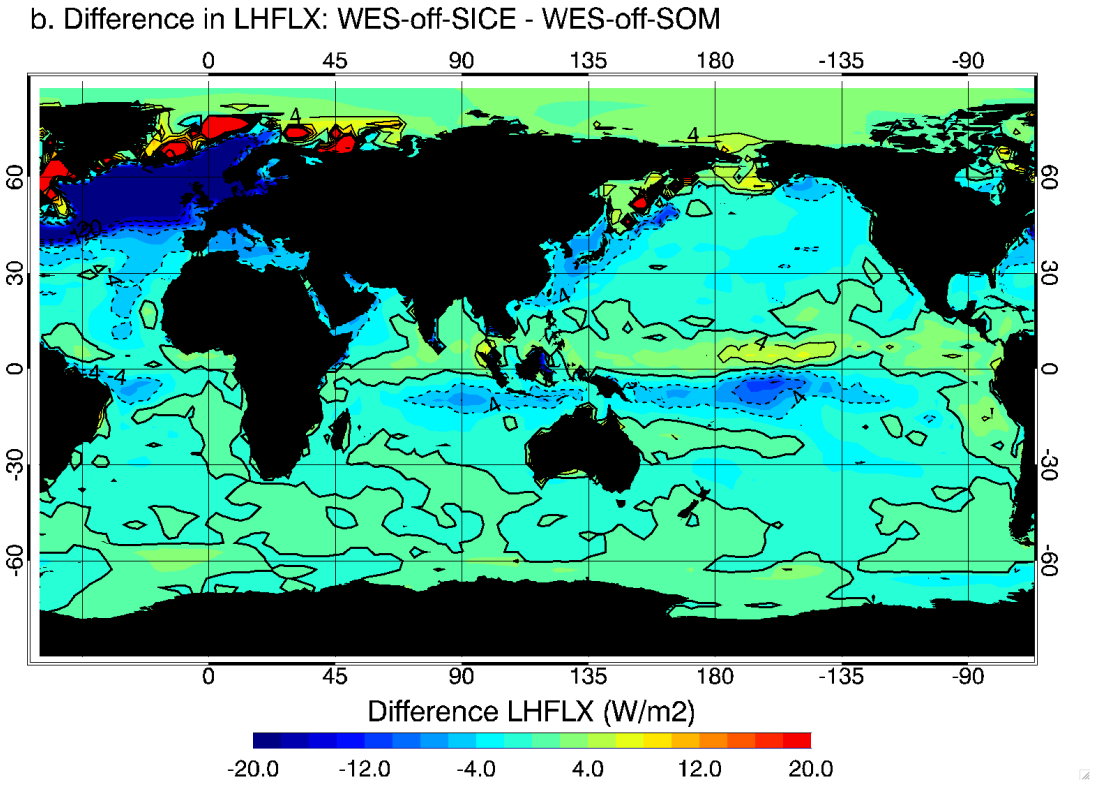

Fig. 52. Difference (WES-off-SICE - WES-off-SOM) in annual mean latent heat flux between the equilibrium state of LGM sea-ice forced WES-off simulation (WES-off-SICE) and the equilibrium state of the unperturbed WES-off run (WES-off-SOM). Contour intervals are 4 W/m^2. Positive values indicate ocean to atmosphere upward heat flux.

4. Transient Response

Chiang and Bitz (2005), who investigate the mechanism for the propagation of cool anomalies from the northern higher latitudes to the tropics and the southward shift of the ITCZ in CCM3 coupled to a SOM, suggest that the WES feedback may be responsible for the southward transport of SST anomalies within the trade wind zone south of about 30°N. Here, we test their hypothesis. Figure 53 shows the time-latitude Hovmoller plot of 3-months running-mean Pacific ocean SST anomalies, where the equilibrium state anomalies are the strongest (Figure 45), averaged over 4 ensemble runs of CCM3-SOM experiment for the first five years of the runs, during which the system approaches equilibrium. The anomalies were computed as deviations from the control run equilibrium state. Cooling reaches the northern trade wind region quickly, reaching amplitudes of about 0.5 K by the end of the first year at about 30°N by advection of cold dry air from the northern high-latitudes (Chiang and Bitz, 2005). Quick widespread cooling of about 0.2 K in the trade wind region south of 30°N up to the deep tropics is also observed within the first two years.

Further southward progression of cooling is restricted at the equatorial region where the anomalous dipole pattern, as seen in the equilibrium state, appears to start forming before the end of the first year, with warming occurring in the southern equatorial Pacific. The cooling in the northern equatorial region then begins to amplify gradually reaching equilibrium by the fourth year. Anomalous convective precipitation which follows the SST also shows a similar amplification of its dipole structure with time as is seen in Figure 54. Chiang and Bitz (2005) propose that the generation of the cross-equatorial anomalous SST dipole and its amplification before it reaches equilibrium are caused by the WES feedback, as is strongly suggested by the progressive amplification of C-shaped anomalous equatorial winds (Figure 55),

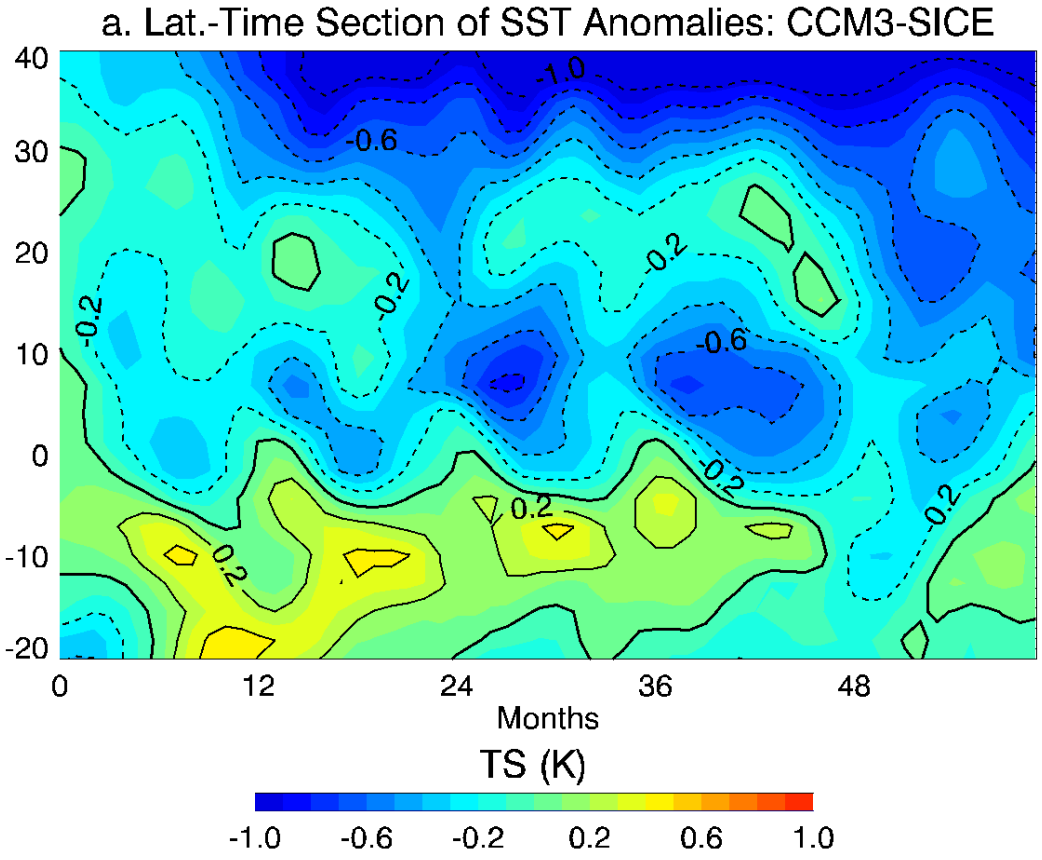

Fig. 53. Time-latitude hovmoeller plot zonally averaged over the Pacific (135°E - 270°E) of SST anomalies averaged over 4 ensemble runs of CCM3-SICE experiment. The SST anomalies are computed as deviations from the control run CCM3-SOM equilbrium state. $t = 0$ corresponds to the model month of September, when abrupt sea-ice anomalies were introduced in the model. Contour intervals are 0.2 K.

and of the associated anomalous latent heat fluxes (Figure 56), with increasing cooling (warming) in the northern (southern) equatorial Pacific. Note the seasonal cycle exhibited by the SST anomalies in the equatorial region (Figure 53), which appears to be synchronized with the seasonal cycle of the climatological ITCZ of the control run. The cold SST anomalies penetrate into the southernmost point in the boreal spring simultaneously with the ITCZ, which also moves south in the spring season. The ITCZ serves as the axis of meridional asymmetry over the equatorial oceans across which the WES feedback mechanizes. The seasonal development of the anomalous dipole about the ITCZ, further supports the presence of the WES feedback in the region.

To clearly identify the role of the WES feedback in the communication of the higher latitude cold signal to the tropics, the transient response of the WES-off-SICE experiment is analyzed. Cold anomalies propagate into the trade wind region in the WES-off-SICE experiment in about the same time frame as the CCM3-SICE experiment even in the absence of the WES feedback, as is seen in the Hovmoller plot of SST (Figure 57). A cooling greater than 0.5 K northward of 10°N is observed by the fifth year similar to that of the CCM3-SICE experiment indicating that processes other than WES feedback are active in the propagation of cold anomalies southwards in the trade wind region. Chiang and Bitz (2005) suggest that humidity plays a key role in the equator-ward propagation of cold anomalies. Transient eddy transport mechanisms have also been proposed (Cheng et al., 2007; Broccoli et al., 2006). Further investigations to understand the precise mechanisms will be conducted in later studies. However, it clearly appears that the WES feedback is not solely responsible for the equator-ward propagation of high-latitude cold anomalies.

A distinct response is observed in the WES-off-SICE experiment south of 10°N as compared to the CCM3-SICE experiment. A very weak cross-equatorial SST dipole

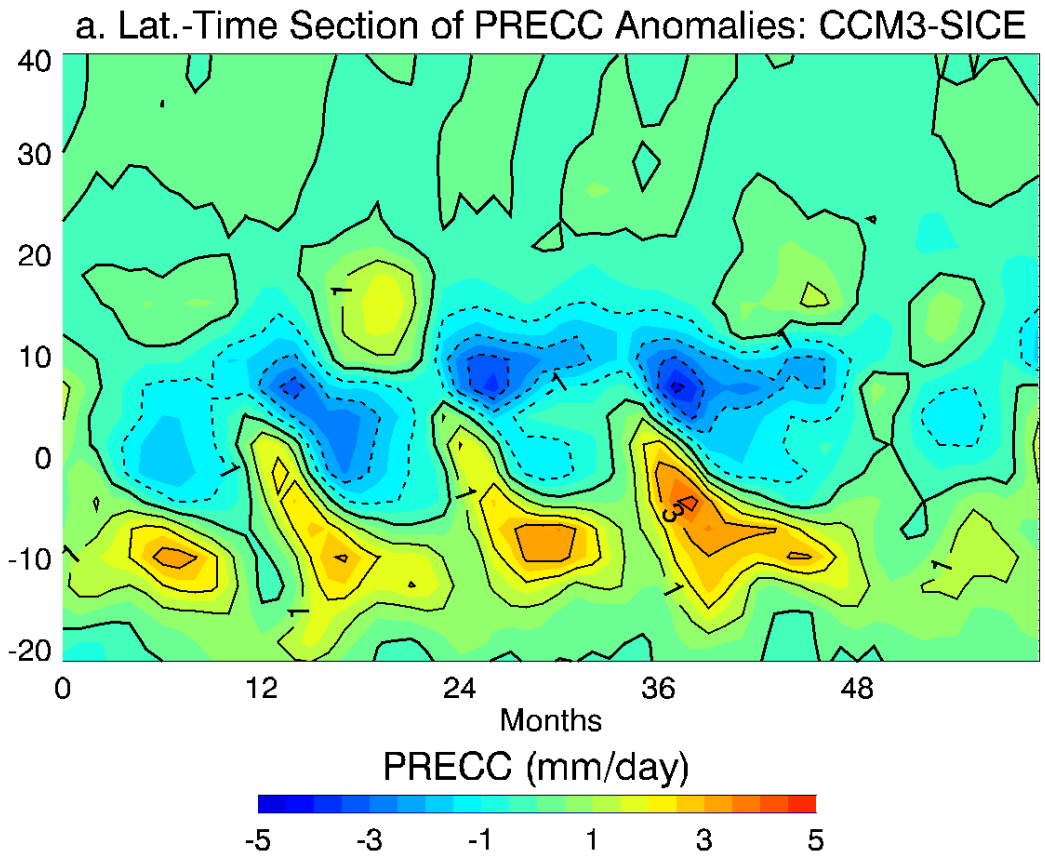

Fig. 54. Same as Figure 53 but for convective precipitation. Contour intervals are 1 mm/day.

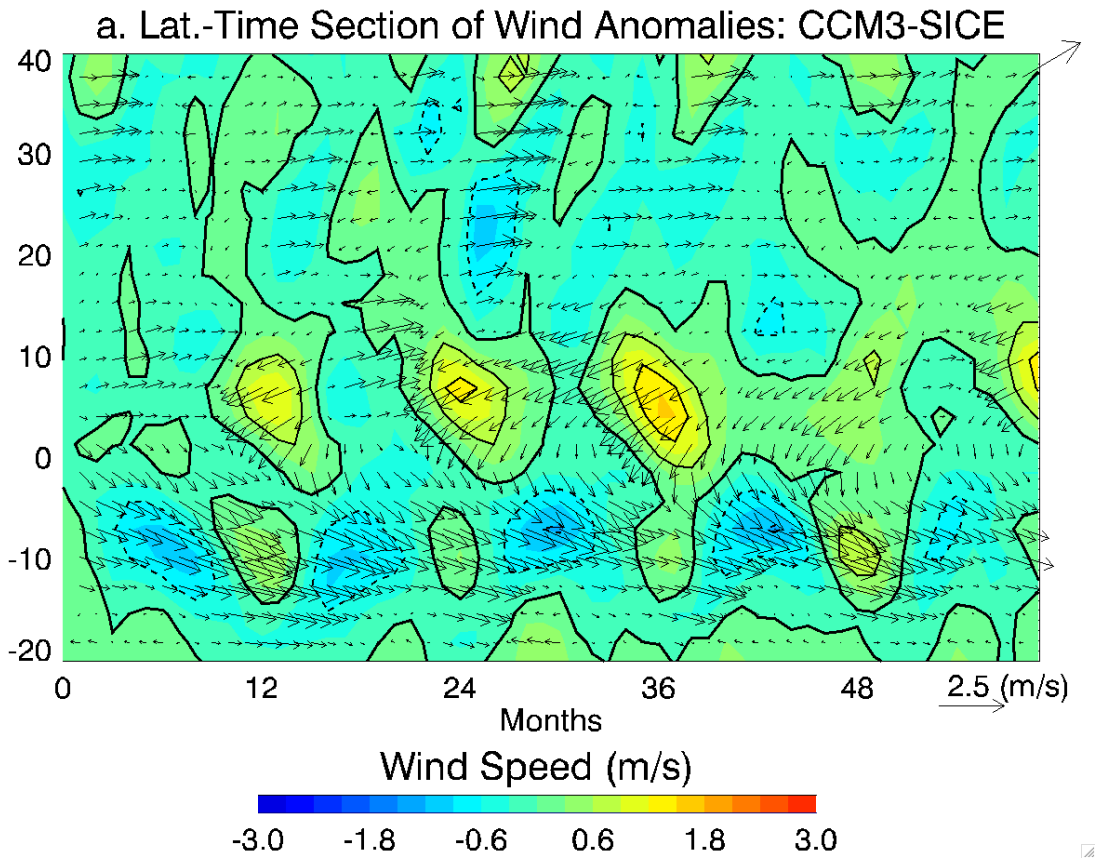

Fig. 55. Same as Figure 53 but for wind speed. Contour intervals are 1 m/s. Anomalous wind vectors are also shown.

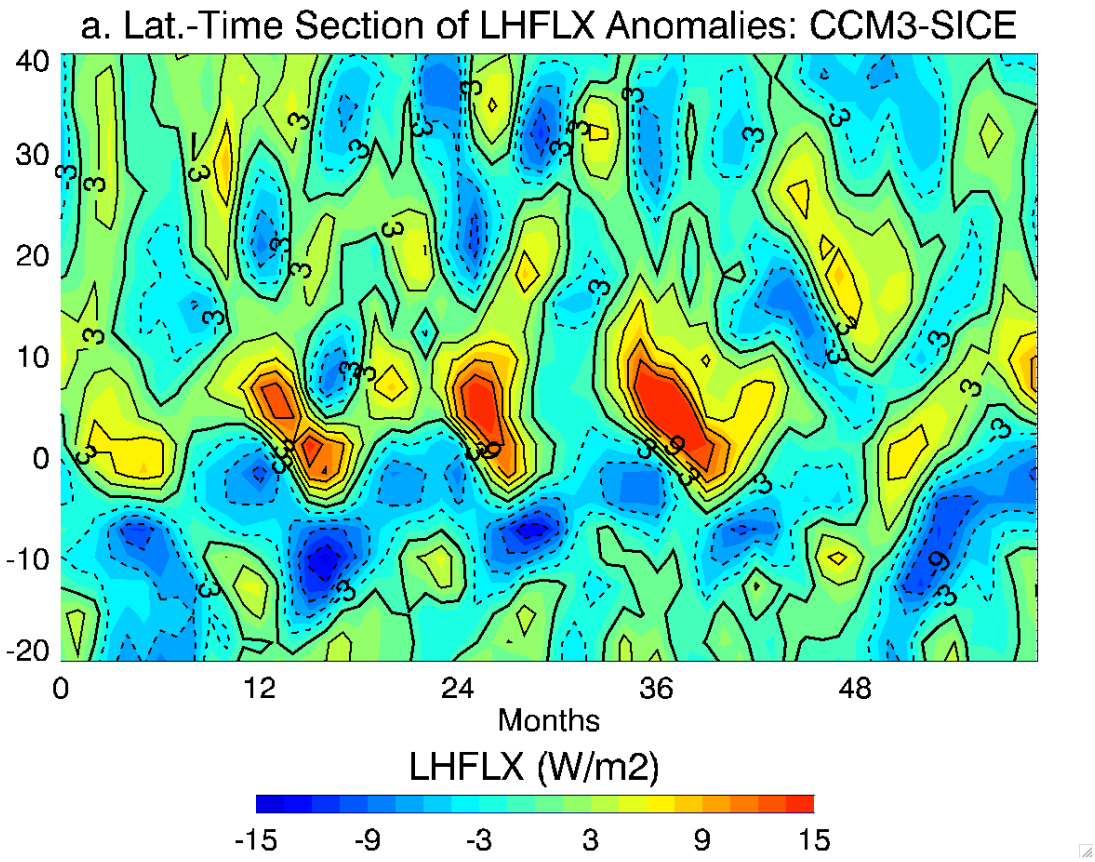

Fig. 56. Same as Figure 53 but for latent heat flux. Contour intervals are 3 W/m^2. Positive values indicate ocean to atmosphere upward heat flux.

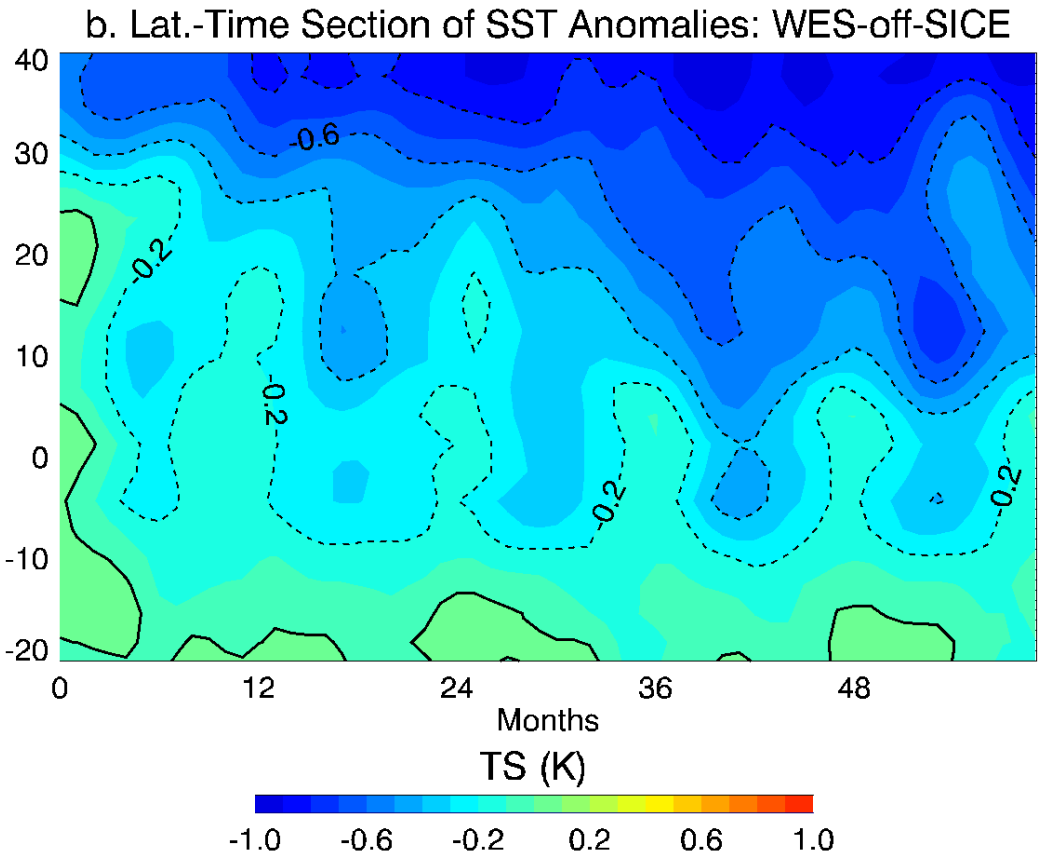

Fig. 57. Time-latitude hovmoeller plot zonally averaged over the Pacific (135°E - 270°E) of SST anomalies averaged over 4 ensemble runs of WES-off-SICE experiment. The SST anomalies are computed as deviations from the unperturbed WES-off-SOM run equilbrium state. $t = 0$ corresponds to the model month of September, when sea-ice anomalies were introduced in the model. Contour intervals are 0.2 K.

in the WES-off-SICE run is seen, with a much weaker amplification with time as the system reaches equilibrium, when compared to the CCM3-SICE experiment. Cold anomalies are observed to attain a magnitude of about 0.2 K in the equatorial region and little warming is seen over the southern equatorial Pacific. The absence of the WES feedback clearly restricts the amplification of the cross-equatorial dipole in the transition phase of the tropical climate from one state to the other. A weaker dipole is observed in the convective precipitation anomalies (Figure 58) as compared to the CCM3-SICE run (Figure 54). In the absence of the WES feedback, surface winds and the latent heat fluxes also show a diminished cross-equatorial response during the transition period (Figures 59 and 60) in the WES-off-SICE experiment confirming the presence of the WES feedback in the region. However, the appearance of the dipole indicates the presence of other mechanisms in the generation of the dipole. Nonetheless, the results of experiments here clearly establish the WES feedback as a dominant mechanism in the development of a CESG, and hence the southward migration of the ITCZ in response to high latitude cooling in CCM3-SOM providing support to the hypothesis of Chiang and Bitz (2005) that the WES feedback plays a role in the transition of equatorial climate.

5. Discussion

In the absence of the WES feedback, a very weak dipole is seen in the eastern and central tropical Pacific as compared to the unmodified sea-ice imposed run, suggesting a dominant role of the WES feedback in the region. The result also indicates that other feedback mechanisms associated with the ITCZ, as mentioned in the Introduction, like deep convective cloud SST feedback, have little impact in the response of the Pacific. The result could also imply that these other feedbacks are inherently tied to the WES feedback, and in the absence of the WES feedback, these feedbacks

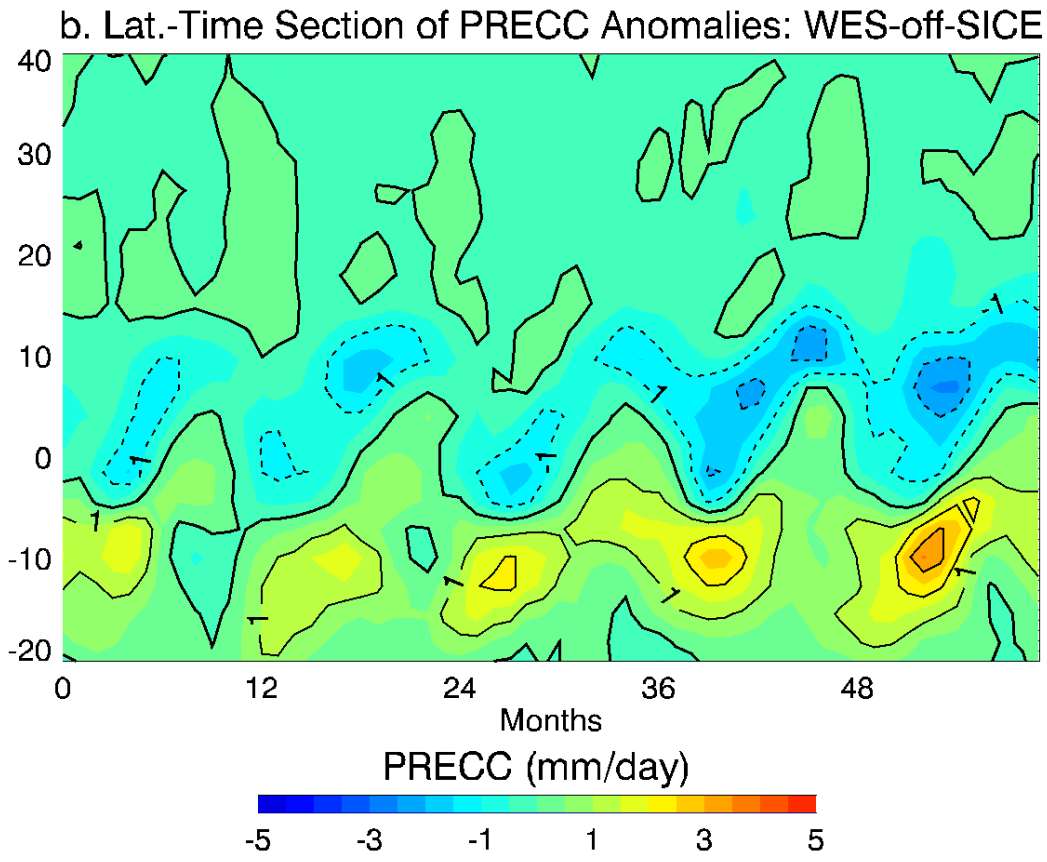

Fig. 58. Same as Figure 57 but for convective precipitation. Contour intervals are 1 mm/day.

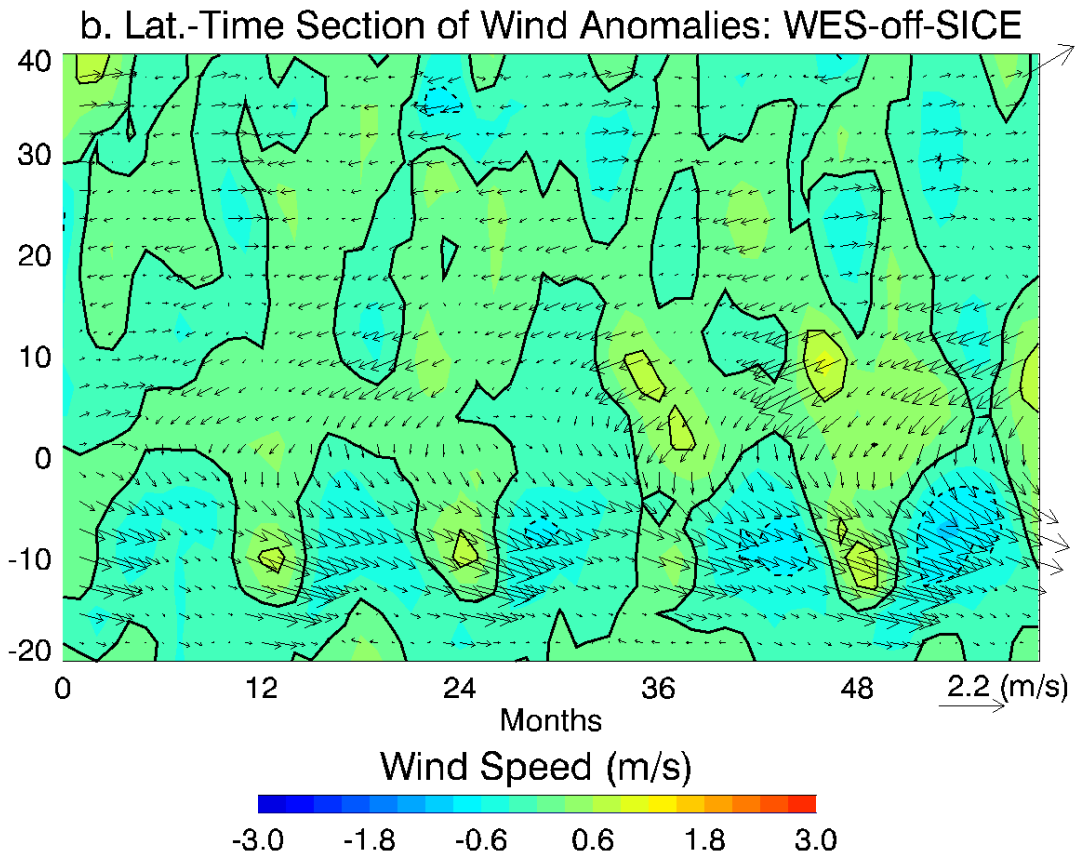

Fig. 59. Same as Figure 57 but for wind speed. Contour intervals are 1 m/s. Anomalous wind vectors are also shown.

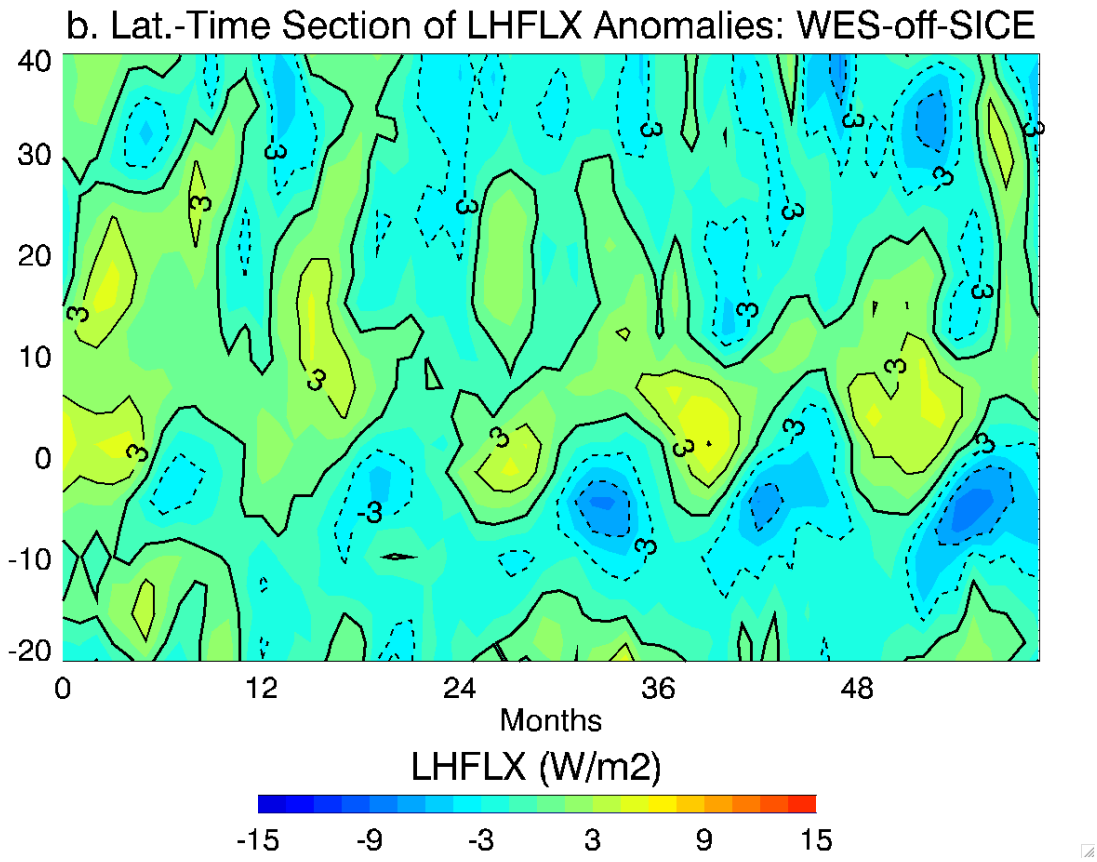

Fig. 60. Same as Figure 57 but for latent heat flux. Contour intervals are 3 W/m^2. Positive values indicate ocean to atmosphere upward heat flux.

lose strength and are unable to generate a response in the tropical Pacific. The argument, however, seems to fail over the Atlantic and the Indian ocean basins, where other mechanisms are able to generate a response, similar to that of the unmodified sea-ice imposed run, even in the absence of the WES feedback. These varied tropical responses can imply various local manifestations of the WES feedback or varied interconnections between the WES feedback and other tropical mechanisms when forced with high latitude anomalous sea-ice. A more in-depth analysis is required to find the linkage between the WES feedback and other mechanisms to better understand tropical response to high-latitude forcings.

The weak role of the WES feedback over the equatorial Atlantic in response to high latitude cooling is surprising. It has been suggested that the WES feedback plays a key role in the meridional mode of the Atlantic (Chang et al., 1997). Other studies (e.g Enfield and Mayer, 1997; Saravanan and Chang, 2000) and experiments done with the WES-off model forced with ENSO conditions in the Pacific for this study, suggest that the WES feedback is a dominant controller in generating realistic responses in the tropical Atlantic. As mentioned in the Introduction, response to the NAO is also suggested to manifest itself through the WES feedback (e.g. Xie and Tanimoto, 1998; Seager et al., 2000). Different roles of the WES feedback in the response to different forcings implies that understanding the variability of the tropics is more challenging, with various phenomena active in the region and possibly interacting with each other. Further, the simulations here were performed with a SOM, which interacts only thermodynamically with the atmosphere. In the presence of dynamical oceans, more complicated phenomena and interactions are possible, understanding of which would require a much detailed study. However, taking a small step towards understanding the tropics, this study clearly identifies that the WES feedback is not dominant in the response of the tropical Atlantic to high latitude cold forcing.

The southward movement of the ITCZ over the equatorial Pacific in response to high latitude cooling in the unmodified run is consistent with that of the results of Chiang and Bitz (2005), as expected as the same AGCM is used here, but different from that of Zhang and Delworth (2005), who note a very weak response over the equatorial Pacific in a AGCM coupled to a SOM as mentioned in the introduction. The response of CCM3-SOM also differs with that of the GFDL model over the equatorial Atlantic in strength (Figure 45). Possible explanations for these different responses could be varying strengths and manifestations of the WES feedback and tele-connection mechanisms between the tropical Atlantic basin and the tropical Pacific basin in the models. A deeper understanding of the reasons for different responses in these simulations, while would improve our knowledge about the tropics, is beyond the scope of this study. The eastern tropical Pacific is influenced by the cooling in the northern Pacific and by the adjacent tropical Atlantic ocean. Further analysis to quantitatively separate the fraction of only thermodynamically developed anomalies over the tropical eastern and central Pacific caused by high latitude Pacific cooling from that of the remote influence of the tropical Atlantic could provide additional potential predictability over eastern equatorial Pacific and hence of ENSO.

A couple of other caveats need to be mentioned. Recent studies show that in addition to the tropical Pacific, the tropical Atlantic climate can also potentially modulate the north Atlantic climate (Okumura et al., 2001; Rajagopalan et al., 1998). Hence, the response of the tropical oceans to high latitude forcings could potentially feedback upon the forcing itself, a phenomenon only partly constrained in experiments here by making the sea-ice non-interactive. In addition, as discussed by Chiang et al. (2003), the SOM does not exhibit mechanisms like the equatorial El Niño or Atlantic Niño phenomena, which themselves respond dynamically as well as thermodynamically to high latitude forcings. As mentioned above, experiments here exclude these mecha-

nisms by design, and focus on purely thermodynamical interactions. Simulations of an AGCM coupled to dynamical ocean models would be needed to completely study the role of the WES feedback in the response of tropical oceans to sea-ice anomalies.

CHAPTER V

SUMMARY

We find evidence for active WES feedback mechanism in tropical climate variability in CCM3 coupled to a SOM. Over the tropical Atlantic, the WES feedback, hypothesized to be associated with the Atlantic meridional mode (Carton et al., 1996; Chang et al., 1997), is believed to be stronger over the deep tropical Atlantic and weaker over the north tropical Atlantic, where the climatological winds are found to be dominant over their perturbations on their influence on latent heat flux fluctuations (Czaja et al., 2002; Saravanan and Chang, 2000). A correlation analysis of factors, namely winds and specific humidity difference, influencing latent heat fluxes in a control CCM3-SOM confirms these results. Strong correlations between u^* and latent heat flux, and weak correlations between specific humidity difference and latent heat flux observed over the deep tropical Atlantic support the existence of the WES feedback there. Stronger correlations between specific humidity difference and latent heat fluxes over the eastern north tropical Atlantic indicate a weaker WES feedback in the region. Strong correlations between u^* and latent heat fluxes also indicate the presence of WES feedback over the tropical western and central Pacific Ocean and the Indian Ocean in accordance with other studies (Chiang and Vimont, 2004; Kawamura et al., 2001). A weak WES feedback in the eastern ocean basins, as indicated by the dominance of humidity in controlling the latent heat fluxes, finds support in a study by Okajima et al. (2003). They find that the presence of a northern asymmetric ITCZ, a characteristic of those regions, causes a weakening of the WES feedback in an idealized GCM.

CCM3-SOM is further applied to understand the mechanistics of the WES feedback on the seasonal to inter-annual time scales. A modified version of the model is

created where the WES feedback is switched off by removing the effects of winds on the surface heat fluxes in the bulk formulations of latent and sensible heat fluxes. A comparison of the modified GCM integrations and the control run provides a platform for testing hypotheses associated with the WES feedback, proposed in the literature as theory and tested mostly by simple dynamic models. A clear indication of the dependence of the deep tropical variability on the WES feedback is found. A reduction to the amount of 40 to 80% is observed in the inter-annual variability of SST, surface heat fluxes, surface wind field, humidity and the convective precipitation field in the WES-off-SOM experiment in the regions where the WES feedback is suggested to be strong by the correlation analysis. A striking change in the mean state of the wind fields and convective precipitation field is also observed in the WES-off-SOM run even though the Q-flux adjustments were made to force the SST of the WES-off-SOM run to match that of the control run.

Comparative analysis of a WES-off run and a control run also indicates that a zonal manifestation of the WES feedback is dominant in the westwards propagation of the equatorial annual cycle originating in the eastern tropical Pacific and Atlantic oceans as proposed by Xie and Philander (1994). The development of the annual cycle in the eastern tropical oceans however is not found to be completely tied to the WES feedback, with a considerable, although weaker, annual cycle still being exhibited in the WES-off experiment. Analysis reveals that the development of the annual cycle in the eastern oceans in the absence of the influence of winds is possibly controlled by local near-surface humidity.

A SVD analysis of CCM3 coupled to a slab ocean model over the tropical Atlantic indicates a cross-equatorial dipole pattern of oceanic and atmospheric anomalies as seen in observational studies (Chang et al., 1997; Ruiz-Barradas et al., 2000), even in the absence of remote forcings like ENSO. This implies that thermodynamic in-

teractions between the atmosphere and the ocean have the potential to integrate the intrinsic atmospheric variability to arrange anomalies in a pattern that resembles the Atlantic meridional mode. This result is similar to the findings of Chang et al. (2001) that in the presence of moderate coupling between the atmosphere and the ocean and atmospheric noise it is possible to generate a dipole-like decadal oscillation in a hybrid coupled model. A distinct time-period of oscillation is not identifiable in the CCM3-SOM integrations because of the lack of ocean dynamics as mentioned in the Introduction. The question of the role of WES feedback in the possible decadal oscillations of the meridional mode either forced or intrinsic hence remains to be answered. Here, the hypothesis that the arrangement into a dipole-like pattern of the tropical Atlantic anomalies is caused by the WES feedback, as suggested by other studies (Chang et al., 1997, 2000) and also indicated by the collocation of coherent SST, latent heat flux and wind anomalies in CCM3-SOM integrations, is tested. A comparison between a CCM3-SOM integration where the WES feedback is switched off and the control run indicates that the free meridional mode of tropical Atlantic variability is indeed enhanced in the presence of the WES feedback at low frequencies.

However, the WES feedback is found not to be essential in the generation of the dipole mode itself. Specific humidity difference between the atmosphere and the ocean surface is capable of independently generating a dipole mode but with a substantially lower inter-annual variance through a feedback mechanism in the WES-off-SOM run. The proposed feedback mechanism still involves cross-equatorial winds caused by initial SST anomalies, which generate a cross-equatorial dipole in the Δq through atmospheric advection causing an amplified dipole of latent heat fluxes and hence of SST, which then further enhance the cross-equatorial winds and the Δq dipole. In the presence of the WES feedback, the mechanism however appears to fail due to stronger SST anomalies which result in strong changes in saturation specific humidity

nullifying the effect of advection of moist air and in fact working to damp the SST anomalies as is seen in the CCM3-SOM simulation. The result here thus indicates a stronger role for humidity in tropical Atlantic climate variability as suggested by Breugem et al. (2007), albeit in the absence of the influence of winds on SST.

Under forced ENSO conditions, the role of WES feedback in modulating tropical Atlantic meridional mode variability becomes evident in our CCM3-SOM experiments forced by an ENSO-like SST cycle in the tropical Pacific. A comparison between ENSO forced runs where the WES feedback is allowed to exist and where the WES feedback is switched off reveal that the coupled response of the Atlantic resembles the meridional mode only in the presence of WES feedback. Otherwise, no discernible coupled response pattern is observed. In the presence of remote forcings like ENSO, humidity- which appeared to generate a meridional mode, although weaker, in the unforced WES-off run, alone fails to sustain the mode and tropical variability appears to be governed by other processes. Penland and Matrosova (1998) find that ENSO disrupts the Atlantic dipole. Our modeling analysis suggests that the disruption occurs if the Atlantic dipole is independent of the influence of surface winds. In the presence of the WES feedback, however, the response of the Atlantic to ENSO events occurs through the meridional mode, even enhancing the mode, as is found in other studies (e.g Ruiz-Barradas et al., 2000; Saravanan and Chang, 2000), amplifying the cross-equatorial gradient of SST, latent heat fluxes, and the winds. The anomalous atmospheric flow associated with the WES feedback also amplifies the cross-equatorial gradient of the surface specific humidity by transporting moisture from one side of the equator to the other. The development of anomalous CESG in the presence of the WES feedback also causes the ITCZ to move northward over the Atlantic during ENSO events consistent with observations and modeling studies (e.g. Moura and Shukla, 1981; Saravanan and Chang, 2000).

The WES feedback is found to amplify the ENSO response in the eastern mid-latitude Atlantic off the Canadian coast, and the north tropical Atlantic in the January to June period, and is found to be incapable of supporting the developed anomalies in the later months of the year due to the loss of dominance of wind speed effect on the latent heat fluxes to the surface humidity effect. The WES feedback is also found to amplify north equatorial anomalies in the July to September period. In addition to the co-location of the relevant SST, wind speed and latent heat flux anomalies in these regions in the CCM3-SOM-ENSO integration, a lack of such anomalies in the WES-off-ENSO integration strongly supports the existence of the WES feedback in these regions, working to intensify the response of ENSO.

The role of the WES feedback in the propagation of cold high latitude anomalies to the tropics and in the southward migration of the ITCZ is also investigated using CCM3 coupled to a slab ocean model forced with LGM sea-ice extent in the northern hemisphere. This study is analogous to fully coupled GCM studies, which simulate the climate response to AMOC slowdown that cools the high latitudes. A period after rapid changes of sea-ice induced by the weakened AMOC have ceased and sea-ice over the entire northern higher latitudes has reached a stable state is considered for the simulations here. As with other experiments in this study, the simulations are further constrained by making the sea-ice thermodynamically non-interactive with the atmosphere and the ocean to completely focus on its climatic impacts in isolation, free from its own complex dynamics, with the goal of investigating the atmospheric tele-connection mechanism from the high latitudes to the tropics.

Consistent with other AGCM coupled to SOM studies (Chiang et al., 2003; Chiang and Bitz, 2005), the analysis reveals a cooling of the entire northern hemisphere when sea-ice is imposed in the northern high latitudes and a southward shift of the ITCZ and the development of CESG, a response similar to those of AMOC slowdown

experiments as mentioned in the introduction (e.g. Stouffer et al., 2006). Cooling of the northern hemisphere up to 10°N at the same rate is also observed when the WES feedback in switched off, a finding in contrast to the proposition of Chiang and Bitz (2005) that the WES feedback is largely responsible for the equator-ward propagation of cold anomalies in the trade wind region. Rapid cooling of the tropics despite the absence of the WES feedback suggests the presence of other large-scale meridional heat transport mechanisms that allow for the communication of high latitude signal to the tropics. Chiang and Bitz (2005) suggest a strong role for humidity, while eddy transport mechanisms have also been suggested (Cheng et al., 2007; Broccoli et al., 2006). Further studies are required to distinctly identify and isolate these other mechanisms.

A. Implications

Thermodynamic coupling provides demonstrable predictability (Saravanan and Chang, 1999, 2004) of the tropical climate. Previous studies and analyses here confirm that a large part of the variability of tropical oceanic climate and the surrounding continents is governed by air-sea feedbacks and particularly by the WES feedback. A realistic representation of these feedback processes in climate models is hence essential for accurate simulation of tropical climate mean and variability, currently suffering from severe biases (Davey et al., 2002). An accurate simulation of these processes would allow us to exploit the potential predictability (Chang et al., 2004) associated with these weakly coupled mechanisms and thus improve predictions of tropical climate on seasonal to decadal time-scales.

Over the Atlantic in particular, the variability of the CESG that is associated with the meridional mode has wide-spread societal impacts influencing rainfall in

Nordeste Brazil (e.g. Moura and Shukla, 1981) and north-western Africa (e.g. Folland et al., 1986). The oscillatory nature of the meridional mode provides potential predictablity (Chang et al., 1997), the tapping of which requires an improved understanding of the mechanisms governing the variability. Further efforts are needed to represent these mechanisms correctly in GCMs, which demonstrate large variability in their representation of air-sea feedbacks (Wang and Carton, 2003) and hence in the variability of the Atlantic, for improved seasonal predictions of the region. An illustration of the disparity of Atlantic variability in different GCMs is seen in the latitudinal extent of the tropical WES feedback in different GCMs, which has been a topic of interest in recent studies. Using a zonally averaged model (Kushnir et al., 2002) show that the low frequency variability of tropical SST decreases if the meridional extent of the WES feedback is confined between 10°N and 10°S. A GCM study by Okumura et al. (2001) reveals that the WES feedback extends into the trade regions affecting the NAO. SVD analysis here however reveals that the tropical WES feedback is limited to about 10°N and 10°S in CCM3 with the latent heat fluxes acting to damp the SSTs at higher latitudes consistent with other studies (Saravanan and Chang, 2000; Chang et al., 2000). Following Kushnir et al. (2002) this implies that the decadal tropical SST variability would differ in CCM3 and the GCM used in their study- the Japanese AGCM, serving as an example for the disparity in the representation of tropical Atlantic variability in different GCMs. An accurate representation of the WES feedback in GCMs would thus serve to improve simulation and hence the predictability of the tropical Atlantic. It has also been demonstrated that the tropical Atlantic variability can potentially influence the NAO (e.g. Rajagopalan et al., 1998) and also the tropical Pacific (e.g. Zhang and Delworth, 2005; Wu et al., 2007), further emphasizing the need for a better understanding of tropical Atlantic climate.

Cooling of the higher latitudes and formation of sea-ice has been associated with a weakening of the AMOC, one of the proposed impacts of global warming induced by green house gases (Gregory and co authors, 2005; Schmittner et al., 2005). The study is aimed at understanding the physical mechanisms that cause a change in the tropical climate, a better knowledge of which would help improve climate models, again with the eventual goal of improving predictability in a warming world.

REFERENCES

Alexander, M. and J. Scott, 2002: The influence of ENSO on air-sea interaction in the Atlantic. *Geophys. Res. Lett.*, **29** (14), 1701.

Alexander, M. A., I. Bladé, M. Newman, J. R. Lanzante, N.-C. Lau, and J. D. Scott, 2002: The atmospheric bridge: The influence of ENSO teleconnections on air-sea interaction over the global oceans. *Journal of Climate*, **15** (16), 2205–2231.

Alexander, M. A. and J. D. Scott, 1997: Surface flux variability over the north Pacific and north Atlantic Oceans. *Journal of Climate*, **10** (11), 2963–2978.

Alley, R. B., D. A. Meese, C. A. Shuman, A. J. Gow, K. C. Taylor, et al., 1993: Abrupt increase in Greenland snow accumulation at the end of the Younger Dryas event. *Nature*, **362** (6420), 527–529.

Barsugli, J. J. and D. S. Battisti, 1998: The basic effects of atmosphere-ocean thermal coupling on midlatitude variability. *Journal of the Atmospheric Sciences*, **55** (4), 477–493.

Bladé, I., 1997: The influence of midlatitude ocean-atmosphere coupling on the low-frequency variability of a GCM. Part I: No tropical SST forcing. *Journal of Climate*, **10** (8), 2087–2106.

Bretherton, C. S., C. Smith, and J. M. Wallace, 1992: An intercomparison of methods for finding coupled patterns in climate data. *Journal of Climate*, **5** (6), 541–560.

Breugem, W.-P., W. Hazeleger, and R. J. Haarsma, 2007: Mechanisms of northern tropical Atlantic variability and response to CO_2 doubling. *Journal of Climate*, **20** (11), 2691–2705.

Broccoli, A. J., 2000: Tropical cooling at the Last Glacial Maximum: An atmosphere-mixed layer ocean model simulation. *Journal of Climate*, **13** (5), 951–976.

Broccoli, A. J., K. A. Dahl, and R. J. Stouffer, 2006: Response of the ITCZ to northern hemisphere cooling. *Geophys. Res. Lett.*, **33**, L01 702.

Broecker, W. S., 2000: Abrupt climate change: Causal constraints provided by the paleoclimate record;. *Earth-Science Reviews*, **51** (1-4), 137–154.

Carton, J. A., X. Cao, B. S. Giese, and A. M. Da Silva, 1996: Decadal and interannual SST variability in the tropical Atlantic Ocean. *Journal of Physical Oceanography*, **26** (7), 1165–1175.

Carton, J. A., G. Chepurin, X. Cao, and B. Giese, 2000: A simple ocean data assimilation analysis of the global upper ocean 1950-95. Part I: Methodology. *Journal of Physical Oceanography*, **30** (2), 294–309.

Cessi, P., K. Bryan, and R. Zhang, 2004: Global seiching of thermocline waters between the Atlantic and the Indian-Pacific Ocean basins. *Geophys. Res. Lett.*, **31**, L04 302.

Chang, P., Y. Fang, R. Saravanan, L. Ji, and H. Seidel, 2006: The cause of the fragile relationship between the Pacific El Niño and the Atlantic Niño. *Nature*, **443** (7109), 324–328.

Chang, P., L. Ji, and H. Li, 1997: A decadal climate variation in the tropical Atlantic ocean from thermodynamic air-sea interactions. *Nature*, **385** (6616), 516–518.

Chang, P., L. Ji, and R. Saravanan, 2001: A hybrid coupled model study of tropical Atlantic variability. *Journal of Climate*, **14** (3), 361–390.

Chang, P. and S. G. Philander, 1994: A coupled ocean-atmosphere instability of relevance to the seasonal cycle. *Journal of the Atmospheric Sciences*, **51** (24), 3627–3648.

Chang, P., R. Saravanan, T. DelSole, and F. Wang, 2004: Predictability of linear coupled systems. Part I: Theoretical analyses. *Journal of Climate*, **17** (7), 1474–1486.

Chang, P., R. Saravanan, L. Ji, and G. C. Hegerl, 2000: The effect of local sea surface temperatures on atmospheric circulation over the tropical Atlantic sector. *Journal of Climate*, **13** (13), 2195–2216.

Chang, P., R. Zhang, W. Hazeleger, C. Wen, X. Wan, et al., 2008: Oceanic link between abrupt changes in the North Atlantic Ocean and the African monsoon. *Nature Geosci*, **1** (7), 444–448.

Charney, J. G., 1963: A note on large-scale motions in the tropics. *Journal of Atmospheric Sciences*, **20**, 607–609.

Chen, D., A. J. Busalacchi, and L. M. Rothstein, 1994: The roles of vertical mixing, solar radiation, and wind stress in a model simulation of the sea surface temperature seasonal cycle in the tropical Pacific Ocean. *J. Geophys. Res.*, **99** (C10), 20 345–20 359.

Cheng, W., C. M. Bitz, and J. C. H. Chiang, 2007: Adjustment of the global climate to an abrupt slowdown of the Atlantic meridional overturning circulation. *Ocean Circulation: Mechanisms and Impacts*, A. Schmittner, J. C. H. Chiang and S. R. Hemming (Eds.), *AGU Monograph*, No. 173, American Geophysical Union, 295–313.

Chiang, J. C. H., M. Biasutti, and D. S. Battisti, 2003: Sensitivity of the Atlantic intertropical convergence zone to last glacial maximum boundary conditions. *Paleoceanography*, **18** (4), 1094.

Chiang, J. C. H. and C. Bitz, 2005: Influence of high latitude ice cover on the marine intertropical convergence zone. *Climate Dynamics*, **25** (5), 477–496.

Chiang, J. C. H., Y. Kushnir, and A. Giannini, 2002: Deconstructing Atlantic intertropical convergence zone variability: Influence of the local cross-equatorial sea surface temperature gradient and remote forcing from the eastern equatorial Pacific. *J. Geophys. Res.*, **107** (D1), 4004.

Chiang, J. C. H. and A. H. Sobel, 2002: Tropical tropospheric temperature variations caused by ENSO and their influence on the remote tropical climate. *Journal of Climate*, **15** (18), 2616–2631.

Chiang, J. C. H. and D. J. Vimont, 2004: Analogous Pacific and Atlantic meridional modes of tropical atmosphere-ocean variability. *Journal of Climate*, **17** (21), 4143–4158.

Curtis, S. and S. Hastenrath, 1995: Forcing of anomalous sea surface temperature evolution in the tropical atlantic during pacific warm events. *J. Geophys. Res.*, **100** (C8), 15,835–15,847.

Czaja, A., P. van der Vaart, and J. Marshall, 2002: A diagnostic study of the role of remote forcing in tropical Atlantic variability. *Journal of Climate*, **15** (22), 3280–3290.

Dahl, K. A., A. J. Broccoli, and R. J. Stouffer, 2005: Assessing the role of North At-

lantic freshwater forcing in millennial scale climate variability: A tropical Atlantic perspective. *Climate Dynamics*, **24** (4), 325–346.

Dansgaard, W., J. W. C. White, and S. J. Johnsen, 1989: The abrupt termination of the Younger Dryas climate event. *Nature*, **339** (6225), 532–534.

Dansgaard, W., S. J. Johnsen, H. B. Clausen, D. Dahl-Jensen, N. S. Gundestrup, et al., 1993: Evidence for general instability of past climate from a 250-kyr ice-core record. *Nature*, **364** (6434), 218–220.

Davey, M., M. Huddleston, K. Sperber, P. Braconnot, F. Bryan, et al., 2002: STOIC: A study of coupled model climatology and variability in tropical ocean regions. *Climate Dynamics*, **18** (5), 403–420.

Denton, G. H., R. B. Alley, G. C. Comer, and W. S. Broecker, 2005: The role of seasonality in abrupt climate change. *Quaternary Science Reviews*, **24** (10-11), 1159–1182.

Deser, C. and M. L. Blackmon, 1993: Surface climate variations over the North Atlantic Ocean during winter: 1900-1989. *Journal of Climate*, **6** (9), 1743–1753.

Dong, B.-W. and R. T. Sutton, 2002: Adjustment of the coupled ocean–atmosphere system to a sudden change in the thermohaline circulation. *Geophys. Res. Lett.*, **29** (15), 1728.

Enfield, D. B. and D. A. Mayer, 1997: Tropical Atlantic sea surface temperature variability and its relation to El Niño-Southern Oscillation. *J. Geophys. Res.*, **102** (C1), 929–945.

Enfield, D. B., A. M. Mestas-Nuñez, D. A. Mayer, and L. Cid-Serrano, 1999: How

ubiquitous is the dipole relationship in tropical Atlantic sea surface temperatures? *J. Geophys. Res.*, **104** (C4), 7841–7848.

Folland, C. K., T. N. Palmer, and D. E. Parker, 1986: Sahel rainfall and worldwide sea temperatures, 1901-85. *Nature*, **320** (6063), 602–607.

Frankignoul, C. and K. Hasselmann, 1977: Stochastic climate models. Part II: Application to sea-surface temperature anomalies and thermocline variability. *Tellus*, **29**, 284–305.

Giannini, A., Y. Kushnir, and M. A. Cane, 2000: Interannual variability of Caribbean rainfall, ENSO, and the Atlantic Ocean. *Journal of Climate*, **13** (2), 297–311.

Gildor, H. and E. Tziperman, 2003: Sea-ice switches and abrupt climate change. *Philos. Trans. R. Soc. London Ser. A*, **3611** (1810), 1935–1942.

Gill, A. E., 1980: Some simple models for heat-induced tropical circulation. *Quarterly Journal of the Royal Meteorological Society*, **106**, 447–462.

Gregory, J. M., K. W. Dixon, R. J. Stouffer, A. J. Weaver, E. Driesschaert, et al., 2005: A model intercomparison of changes in the Atlantic thermohaline circulation in response to increasing atmospheric CO_2 concentration. *Geophys. Res. Lett.*, **32**, L12 703.

Hasselmann, K., 1976: Stochastic climate models. Part I. *Tellus*, **28**, 473–485.

Held, I. M. and A. Y. Hou, 1980: Nonlinear axially symmetric circulations in a nearly inviscid atmosphere. *Journal of the Atmospheric Sciences*, **37** (3), 515–533.

Horel, J. D., 1982: On the annual cycle of the tropical Pacific atmosphere and ocean. *Monthly Weather Review*, **110**, 1863–1878.

Hostetler, S. W. and A. C. Mix, 1999: Reassessment of ice-age cooling of the tropical ocean and atmosphere. *Nature*, **399** (6737), 673–676.

Houghton, R. W. and Y. M. Tourre, 1992: Characteristics of low-frequency sea surface temperature fluctuations in the tropical Atlantic. *Journal of Climate*, **5** (7), 765–772.

Huang, B. and J. Shukla, 1997: Characteristics of the interannual and decadal variability in a general circulation model of the tropical atlantic ocean. *Journal of Physical Oceanography*, **27** (8), 1693–1712.

Huang, R. X., M. A. Cane, N. Naik, and P. Goodman, 2000: Global adjustment of the thermocline in response to deepwater formation. *Geophys. Res. Lett.*, **27** (6), 759–762.

Hurrell, J. W., J. J. Hack, B. A. Boville, D. L. Williamson, and J. T. Kiehl, 1998: The dynamical simulation of the NCAR Community Climate Model version 3 (CCM3). *Journal of Climate*, **11** (6), 1207–1236.

Kaspi, Y., R. Sayag, and E. Tziperman, 2004: A "triple sea-ice state" mechanism for the abrupt warming and synchronous ice sheet collapses during Heinrich events. *Paleoceanography*, **19** (PA3004).

Kawamura, R., T. Matsuura, and S. Iizuka, 2001: Role of equatorially asymmetric sea surface temperature anomalies in the Indian Ocean in the Asian summer monsoon and El Niño-Southern Oscillation coupling. *J. Geophys. Res.*, **106** (D5), 4681–4693.

Kawase, M., 1987: Establishment of deep ocean circulation driven by deep-water production. *Journal of Physical Oceanography*, **17** (12), 2294–2317.

Kennett, J. P. and B. L. Ingram, 1995: A 20,000-year record of ocean circulation and climate change from the Santa Barbara basin. *Nature*, **377** (6549), 510–514.

Kiehl, J. T., J. J. Hack, G. B. Bonan, B. A. Boville, B. P. Briegleb, D. L. Williamson, and P. J. Rasch, 1996: Description of the NCAR community climate model. Technical Note TN-420+SR, NCAR.

Kiehl, J. T., J. J. Hack, G. B. Bonan, B. A. Boville, D. L. Williamson, and P. J. Rasch, 1998: The National Center for Atmospheric Research Community Climate Model: CCM3. *Journal of Climate*, **11** (6), 1131–1149.

Klein, S. A., B. J. Soden, and N.-C. Lau, 1999: Remote sea surface temperature variations during ENSO: Evidence for a tropical atmospheric bridge. *Journal of Climate*, **12** (4), 917–932.

Kushnir, Y., R. Seager, J. Miller, and J. C. H. Chiang, 2002: A simple coupled model of tropical Atlantic decadal climate variability. *Geophys. Res. Lett.*, **29** (23), 2133.

Lau, N.-C. and M. J. Nath, 1996: The role of the atmospheric bridge in linking tropical Pacific ENSO events to extratropical SST anomalies. *Journal of Climate*, **9** (9), 2036–2057.

Lau, N.-C. and M. J. Nath, 2001: Impact of ENSO on SST variability in the North Pacific and North Atlantic: Seasonal dependence and role of extratropical sea-air coupling. *Journal of Climate*, **14** (13), 2846–2866.

Li, C., D. S. Battisti, D. P. Schrag, and E. Tziperman, 2005: Abrupt climate shifts in Greenland due to displacements of the sea ice edge. *Geophys. Res. Lett.*, **32**, L19 702.

Li, T. and S. G. H. Philander, 1996: On the annual cycle of the eastern equatorial Pacific. *Journal of Climate*, **9** (12), 2986–2998.

Lindzen, R. S. and S. Nigam, 1987: On the role of sea surface temperature gradients in forcing low-level winds and convergence in the tropics. *Journal of the Atmospheric Sciences*, **44** (17), 2418–2436.

Liu, Z., 1996: Modeling equatorial annual cycle with a linear coupled model. *Journal of Climate*, **9** (10), 2376–2385.

Lynch-Stieglitz, J., 2004: Ocean science: Hemispheric asynchrony of abrupt climate change. *Science*, **304** (5679), 1919–1920.

Manabe, S. and A. J. Broccoli, 1985: The influence of continental ice sheets on the climate of an ice age. *J. Geophys. Res.*, **90** (D1), 2167–2190.

Maykut, G. A. and N. Untersteiner, 1971: Some results from a time-dependent thermodynamic model of sea ice. *J. Geophys. Res.*, **76** (6), 1550–1575.

Mehta, V. M., 1998: Variability of the tropical ocean surface temperatures at decadal-multidecadal timescales. Part I: The Atlantic Ocean. *Journal of Climate*, **11** (9), 2351–2375.

Mitchell, T. P. and J. M. Wallace, 1992: The annual cycle in equatorial convection and sea surface temperature. *Journal of Climate*, **5** (10), 1140–1156.

Moura, A. D. and J. Shukla, 1981: On the dynamics of droughts in northeast Brazil: Observations, theory and numerical experiments with a general circulation model. *Journal of the Atmospheric Sciences*, **38** (12), 2653–2675.

Nobre, P. and J. Shukla, 1996: Variations of sea surface temperature, wind stress, and rainfall over the tropical Atlantic and South America. *Journal of Climate*, **9** (10), 2464–2479.

Okajima, H., S.-P. Xie, and A. Numagati, 2003: Interhemispheric coherence of tropical climate variability: Effect of the climatological ITCZ. *Journal of the Meteorological Society of Japan*, **81** (6), 1371–1386.

Okumura, Y. and S.-P. Xie, 2004: Interaction of the Atlantic equatorial cold tongue and the African monsoon. *Journal of Climate*, **17** (18), 3589–3602.

Okumura, Y., S.-P. Xie, A. Numaguti, and Y. Tanimoto, 2001: Tropical atlantic air-sea interaction and its influence on the NAO. *Geophys. Res. Lett.*, **28** (8), 1507–1510.

Penland, C. and L. Matrosova, 1998: Prediction of tropical Atlantic sea surface temperatures using linear inverse modeling. *Journal of Climate*, **11** (3), 483–496.

Peterson, L. C., G. H. Haug, K. A. Hughen, and U. Rohl, 2000: Rapid changes in the hydrologic cycle of the tropical Atlantic during the last glacial. *Science*, **290** (5498), 1947–1951.

Philander, S. G. H. and Y. Chao, 1991: On the contrast between the seasonal cycles of the equatorial Atlantic and Pacific Oceans. *Journal of Physical Oceanography*, **21** (9), 1399–1406.

Philander, S. G. H., D. Gu, G. Lambert, T. Li, D. Halpern, N. C. Lau, and R. C. Pacanowski, 1996: Why the ITCZ is mostly north of the equator? *Journal of Climate*, **9** (12), 2958–2972.

Rajagopalan, B., Y. Kushnir, and Y. M. Tourre, 1998: Observed decadal midlatitude and tropical Atlantic climate variability. *Geophys. Res. Lett.*, **25** (21), 3967–3970.

Ruiz-Barradas, A., J. A. Carton, and S. Nigam, 2000: Structure of interannual-to-decadal climate variability in the tropical Atlantic sector. *Journal of Climate*, **13** (18), 3285–3297.

Saravanan, R., 1998: Atmospheric low-frequency variability and its relationship to midlatitude SST variability: Studies using the NCAR Climate System Model. *Journal of Climate*, **11** (6), 1386–1404.

Saravanan, R. and P. Chang, 1999: Oceanic mixed layer feedback and tropical Atlantic variability. *Geophys. Res. Lett.*, **26** (24), 3629–3632.

Saravanan, R. and P. Chang, 2000: Interaction between tropical Atlantic variability and El Niño-Southern Oscillation. *Journal of Climate*, **13** (13), 2177–2194.

Saravanan, R. and P. Chang, 2004: Thermodynamic coupling and predictability of tropical sea surface temperature. *Earth's climate: The Ocean-Atmosphere Interaction*, C. Wang and S.-P. Xie and J. A. Carton (Eds.), *Geophysical Monograph*, No. 147, American Geophysical Union, 171–180

Schmittner, A., M. Latif, and B. Schneider, 2005: Model projections of the North Atlantic thermohaline circulation for the 21st century assessed by observations. *Geophys. Res. Lett.*, **32**, L23 710.

Schneider, E. K., 1977: Axially symmetric steady-state models of the basic state for instability and climate studies. Part II: Nonlinear calculations. *Journal of the Atmospheric Sciences*, **34** (2), 280–296.

Seager, R., D. Battisti, M. Gordon, N. Naik, A. Clement, and M. Cane, 2002: Is the gulf stream responsible for Europe's mild winters? *Q. J. R. Meteorol. Soc.*, **128**, 2563–86.

Seager, R., Y. Kushnir, P. Chang, N. Naik, J. Miller, and W. Hazeleger, 2001: Looking for the role of the ocean in tropical Atlantic decadal climate variability. *Journal of Climate*, **14** (5), 638–655.

Seager, R., Y. Kushnir, M. Visbeck, N. Naik, J. Miller, G. Krahmann, and H. Cullen, 2000: Causes of Atlantic Ocean climate variability between 1958 and 1998. *Journal of Climate*, **13** (16), 2845–2862.

Servain, J., I. Wainer, J. P. M. Jr., and A. Dessier, 1999: Relationship between the equatorial and meridional modes of climatic variability in the tropical Atlantic. *Geophys. Res. Lett.*, **26** (4), 485–488.

Sobel, A. H. and C. S. Bretherton, 2000: Modeling tropical precipitation in a single column. *Journal of Climate*, **13** (24), 4378–4392.

Stouffer, R. J., J. Yin, J. M. Gregory, K. W. Dixon, M. J. Spelman, et al., 2006: Investigating the causes of the response of the thermohaline circulation to past and future climate changes. *Journal of Climate*, **19** (8), 1365–1387.

Stuiver, M. and P. M. Grootes, 2000: GISP2 oxygen isotope ratios. *Quaternary Research*, **53** (3), 277–284.

Takahashi, K. and D. S. Battisti, 2007: Processes controlling the mean tropical pacific precipitation pattern. Part I: The Andes and the eastern Pacific ITCZ precipitation pattern. part i: The andes and the eastern pacific itcz. *Journal of Climate*, **20** (14), 3434–3451.

Tanimoto, Y. and S.-P. Xie, 2002: Inter-hemispheric decadal variations in SST, surface wind, heat flux and cloud cover over the Atlantic Ocean;. *Journal of the Meteorological Society of Japan*, **80** (5), 1199–1219.

Thorndike, A. S., 1992: A toy model linking atmospheric thermal radiation and sea ice growth. *J. Geophys. Res.*, **97** (C6), 9401–9410.

Timmermann, A., S. I. An, U. Krebs, and H. Goosse, 2005: ENSO suppression due to weakening of the North Atlantic thermohaline circulation. *Journal of Climate*, **18** (16), 3122–3139.

Timmermann, A., Y. Okumura, S.-I. An, A. Clement, B. Dong, et al., 2007: The influence of a weakening of the Atlantic meridional overturning circulation on ENSO. *Journal of Climate*, **20** (19), 4899–4919.

Vellinga, M. and R. A. Wood, 2002: Global climatic impacts of a collapse of the Atlantic thermohaline circulation. *Climatic Change*, **54** (3), 251–267.

Wallace, J. M. and D. S. Gutzler, 1981: Teleconnections in the geopotential height field during the northern hemisphere winter. *Monthly Weather Review*, **109** (4), 784–812.

Wallace, J. M., C. Smith, and Q. Jiang, 1990: Spatial patterns of atmosphere-ocean interaction in the northern winter. *Journal of Climate*, **3** (9), 990–998.

Wang, B., 1994: On the annual cycle in the tropical eastern central Pacific. *Journal of Climate*, **7** (12), 1926–1942.

Wang, J. and J. A. Carton, 2003: Modeling climate variability in the tropical Atlantic atmosphere. *Journal of Climate*, **16** (23), 3858–3876.

Wu, L., F. He, Z. Liu, and C. Li, 2007: Atmospheric teleconnections of tropical Atlantic variability: Interhemispheric, tropical-extratropical, and cross-basin interactions. *Journal of Climate*, **20** (5), 856–870.

Wu, L. and Z. Liu, 2002: Is tropical Atlantic variability driven by the north Atlantic oscillation? *Geophys. Res. Lett.*, **29** (13), 1653.

Xie, S.-P., 1994: On the genesis of the equatorial annual cycle. *Journal of Climate*, **7** (12), 2008–2013.

Xie, S.-P., 1996: Westward propagation of latitudinal asymmetry in a coupled ocean-atmosphere model. *Journal of Atmospheric Sciences*, **53** (22), 3236–3250.

Xie, S.-P., 1999: A dynamic ocean-atmosphere model of the tropical Atlantic decadal variability. *Journal of Climate*, **12** (1), 64–70.

Xie, S.-P., 2005: The shape of continents, air-sea interaction, and the rising branch of the Hadley circulation, *The Hadley Circulation: Past, Present and Future*, H. F. Diaz and R. S. Bradley (Eds.), Kluwer Academic Publishers, 121–152

Xie, S.-P. and J. Carton, 2004: Tropical Atlantic variability: Patterns, mechanisms, and impacts. *Earth's Climate: The Ocean-Atmosphere Interaction*, C. Wang and S.-P. Xie and J. A. Carton (Eds.), *Geophysical Monograph*, No. 147, American Geophysical Union, 121–142

Xie, S.-P., Y. Okumura, T. Miyama, and A. Timmermann, 2008: Influences of Atlantic climate change on the tropical Pacific via the central American isthmus. *Journal of Climate*, **21** (15), 3914–3928.

Xie, S.-P. and S. Philander, 1994: A coupled ocean-atmosphere model of relevance to the ITCZ in the eastern Pacific. *Tellus*, **46A**.

Xie, S.-P. and Y. Tanimoto, 1998: A pan-Atlantic decadal climate oscillation. *Geophys. Res. Lett.*, **25** (12), 2185–2188.

Yang, J., 1999: A linkage between decadal climate variations in the Labrador Sea and the tropical Atlantic Ocean. *Geophys. Res. Lett.*, **26** (8), 1023–1026.

Yukimoto, S., M. Endoh, Y. Kitamura, A. Kitoh, T. Motoi, and A. Noda, 2000: ENSO-like interdecadal variability in the Pacific Ocean as simulated in a coupled general circulation model. *J. Geophys. Res.*, **105** (C13).

Zhang, R. and T. L. Delworth, 2005: Simulated tropical response to a substantial weakening of the Atlantic thermohaline circulation. *Journal of Climate*, **18** (12), 1853–1860.

VITA

Salil Mahajan received his Bachelor of Architecture degree from the Indian Institute of Technology, Kharagpur, India in 2002. He entered the Department of Atmospheric Sciences at Texas A&M University in 2003 and earned his Master of Science degree in December 2004. He continued his academic pursuit in the department and earned his Ph.D. in December 2008.

Salil may be reached at the Department of Atmospheric Sciences, 3150 TAMU, Texas A&M University, College Station, Texas-77843-3150. His email is salilmahajan@tamu.edu